ADVANCED MASTERS IN STRUCTURAL ANALYSIS
OF MONUMENTS AND HISTORICAL CONSTRUCTIONS

Master's Thesis

Thomas E. Morrison

Advanced Numerical Tool to Analyze Monitoring Data

This Masters Course has been funded with support from the European Commission. This publication reflects the views only of the author, and the Commission cannot be held responsible for any use which may be made of the information contained therein.

Portugal I 2008

DECLARATION

Name: Thomas E Morrison

Email: tomemorrison@gmail.com

Passport nº: _____

Title of the MSc Dissertation: Advanced Numerical Tool to Analyze Monitoring Data

Supervisor(s): Professor Ramos

Year: 2007 / 2008

I hereby declare that the MSc Consortium responsible for the Advanced Masters in Structural Analysis of Monuments and Historical Constructions is allowed to store and make available electronically the present MSc Dissertation.

University: University of Minho

Date: _____

Signature: _____

I hereby declare that this MSc Dissertation is an original work by the author.

University: University of Minho

Date: _____

Signature: _____

Acknowledgements

Without the help and support of many this thesis could never have been completed. I can't possibly mention all the forms of support that have been provided to me over the last four months. The process has been challenging and somewhat overwhelming, so please forgive potential inadvertent omissions.

- I would like to thank the European Union for providing the essential finical support through the Erasmus Mundus Scholarship, as well as the selection committee of the Advanced Masters in Structural Analysis of Monuments and Historical Construction who saw in me a worthy candidate for this program and scholarhip.
- I thank my supervisor, Professor Luis Ramos. He not only motivated me but also kept me focused. His feedback was invaluable, always finding time to answer my questions.
- I greatly acknowledge the help of Sandra Pereira guiding me through the intangibles of Univeristy and course program requirements.
- I thank Oliver Baettig, for his helpful edits on one of the more difficult parts of my thesis.
- Finally, I would like to thank Bilge, Paolo, Shweta, and Supawat for the discussions we had working on this short term thesis project.

Life-long thanks go to my parents, Carol and Luke, for far more than I could ever summarize in a short message. My daughter, Dorothy, and her unmatched skill of making me smile. And most importantly, thank you Claire, for being the rock I couldn't stand without.

Abstract

Long term structural health monitoring systems are finding increased use in many fields, including preservation of historic structures. Advances in structural monitoring systems have made it possible to place large numbers of structural and environmental sensors on a structure, and receive almost continuous data in real time. One difficulty created by these advances is that large amounts of data are generated and require analysis; a process that, without assistance, demands significant labour. The numerical tool presented in this thesis is a stepping stone towards an automated data analysis program.

This thesis begins with a review of structural health monitoring systems, including sensors, data acquisition systems, and various data analysis techniques. Based on this state of the art, the numerical tool, named MIROVY, was developed in two sections. First, the tool receives the sensor data and processes it with typical analysis techniques such as direct results analysis, simple statistical analysis, static regression analysis and dynamic regression analysis. These methods are currently employed by professionals in the structural health monitoring field to determine if any structural damage or instabilities exist. These methods can also be used to determine the effect of surrounding construction work on an existing building.

Second, the numerical tool aims at modeling the structural response in the hope of creating a damage detection system. Potentially, this will provide an alarm if a structural problem occurs.

Third, the numerical tool is tested on two case studies: Oporto Cathedral, located in Porto, Portugal; and the Monastery of Jerónimos, located in Lisbon, Portugal. These historical structures have monitoring systems in place as well as several years of record history, providing the numerical tool with test data.

Results of the case studies tests show that MIROVY is a good initial step in the direction of automated user-friendly monitoring data analysis systems. In its present state the program is beneficial to professionals in the field in its ability to analyze input data with minimum pre-processing and provide graphical and text feedback quickly and easily.

Resumo

A monitorização estrutural a longo prazo tem aumentado as suas aplicações em muitas áreas, incluindo na preservação do património histórico. Os avanços recentes dos sistemas de monitorização estruturais tornaram possível a instalação de um número significativo de sensores estruturais e ambientais, sendo possível receber e monitorizar em tempo real todos os dados. Uma dificuldade criada com esta situação prende-se com o facto de que grandes quantidades de dados necessitam de uma análise robusta, um processo em que sem a assistência de ferramentas numéricas pode requerer um esforço significativo por parte do analisador. A ferramenta numérica apresentada nesta tese pretende ser um primeiro passo para a criação de um instrumento robusto para a análise automática dos dados provenientes dos sistemas de monitorização.

Nesta tese, os sistemas de monitorização estruturais foram revistos, incluindo os sensores, os sistemas de aquisição de dados e várias técnicas de análise de dados. Com base nesta revisão, a ferramenta numérica foi desenvolvida em duas partes.

Em primeiro lugar, a ferramenta foi desenvolvida para ler os dados de sistemas de monitorização e para os processar através de técnicas correntes, tais como a análise directa de resultados, simples análises estatísticas, e análises de regressões lineares. Estes métodos são, tipicamente, os mais usados pelos profissionais da monitorização estrutural para detectar algum fenómeno não estabilizado nas estruturas, ou averiguar os efeitos do decorrer de trabalhos significativos nas mediações de uma construção importante.

Em segundo lugar, com a ferramenta numérica pretende-se modelar a resposta estrutural das construções com o objectivo de criar um sistema de detecção de dado robusto. Idealmente, esta ferramenta poderá proporcionar um sistema automático de alarmes quando qualquer problema estrutural ocorrer.

Ambas as partes da ferramenta numérica foram testadas em dois casos de estudo: na Catedral da cidade do Porto e no Mosteiro dos Jerónimos em Lisboa. Estes monumentos têm instalados sistemas de monitorização com registos de vários anos, proporcionando um teste à ferramenta com dados reais.

Para ambos os casos de estudo, os resultados obtidos demonstraram que a presente ferramenta numérica é um importante passo para monitorização automática. Na versão actual, a ferramenta é

bastante útil para os analistas. Dentro das suas potencialidades destacam-se a capacidade para importar os dados sem a necessidade de pré-processamento e a capacidade para gerar informação gráfica e numérica de uma forma rápida e fácil de ser assimilada pelos utilizadores.

Table of Contents

ACKNOWLEDGEMENTS ..... **V**

ABSTRACT ..... **VII**

RESUMO ..... **IX**

TABLE OF CONTENTS ..... **XI**

LIST OF FIGURES ..... **XIII**

LIST OF TABLES ..... **XVII**

1 INTRODUCTION **1**

2 MONITORING SYSTEMS **3**

2.1 SENSORS 3
2.1.1 Static Monitoring Sensors *4*
2.1.2 Dynamic Monitoring Sensors *11*
2.1.3 MEMS Sensors *12*
2.2 DATA ACQUISITION SYSTEMS 12
2.2.1 Data Acquisition Systems for Static Monitoring *13*
2.2.2 Data Acquisition Systems for Dynamic Monitoring *13*
2.3 WIRELESS MONITORING SYSTEMS 14
2.4 GENERAL REMARKS 15

3 MONITORING ANALYSIS **16**

3.1 DIRECT RESULTS ANALYSIS 16
3.2 SIMPLE STATISTICAL ANALYSIS 18
3.2.1 Mean and Standard Deviation *18*
3.2.2 Histogram *20*
3.2.3 Probability Density Function *21*
3.3 REGRESSION ANALYSIS WITH STATIC MODELS 23
3.3.1 Linear Regression *23*
3.3.2 Logistic Regression *25*
3.3.3 Polynomial Regression *26*
3.3.4 Logarithmic and Exponential Regression *26*
3.3.5 Normalized Regression Analysis *27*
3.4 REGRESSION ANALYSIS WITH DYNAMIC MODELS 27
3.4.1 Auto Regressive Moving Average *27*
3.4.2 Auto Regressive Models with Exogeneous Inputs *28*
3.5 COMMON REGRESSION QUALITY CRITERIA 28
3.6 ANALYSIS WITH NUMERICAL MODELS 30
3.7 UNCERTAINTY ANALYSIS 31
3.8 TYPICAL MONITORING USED WITH STRUCTURAL INTERVENTIONS 32
3.9 GENERAL REMARKS 34

4 DEVELOPMENT OF MIROVY, THE NUMERICAL TOOL **35**

4.1 ARCHITECTURAL DESCRIPTION 35
4.1.1 Model Skeleton *35*
4.1.2 Data Input *37*
4.1.3 Single Signal Option *37*
4.1.4 Time Selection *37*

4.1.5 Direct Results Analysis 38
4.1.6 Simple Statistical Analysis 39
4.1.7 Time Selection and Specific Data Filters 39
4.1.8 Regression Analysis – Static Modeling 40
4.1.9 Regression Analysis – Dynamic Modeling 40
4.2 DETAILED DESCRIPTION OF THE FEATURES 41
4.2.1 Data Input 41
4.2.2 Single Signal Option 42
4.2.3 Time Selection 43
4.2.4 Direct Results Analysis 43
4.2.5 Simple Statistical Analysis 45
4.2.6 Time Selection and Specific Data Filter 47
4.2.7 Regression Analysis – Static Modeling 48
4.2.8 Regression Analysis – Dynamic Modeling 51
4.3 GENERAL REMARKS 52

5 APPLICATIONS TO TWO CASE STUDIES 53

5.1 OPORTO CATHEDRAL 53
5.1.1 Sensors 54
5.1.2 Creation of Data Files 56
5.1.3 Direct Results Analysis 57
5.1.4 Simple Statistical Analysis 60
5.1.5 Regression Analysis 61
5.1.6 Enhanced Analysis with the Advanced Numerical Tool 62
5.1.7 General Notes on Oporto Cathedral 79
5.2 MONASTERY OF JERÓNIMOS 79
5.2.1 Sensor Locations 80
5.2.2 Creation of Data File 82
5.2.3 Direct Results Analysis 82
5.2.4 Simple Statistical Analysis 85
5.2.5 Regression Analysis 86
5.2.6 Enhanced Analysis with the Advanced Numerical Tool 87
5.2.7 General Notes on Jerónimos Monastery 96
5.3 GENERAL REMARKS 96

6 MODELING THE STRUCTURAL RESPONSE FOR ALARMS DEFINITION 97

6.1 ARCHITECTURE 97
6.2 PROCEDURES 98
6.2.1 Direct Damage Detection 99
6.2.2 ARX Damage Detection 100
6.2.3 Visual ARX Damage Detection 101
6.3 APPLICATION TO OPORTO CATHEDRAL 102
6.4 APPLICATION TO MONASTERY OF JERÓNIMOS 107
6.5 GENERAL REMARKS 109

7 CONCLUSIONS 110

7.1 CRITICAL REVIEW OF THE NUMERICAL TOOL 110
7.2 FUTURE POTENTIAL FOR NUMERICAL TOOL 111

REFERENCES 113

APPENDIX A: POST REPORT ENHANCEMENTS TO NUMERICAL TOOL 121

APPENDIX B: NUMERICAL TOOL USER MANUAL 123

List of Figures

FIGURE 1: STRUCTURAL HEALTH MONITORING SYSTEM (ISIS CANADA, 2004) 3
FIGURE 2: TYPES OF TEMPERATURE SENSORS: (A) THERMOCOUPLE; (B) ELECTRICAL RESISTANCE; AND (C) FIBRE OPTIC (MARQUES, 2007) 4
FIGURE 3: WIND SENSOR, SPEED AND DIRECTION (NOVALYNX CORPORATION, 1988) 5
FIGURE 4: COMBINATION TEMPERATURE HUMIDITY METER (LABORATORY ELECTRONICS, 2008) 6
FIGURE 5: TILT METERS (GEOMECHANICS, 2008) 6
FIGURE 6: CRACK MONITORING WITH LDVT ON PRAGUE NEW TOWN HALL (DRDACKY, 2008) 7
FIGURE 7: STRAIN GAUGE FOR THREE PRINCIPLE STRESSES (OMEGA, 2003) 8
FIGURE 8: WHEATSTONE BRIDGE (ENCKELL, 2006) 8
FIGURE 9: LOAD CELLS (IQS, 2008) 9
FIGURE 10: PRESSURE CELLS: (A) TOTAL PRESSURE CELL; (B) VW PRESSURE CELL FOR TUNNELS; (C) VW STRESS STATION (DGSI, 2008) 10
FIGURE 11: FORCE TRANSDUCER: (A) CLOSE UP VIEW; (B) INSTALLED BELOW COLUMN (CANBAY, ERSOY, & TUGRUL, 2004) 10
FIGURE 12: SAMPLE GEOPHONE (SENSHE TECH, 2007) 11
FIGURE 13: VARIOUS ACCELEROMETERS (HONEYWELL, 2004) 12
FIGURE 14: DATA ACQUISITION HARDWARE: (A) A PARALLEL PORT, AND; (B) A PLUG IN BOARD, DATA ACQUISITION SYSTEMS (OMEGA, 2007) 13
FIGURE 15: STRONG MOTION RECORDER (GEOSIG, 2008) 14
FIGURE 16: SAMPLE RAW SIGNAL 16
FIGURE 17: APPLIED MOVING AVERAGE METHOD 17
FIGURE 18: SIGNAL OF MEAN SIX AND STANDARD DEVIATION ONE 18
FIGURE 19: SAMPLE HISTOGRAM 20
FIGURE 20: PROBABILITY MASS AND DENSITY FUNCTIONS. 22
FIGURE 21: SAMPLE LOGISTIC REGRESSION CURVE 26
FIGURE 22: FEM ASSUMPTIONS (KABELLE, 2007) 30
FIGURE 23: PLOT OF UNFILTERED DATA 44
FIGURE 24: DATA BEFORE AND AFTER MOVING AVERAGE FILTER 45
FIGURE 25: SAMPLE OF HISTOGRAM AND CUMULATIVE DISTRIBUTION FUNCTION CREATED BY THE NUMERICAL TOOL 47
FIGURE 26: PLOTTED POLYNOMIAL REGRESSION ANALYSIS RELATIONS. 49
FIGURE 27: STATIC, MULTIPLE REGRESSION ANALYSIS RESULTS 50
FIGURE 28: COMPARISON OF DATA AND ARX MODEL 51
FIGURE 29: OPORTO CATHEDRAL (VIRTUAL PORUGAL, 2008) 53
FIGURE 30: LOCATION OF SENSORS IN OPORTO CATHEDRAL (RAMOS & LOURENCO, 2007) 54

FIGURE 31: OPORTO CATHEDRAL (A) CRACK METER (B) EXTENSOMETER (C) TILT METER 55

FIGURE 32: OPORTO CATHEDRAL (A) TEMPERATURE HUMIDITY SENSOR (B) WIND VELOCITY SENSOR 56

FIGURE 33: SAMPLE UNFILTERED PLOTS WITH UPPER AND LOWER BOUNDS AT THREE STANDARD DEVIATIONS 58

FIGURE 34: DATA FILTERED WITH MOVING AVERAGE FILTER COMPARED TO UNFILTERED 59

FIGURE 35: CLOSE UP ON DATA FILTERED WITH MOVING AVERAGE COMPARED TO UNFILTERED 59

FIGURE 36: HISTOGRAM SAMPLE FROM OPORTO CATHEDRAL 61

FIGURE 37: CRACK METER 2 SIGNAL, UNFILTERED WITH UPPER AND LOWER BOUNDS 63

FIGURE 38: CRACK METER 2 SIGNAL, AFTER FILTERING 64

FIGURE 39: CRACK METER 2, HISTOGRAM 64

FIGURE 40: RELATION BETWEEN CRACK METER 2 AND SURFACE TEMPERATURE 2 65

FIGURE 41: CRACK METER 2, MULTIPLE REGRESSION ANALYSIS RESULTS 66

FIGURE 42: CRACK METER 2, MULTIPLE REGRESSION RESIDUALS 67

FIGURE 43: CRACK METER 2, ARX MODEL RESULTS 68

FIGURE 44: EXTENSOMETER ABOVE, FILTERED DATA 69

FIGURE 45: EXTENSOMETER ABOVE, HISTOGRAM 69

FIGURE 46: EXTENSOMETER ABOVE, STATIC REGRESSION 70

FIGURE 47: OPORTO CATHEDRAL TILT METER DIRECTIONS (RAMOS & LOURENCO, 2007) 72

FIGURE 48: TILT METER 2, FILTERED DATA 72

FIGURE 49: TILT METER 2, HISTOGRAM 73

FIGURE 50: TILT METER 2, RELATION TO TEMPERATURE 74

FIGURE 51: TILT METER 2, NIGHT TIME RELATION TO TEMPERATURE 74

FIGURE 52: TILT METER 2, MULTIPLE REGRESSION ANALYSIS 75

FIGURE 53: RELATIVE HUMIDITY, HISTOGRAM 76

FIGURE 54: RELATIVE TEMPERATURE, FILTERED DATA 77

FIGURE 55: WIND DIRECTION AND SPEED, HISTOGRAM 78

FIGURE 56: SURFACE TEMPERATURE 1, FILTERED DATA 79

FIGURE 57: MONASTERY OF JERÓNIMOS (FREIRE, 2008) 80

FIGURE 58: SENSOR LOCATIONS IN THE MONASTERY OF JERÓNIMOS (COURTESY OF PROF. RAMOS, UNIVERSITY OF MINHO) 81

FIGURE 59: JERÓNIMOS MONASTERY, UNFILTERED DATA WITH UPPER AND LOWER BOUNDS 83

FIGURE 60: JERÓNIMOS MONASTERY, DATA FILTERED WITH MOVING AVERAGE COMPARED TO UNFILTERED DATA 84

FIGURE 61: JERÓNIMOS MONASTERY, CLOSE UP VIEW OF FILTERED AND UNFILTERED DATA 84

FIGURE 62: JERÓNIMOS MONASTERY, HISTOGRAM SAMPLE 86

FIGURE 63: JERÓNIMOS MONASTERY, CUMULATIVE DISTRIBUTION FUNCTION SAMPLE 86

FIGURE 64: JERÓNIMOS MONASTERY, TILT METER NORTH FILTERED DATA 88

FIGURE 65: JERÓNIMOS MONASTERY, TILT METER SOUTH FILTERED DATA 88
FIGURE 66: JERÓNIMOS MONASTERY, TILT METER NORTH HISTOGRAM 89
FIGURE 67: JERÓNIMOS MONASTERY, TILT METER SOUTH HISTOGRAM 89
FIGURE 68: JERÓNIMOS MONASTERY, TILT METER NORTH STATIC REGRESSION 90
FIGURE 69: JERÓNIMOS MONASTERY, TILT METER SOUTH STATIC REGRESSION....91
FIGURE 70: JERÓNIMOS MONASTERY, ARX MODEL OF NORTH TILT METER....92
FIGURE 71: JERÓNIMOS MONASTERY, ARX MODEL OF SOUTH TILT METER 93
FIGURE 72: JERÓNIMOS MONASTERY TEMPERATURE SENSOR 94
FIGURE 73: JERÓNIMOS MONASTERY, HUMIDITY DATA 95
FIGURE 74: JERÓNIMOS MONASTERY, WIND DATA 95
FIGURE 75: VISUAL ARX DAMAGE DETECTION, FIRST PLOT 102
FIGURE 76: VISUAL ARX DAMAGE DETECTION, SECOND PLOT 102
FIGURE 77: OPORTO CATHEDRAL, CRACK METER 2, VISUAL ARX DAMAGE DETECTION 105
FIGURE 78: OPORTO CATHEDRAL, TILT METER 1 A, VISUAL ARX PLOT 1....106
FIGURE 79: OPORTO CATHEDRAL, TILT METER 1 A, VISUAL ARX PLOT 2....106
FIGURE 80: JERÓNIMOS MONASTERY, SOUTH TILT METER VISUAL ARX DAMAGE DETECTION 108
FIGURE 81: JERÓNIMOS MONASTERY, SOUTH TILT METER, VISUAL ARX, SHORT HISTORY 108

List of Tables

TABLE 1: THREE STAGE MONITORING SYSTEM 33
TABLE 2: RANKIN DAMAGE CATEGORIES (RANKIN, 1988) 33
TABLE 3: OPERATING PROCESS OF MIROVY 36
TABLE 4: ARCHITECTURAL OUTLINE OF DATA INPUT SUB-PROGRAM 37
TABLE 5: ARCHITECTURAL OUTLINE OF THE DIRECT RESULTS ANALYSIS 38
TABLE 6: ARCHITECTURAL OUTLINE OF THE SIMPLE STATISTICAL ANALYSIS 39
TABLE 7: ARCHITECTURAL OUTLINE OF STATIC REGRESSION ANALYSIS SUB-PROGRAM 40
TABLE 8: ARCHITECTURAL OUTLINE OF DYNAMIC REGRESSION ANALYSIS 41
TABLE 9: OPORTO SENSOR TYPE AND ID 55
TABLE 10: MAXIMUM AND MINIMUM SIGNAL VALUES BEFORE AND AFTER OUTLIER REMOVAL 57
TABLE 11: SIMPLE STATISTICAL ANALYSIS BY SIGNAL 60
TABLE 12: MATRIX OF THE OPORTO CATHEDRAL COEFFICIENTS OF DETERMINATION 62
TABLE 13: CRACK METER 2, SINGLE REGRESSION ERROR INDICATORS 65
TABLE 14: CRACK METER 2, MULTIPLE REGRESSION ERROR INDICATORS 66
TABLE 15: CRACK METER 2, ARX REGRESSION ERROR INDICATORS 68
TABLE 16: EXTENSOMETER ABOVE, STATIC REGRESSION ERROR SUMMARY 70
TABLE 17: TILT METER 2, COMPARED QUALITY CRITERIA 75
TABLE 18: MONASTERY OF JERÓNIMOS SENSOR TYPES 81
TABLE 19: JERÓNIMOS MONASTERY, SENSOR NAME CONVERSION CHART 81
TABLE 20: JERÓNIMOS MONASTERY: MAXIMUM AND MINIMUM SIGNAL VALUES BEFORE AND AFTER OUTLIER REMOVAL 83
TABLE 21: JERÓNIMOS MONASTERY, SIMPLE STATISTICAL ANALYSIS BY SIGNAL 85
TABLE 22: JERÓNIMOS MONASTERY, COEFFICIENTS OF DETERMINATION 87
TABLE 23: JERÓNIMOS MONASTERY, STATIC REGRESSION 91
TABLE 24: JERÓNIMOS MONASTERY, ARX MODEL 93
TABLE 25: ARCHITECTURAL OUTLINE OF DAMAGE DETECTION PROGRAM 98
TABLE 26: BASE AND TEST DATA LENGTHS 99
TABLE 27: INPUT VARIABLES FOR DAMAGE DETECTION OF OPORTO CATHEDRAL 103
TABLE 28: RESULTING ALARMS FROM DAMAGE DETECTION ANALYSIS OF OPORTO CATHEDRAL 103
TABLE 29: JERÓNIMOS MONASTERY, DAMAGE DETECTION INPUT VALUES 107
TABLE 30: JERÓNIMOS MONASTERY, DAMAGE DETECTION ALARMS 107
TABLE 31: JERÓNIMOS MONASTERY, VISUAL ARX, ERROR IN ARX MODEL 109

Erasmus Mundus Programme:	ADVANCED MASTERS IN STRUCTURAL ANALYSIS OF MONUMENTS AND HISTORICAL CONSTRUCTIONS
Consortium Institutions:	UNIVERSITY OF MINHO, PORTUGAL
	CZECH TECHNICAL UNIVERSITY IN PRAGUE, CZECH REPUBLIC
	UNIVERSITY OF PADOVA, ITALY
	TECHNICAL UNIVERSITY OF CATALONIA, SPAIN
Satellite Participant:	INSTITUTE OF THEORETICAL AND APPLIED MECHANICS, CZECH REPUBLIC

1 INTRODUCTION

Advancements in the field of structural health monitoring have enabled easy installation of complex structural monitoring systems, capable of providing users with an abundance of sensor feedback. Currently the labour requirements to process this large amount of information can outweigh the benefits of using state of the art structural health monitoring systems, and in extreme cases can cause the user to miss important information. MIROVY, the advanced numerical tool (also referred to as numerical tool or program) presented in this thesis, is designed to assist in the analysis of structural monitoring systems, specifically for monitoring historical structures.

Environmental sensors that record data on environmental conditions, and structural sensors that record data on static and dynamic structural movements, provide the foundation of structural health monitoring. A complete monitoring system requires knowledge of both the environmental input and the structural response. These systems provide a constant flow of data to the data acquisition systems. The data acquisition system collects this data for the user to analyze.

Data from the data acquisition system is processed by a variety of methods. An investigation into structural stability can include filtering the data, undertaking direct data analysis, running statistical analyse, and painstaking regression analysis of the data. This data processing is laborious.

MIROVY is designed to receive data from data acquisition systems with a minimum amount of pre-processing, and assist the user in their structural analysis. The program architecture approaches the data analysis in a step by step approach. The numerical tool can provide the direct data analysis for the user to review, along with built in noise filters. Further steps include basic statistical analysis and regression analysis. MIROVY is capable of running static regression analysis, single or multiple, as well as conducting dynamic regression analysis using an auto regressive model with exogenous inputs (ARX model).

Two case studies, Oporto Cathedral and the Monastery of Jerónimos, are historical structures used to test MIROVY. The advanced numerical tool provides all the basic information on the sensors being analyzed, including conducting the regression analysis and providing feedback on the accuracy of the models.

Many structural monitoring systems are installed with the objective of detecting structural damage, and estimating the severity of damage. This can be done through careful analysis of the sensor data;

through modeling the structure and creating alarm definitions; or both. The numerical tool also provides a final section for damage detection. Using both simple modeling and advanced ARX models the numerical tool provides feedback to assist the user in determining structural damage or instability.

Again the two case studies are used to test the numerical tool. MIROVY is able to run several analyses of the data, thus providing feedback and reducing the labour requirements. In this version of the advanced numerical tool final alarms should be defined with professional review of the structural analysis.

2 MONITORING SYSTEMS

Structural health monitoring systems are typically composed of sensors, on-site data acquisition systems, communication systems, data processing, and data storage, as shown in Figure 1. Properly stored data should be available for future analysis from outside parties (ISIS Canada, 2004). The monitoring part of the system is composed of the sensors and the on-site data acquisition system.

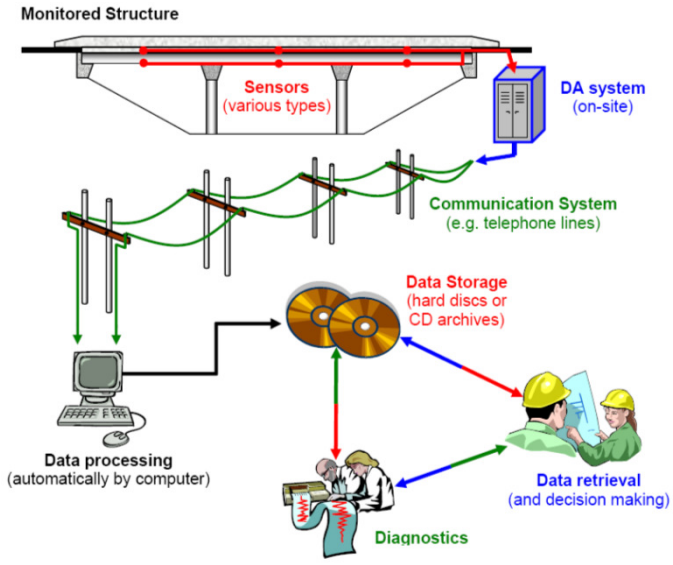

Figure 1: Structural Health Monitoring System (ISIS Canada, 2004)

2.1 Sensors

The sensors used to collect the data are the basis of any structural health monitoring system. Different sensors can be selected for various types of data collection, enabling the end user to collect data on temperature, wind, movement, deformations, displacements, stress and strain, plus other structural and environmental quantities. Structural monitoring can be broken down into two groups, static monitoring, and dynamic monitoring. Static monitoring is made up of systems that require less frequent data collection, for example one sample every hour. These sensors focus on the static issues of a structure such as crack development and tilt. Dynamic monitoring includes systems requiring tens to thousands of samples per second (Ramos & Lourenço, 2005) and focus on finding dynamic properties of a structure such as modal properties and natural frequencies. Placement and selection of sensors are very important. Poorly placed sensors may not receive as strong a signal as the structure is

actually experiencing. Selection of sensors with inapproapreate range or resolution could result in the sensor failing to report the changing conditions.

Within the scope of this thesis, only long-term, fully automated sensors are considered.

2.1.1 Static Monitoring Sensors

Static monitoring focuses on the static behaviour of a structures as well as conditions that change over a time period of hours at most. If static testing were conducted, the test would be short term with the use of fully defined loads (Enckell, 2006). Static monitoring can include, but is not limited to, static testing. Often static monitoring can be conducted over a period of several years with undefined loads (see case studies in section 5). Selection of sensors based on a range and resolution that match use and requirements is important. The following subsections present a group of static sensors.

2.1.1.1 Temperature Sensors

Temperature records in structural health monitoring are considered static. The temperature will change over the course of a day, and with one data point an hour it is possible to get a representative curve. In temperate climates a temperature sensor which records from minus twenty degrees to positive one hundred degrees Centigrade is sufficient when being used on an existing structure (Ramos & Lourenço, 2005). There are, however, many different types of temperature sensors available to choose from, including fibre optic, infrared, electrical resistance, thermocouple and combined sensors. Examples of temperature sensors are shown in Figure 2.

(a) (b) (c)

Figure 2: Types of temperature sensors: (a) thermocouple; (b) electrical resistance; and (c) fibre optic (Marques, 2007)

The use of temperature sensors in the analysis of existing structures is important because it assists in determining possible causes of damage through correlation between temperature changes and structural movements (Marques, 2007). Since temperature can also vary between different parts of the structure, thereby causing damage, several location should be selected for analysis. Typically, combined sensors are used to measure relative air humidity and air temperature. However, surface

temperature sensors are most recommended as the surface temperature is more directly related to static changes (Ramos L. F., 2007).

2.1.1.2 Wind Sensors

Wind sensors are required to identify potential correlations between wind velocity and structural movement. The direction and velocity of the wind are measured by sensors placed outside the structure. Most wind sensors are referred to as anemometers. An anemometer should be selected based on required operating temperature, moisture, and potential wind velocity for the site under consideration. The desired resolution should also be considered when making this selection (ISIS Canada, 2004). Figure 3 shows a simple, accurate, and versatile wind sensor.

Figure 3: Wind Sensor, speed and direction (NovaLynx Corporation, 1988)

2.1.1.3 Moisture Meters

High moisture levels can lead to serious structural problems if not monitored. The increased potential of biological damage to the structure, especially to timber members, cannot be overlooked; nor can potential hygienic problems (Sandrolini & Franzoni, 2006). Capillary rise, condensation, rain, pipe leaks, and flood are major sources of moisture, while testing for moisture content in masonry walls may also cause minor moisture problems. In the case of long term monitoring of in-wall moisture contents, the most consistent system is based on using material plugs which can be taken to the laboratory for testing, then placed back in location (Sandrolini & Franzoni, 2006).

However, for continuous monitoring systems the previous solution is not adequate. A simplified moisture monitor is the most common method for monitoring the moisture in the air throughout the structure. While it is possible to install individual moisture meters at many points, it is normally

sufficient to use a combined sensor for the purposes of structural health monitoring. A combined sensor will provide temperature and relative humidity (Ramos L. F., 2007). A sample sensor is shown in Figure 4. If accurate measurements of humidity are required in several locations three basic types of humidity sensors are available; capacitor based sensors, resistor based sensors, and thermo-conducting sensors (Marques, 2007). Such special circumstances apply to art galleries and archives.

Figure 4: Combination temperature humidity meter (Laboratory Electronics, 2008)

2.1.1.4 Tilt Meters

Tilt meters are designed to monitor inclinations and rotations, typically using various sensors in combinations with a bubble level or levels (Marques, 2007). Systems can be uniaxial or biaxial; some containing temperature probes and all are commercially available in many different models (Geomechanics, 2008). Figure 5 shows a digital biaxial all weather tilt meter, and an analog uniaxial moisture resistant tilt meter.

Figure 5: Tilt Meters (Geomechanics, 2008)

2.1.1.5 Crack Meters

In structural health monitoring crack meters are most commonly used when monitoring masonry structures, since cracking in masonry is common, but does not always indicate failure of the material. However, these masonry cracks should be monitored to determine if they are active or dormant. There are three basic types of crack meters in use: transducer based meters, electrical resistance based meters, and mechanical crack meters. Of these, the Linear Variable Differential Transformer, or LVDT, is the most commonly used (Marques, 2007). A LVDT sensor can operate as either an inductive transducer or electrical resistance based sensor. Crack meters are often used to ensure that existing structures are not damaged by nearby construction work, as shown in Figure 6. Several crack meters are also used when carrying out destructive tests such as single and double flat-jack tests (Binda & Tiraboschi, 1999).

Figure 6: Crack monitoring with LDVT on Prague New Town Hall (Drdacky, 2008)

2.1.1.6 Strain Gauges

A wire with a given current passing through it will have a resulting resistance, based on the length, cross sectional area, material, and density. A strain gauge functions using this principle. Thin wires are attached to the surface, and any elongation of the surface results in an elongation of the wires, which can be measured accurately by the change in resistance of the wires. Changes in temperature

can also have an effect and should be taken into account (Window, 1992). Typical designs of strain gauges are to measure strain in one direction, two perpendicular directions, or in the directions of the three principal stresses, shown in Figure 7. All of these types of gauges have become readily available and affordable (Enckell, 2006). The resulting data can be combined with the modulus of elasticity to give the stress in a material.

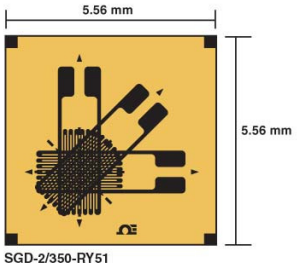

Figure 7: Strain gauge for three principle stresses (OMEGA, 2003)

For certain applications the strain gauges are used in combination with a Wheatstone bridge to improve accuracy. The Wheatstone bridge is an electrical assembly of four resistors, one of unknown resistance, one of known and adjustable resistance, and two of known resistance, as shown in Figure 8.

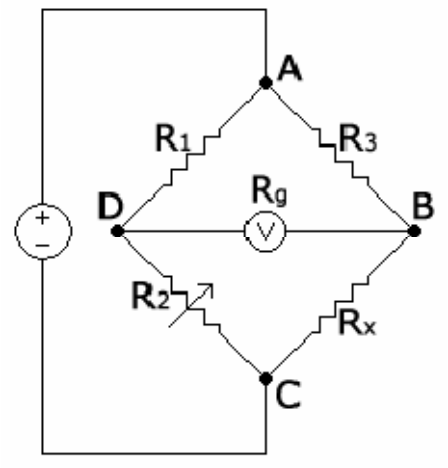

Figure 8: Wheatstone bridge (Enckell, 2006)

Rx is the unknown resistor, and R2 is the know resistor with adjustable resistance. A voltage meter is placed in-between the two sides of the assembly as a bridge. The principle is based on the idea that zero voltage can be very accurately measured. To find Rx, R2 is adjusted until the voltage across the bridge is equal to zero. Using the knowledge of R1 and R3 it is then possible to accurately determine

Rx. This method gives more accurate results over larger areas than the much smaller single strain gauge is capable (Window, 1992). The strain gauges are used in this design as the Rx resistor

2.1.1.7 Load Cells

Load cells convert load or pressure into an electric signal. The most common type of load cell, and discussed in section 2.1.1.6, is the strain gauge. Other common types of load cells include the hydraulic load cell, useful in outdoor environments that have transient voltage risks, and piezo-electric load cells, which are well suited to measuring dynamic forces (Society of Robots, 2008). Potential applications of load cells in structural engineering include: use on wind or radio towers to monitor stresses; monitoring suspension bridge cables; and monitoring of tie rods (FUTEK, 2008). Modern research in the area of load cells includes work on compact six-component load cells for determining strain distribution on plates (Joo, Na, & Kang, 2002).

Figure 9: Load cells (IQS, 2008)

2.1.1.8 Pressure Cells

Pressure cells are used to measure effective stress and pore-water pressure. Typically these sensors are used for geotechnical applications, monitoring soil pressures. The four main kinds of pressure cells are the total pressure cell, the jackout pressure cell, the VW pressure cell for tunnels, and the VW stress station pressure cells. The total pressure cell, shown in Figure 10 (a), is for determining total pressure on a structure, and is capable of determining magnitude, distribution and orientation of the stress. A jackout pressure cell is for soft soils, and uses a hydraulic jack to keep the sensor in contact with the soil. The VW pressure cell, shown in Figure 10 (b), is designed specifically for the outer liner of a tunnel. The VW stress station, shown in Figure 10 (c), is designed for use in boreholes and breaks a monitor's stress into its three principle axes (DGSI, 2008).

(a) (b) (c)

Figure 10: Pressure cells: (a) Total Pressure Cell; (b) VW Pressure Cell for Tunnels; (c) VW Stress Station (DGSI, 2008)

2.1.1.9 Force Transducers

Force transducers are used to measure axial force, shear force, and bending moment without affecting the behaviour of the structure. They are typically installed at the bottom of columns, or at either end of ties. Many force transducers are actually composed of a series of load cells organized in a way to give more effective results (Canbay, Ersoy, & Tugrul, 2004). Force transducers are often created much larger than other sensors, as shown in Figure 11.

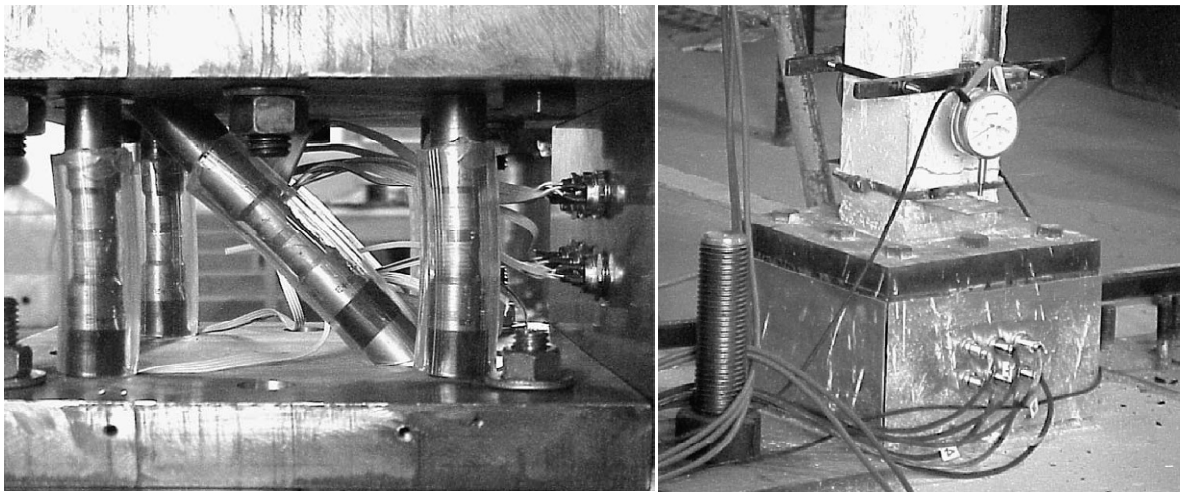

Figure 11: Force Transducer: (a) close up view; (b) installed below column (Canbay, Ersoy, & Tugrul, 2004)

2.1.1.10 Other Static Sensors

Other sensors that could be used in static monitoring include pressure meters, topographical survey system, optical survey system, and hydrological systems (SISGEO, 1993). These systems are less commonly used in structural health monitoring, but should be considered for special cases.

2.1.2 Dynamic Monitoring Sensors

Dynamic monitoring is used to find the structures damping frequencies, as well as modal shapes and natural frequencies. Testing can be done by forced vibration, where the user imparts a known vibration to the structure, or by ambient vibration, where the surrounding naturally occurring vibrations are used to create input (Enckell, 2006). It is also possible to detect damage based on changes in dynamic properties such as changes in natural frequencies (Salawu, 1997).

2.1.2.1 Geophones

A geophone is a sensor designed to observe the velocity of a point, seen in Figure 12. The ground motion is converted into voltage, using either a magnetic spring set up, or newer micro electro mechanical systems (MEMS) technology (Enckell, 2006). These sensors are not used as often as the accelerometers for structural health monitoring.

Figure 12: Sample geophone (SENSHE TECH, 2007)

2.1.2.2 Accelerometers

Accelerometers are the most used sensors in dynamic structural health monitoring. They come in a wide range of sizes and capabilities (see Figure 13), each designed to meet different requirements. There are five basic kinds of accelerometers:

1. piezoelectric,
2. piezoresistive,
3. modern micro electro mechanical (MEMS),
4. capacitive, and
5. force balanced.

The accelerometers convert the structural movement into electronic signals, which can be recorded and manipulated to give displacement, velocity, modal shapes, and modal frequencies (Enckell, 2006).

Figure 13: Various accelerometers (Honeywell, 2004)

2.1.3 MEMS Sensors

Micro electromechanical systems, or MEMS sensors as they are commonly referred to, are very small sensors which work with a combination of electrical and mechanical parts. These sensors can be as small as several micrometers or as large as several millimetres, and are created with precise machining (Enckell, 2006). MEMS sensors can be created to work as accelerometers, humidity sensor, temperature sensors, or pressure sensors. While this technology is in its initial stages of development, it is expected to see large scale use in structural health monitoring (EMPA, et al., 2004). The MEMS sensors are increasingly being used in conjunction with wireless monitoring systems, with significant tests being conducted in this area in by Jerome Lynch (Lynch J. P., 2005); (Lynch J. P., 2007); (Lynch, Y., Swartz, Lu, & Loh, 2008); and (Pei, Kapoor, Graves-Abe, Sugeng, & Lynch, 2008).

2.2 Data Acquisition Systems

Data acquisition systems receive the raw data from the sensors and convert it into a more user friendly format. Depending on the sensors in use, some data acquisition systems are required to send a signal to the sensor as well as receiving the feedback (ISIS Canada, 2004). Some data acquisition systems will condition the signal to reduce possible error. This conditioning can include, but is not limited to, increasing resolution, decreasing noise, filtering out unwanted signals, and preparing signals for the computer (Ramos L. F., 2007). Depending on the monitoring being undertaken it may be possible to use one type of data acquisition system for the entire structural health monitoring system, but due to the different data gathered for the static monitoring system and the dynamic monitoring system it is not uncommon for the data acquisition systems to be separate (Hubin, 2002).

2.2.1 Data Acquisition Systems for Static Monitoring

There are four basic types of data acquisition systems that could be used in conjunction with static monitoring. A serial communication data acquisition system is the typical choice for structural health monitoring. It is capable of collecting processing and storing data if no computer is present. USB data acquisition systems work as one step from the sensor to the computer, converting the data but not storing. A data acquisition plug in board is similar to the USB system, only the board is hardware installed into the computer. The parallel port data acquisition system also requires a connection to a computer, but is able to process much higher rate files than the USB or plug in board (OMEGA, 2007). Many serial communication systems are also able to provide remote downloading by phone line, enabling users to gather data continuously without the need to visit the site (Ramos L. F., 2007).

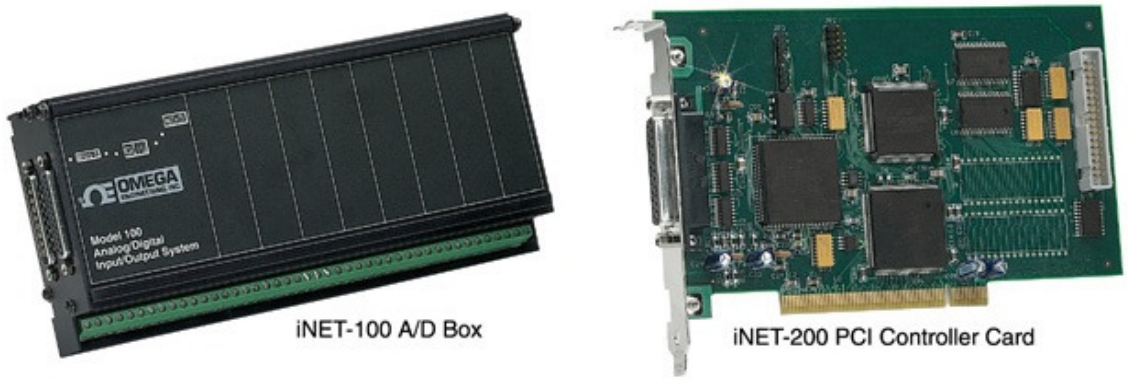

(a) (b)

Figure 14: Data acquisition hardware: (a) a parallel port, and; (b) a plug in board, data acquisition systems (OMEGA, 2007)

2.2.2 Data Acquisition Systems for Dynamic Monitoring

When collecting data from the dynamic monitoring systems requirements for the data acquisition system can differ from requirements for the static system. In the dynamic system it is possible to have several thousand samples being collected per second, creating an extremely large amount of information. Typically it is best to collect data only over the most beneficial time periods, when the greatest number of frequencies are covered. Data collection should include periodic ambient vibration checks to detect changes in the natural frequencies of the structure (Ramos L. F., 2007).

While it is possible to use the same data acquisition systems for dynamic monitoring as for static monitoring, the strong motion recorder is most often preferred. Strong motion recorders, example shown in Figure 15, were originally designed for recording seismic events. The recorders are capable of collecting data at high frequencies, and can record only after a trigger event initiates the recording, concluding when the signal drops below a predetermined amplitude (GEOSIG, 2008). This system is well suited to seismic events since significant events do not occur often. When they do occur, it is preferable to have more data available for analysis. Strong motion recorders are also well suited for dynamic monitoring of structures because they require little maintenance and are capable of giving the most valuable feedback.

Figure 15: Strong Motion Recorder (GEOSIG, 2008)

2.3 Wireless Monitoring Systems

Wireless monitoring systems is a fast gowning and much anticipated area in structural monitoring. These systems are composed of standard sensors and data acquisition systems, connected wirelessly instead of by cables. Some sensors and data acquisition systems have the wireless ports built in, but otherwise the system functions as a typical wired structural health monitoring system. Advances in wireless sensors should help to reduce costs of structural health monitoring systems through reduction of wire installation costs. In 2002 costs for wire installation in new structures was estimated at $2.20 per meter, while it cost $7.19 per meter in existing structures (Jang, Healy, & Skibniewski, 2008). This translates into an average of forty five to seventy five percent of the cost for a structural monitoring system being put towards wire installations (Jang, Healy, & Skibniewski, 2008). Wireless sensors reduce this cost significantly. There are still several obstacles for the wireless systems to overcome, including nodal determination and power supply, but the field is promising. With regards to use in historical structures, there is the additional problem of signal strength since many masonry structures have very thick walls which can impair signal transmission.

2.4 General Remarks

Most historical structure monitoring is done on masonry structures. Moisture, temperature, crack and tilt meters are the most commonly used sensors. These systems are different from structural health monitoring systems used on bridges due to fewer sensors and less cable requirements. Historical structures also undergo more movement than modern structures, requiring sensors that have a larger range than would be suggested for structural health monitoring of modern structures. Nonetheless the use of data acquisition systems in historical structures is not significantly different from the data acquisition systems used in modern structures.

3 MONITORING ANALYSIS

Data analysis is one of the main steps in structural monitoring. Much of the data received can be difficult to interpret for use in engineering calculations. Fortunately, there are many methods available to reduce the noise of a signal and ease interpretation.

3.1 Direct Results Analysis

Direct results analysis refers to analyzing data without a statistical approach. Reviewing raw signals poses great difficulty due to the noise of the signal. The noise creates an output that is unclear. Without using more advanced statistical analysis methods, there are more direct methods to signal noise reduction. Figure 16 shows a sample of raw data signal with noise. In some cases the raw signal contains values that are significant further from the mean than is normal. These values may be considered outlyers, points that are assumed to be erroneous, and are removed from the data.

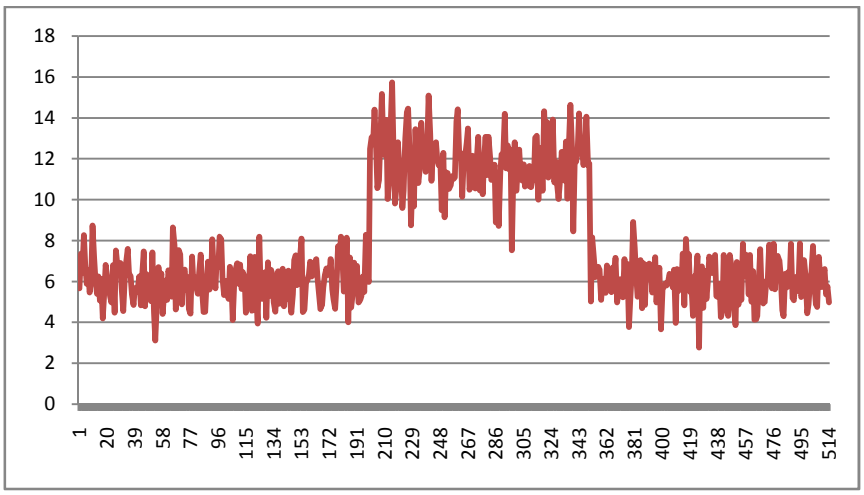

Figure 16: Sample raw signal

The simplest process used to reduce signal noise in direct results analysis is the moving average method. This method works by taking the average of several points at each location to smooth the signal. The equation for moving average is shown below, where $x[\,]$ is noisy signal, $y[\,]$ is the cleaned signal, and M is the number of points in the moving average. The moving average equation, (1), demonstrates the simplicity of the process (Smith, 2003). The number of points in the moving average is also referred to as the moving average window size.

$$y[i] = \frac{1}{M}\sum_{j=0}^{M-1} x[i+j] \qquad (1)$$

Some data points at the end of the signal can be lost using the simplest form of the moving average method, while the output function may be moved slightly to the left of the actual. This leftward movement of the signal can be avoided by using an initial value $x\left[i - \frac{M-1}{2} + j\right]$ instead of $x[i+j]$. It is best to select M as an odd number in order to create symmetrical averaging when using $x\left[i - \frac{M-1}{2} + j\right]$ (Smith, 2003). Two analyses of the raw signal shown in Figure 16 using a basic moving average method with five average points and thirty one average points is shown in Figure 17. These figures also show the unusable data at the end of the signal. While the moving average is well suited to many signal types, it is poorly suited to signals in the frequency domain. There are some noise filters based on the moving average filter that better process these signals better, such as multiple pass moving average filters (Smith, 2003).

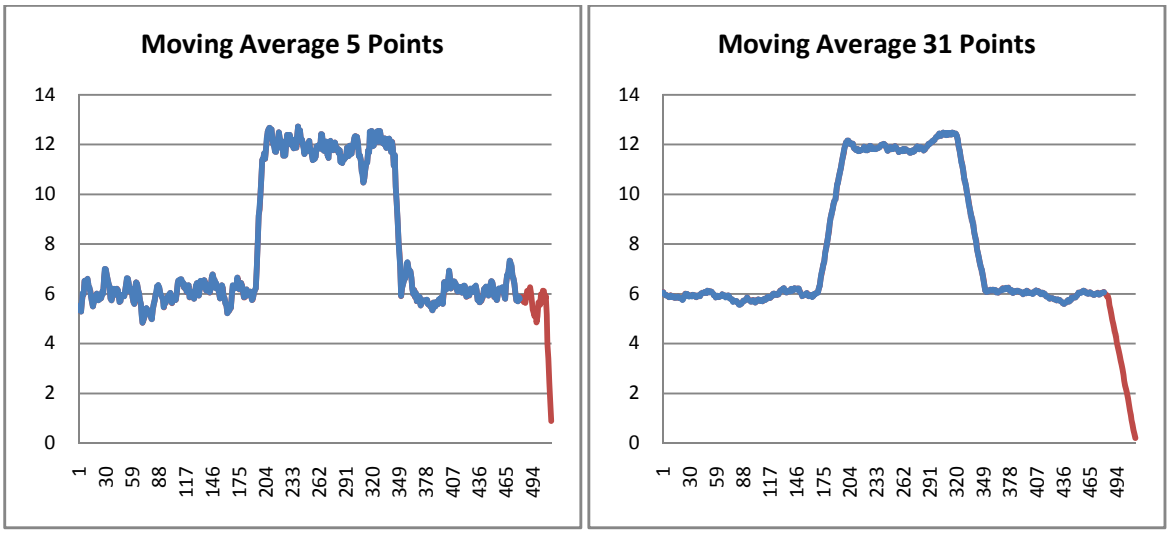

Figure 17: Applied Moving Average Method

In the case that more than one signal must be separated, functions like the windowed-sinc filter can be used (Smith, 2003). This method is costly in terms of computer processing time, but produces dependable results using the Fourier transform (Smith, 2003).

3.2 Simple Statistical Analysis

Basic statistical analysis is best used to determine probability of event occurrence. One signal can be decomposed such that the probability for certain events in that signal can be easily and accurately obtained. This data can be combined with other data to determine probability of several different events occurring simultaneously. It is also possible to analyze sections of the signal to determine the most likely events, and plot the signal with these separate sections.

3.2.1 Mean and Standard Deviation

To explain statistical analysis it helps to know some of the basics of statistics and how they apply to the digital signals. The digital signal supplies data over time that can vary between an upper and lower bound. Typically this signal is a voltage that can vary between certain values, as defined by the sensor, and recoded by the data acquisition system (Smith, 2003). When all of this data is reviewed it will have an average value, referred to in statistics as the mean value, and represented by μ. The retrieved data can be very similar to the mean or more widely dispersed, creating what is referred to as the standard deviation, which is represented by σ (Soong, 2004). The line shown in Figure 18 has a mean value of six, and a standard deviation of one.

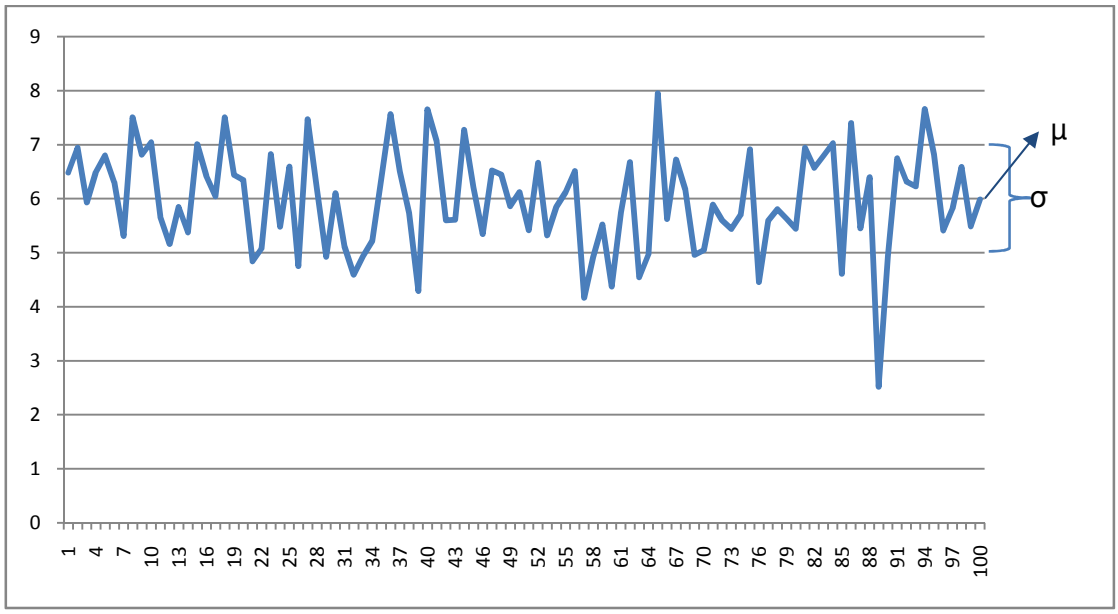

Figure 18: Signal of mean six and standard deviation one

The mean and standard deviation can be easily represented mathematically, as shown in equations (2) and (3). *N* represents the number of data points being taken into consideration, while x_i is the value

of the data point i. Equation output μ is the mean value, and σ is the standard deviation, σ^2 is called the variance. The standard deviation is the square root of the variance. In order to reduce error in samples containing few data points, the square of the standard deviation is calculated using one over N minus one, instead of simply one over N. In samples containing a large number of data points the minus one becomes insignificant (Smith, 2003).

$$\mu = \frac{1}{N}\sum_{i=0}^{N-1} x_i \qquad (2)$$

$$\sigma^2 = \frac{1}{N-1}\sum_{i=0}^{N=1} (x_i - \mu)^2 \qquad (3)$$

Using this information, signals can be simplified and compared. More complex signals can be broken down into smaller sections to allow for changes in feedback.

In cases of continuously incoming data, running statistics can be used. Running statistics refers to statistics that continuously recalculate the mean and standard deviation as new data arrives. If the recalculations are done in the initial form this method can become inefficient due to power and memory demands on the computer. However, simplified methods and equations have been created to deal with the data more easily (Smith, 2003).

With the mean and standard deviation it is also possible to calculate the signal to noise ratio and the coefficient of variation (CV), both being similar concepts.

$$Signal\ to\ Noise\ Ratio = \frac{mean}{standard\ deviation} = \frac{\mu}{\sigma} \qquad (4)$$

$$CV = \frac{standard\ deviation}{mean} \times 100 = \frac{\sigma}{\mu} \times 100 \qquad (5)$$

With more accurate results, the signal to noise ratio is higher and the coefficient of variation is lower. These relations are often used in comparing results.

Processes that have means which change over time are called non-stationary. A non-stationary signal will have a high coefficient of variation if treated in the simplified manner shown above. These

signals should instead be broken up into sections and have the mean and standard deviations calculated for each section, which should reduce the coefficient of variation. If the coefficient of variation remains high in any of the sections, the size of the section could be further reduced. For computer analysis a predefined section size is chosen, and the non-stationary signal is converted into a stepped function. If required the stepped function can be further manipulated to give a smoother curved function. Selection of the proper size of the sections is important, as sections that are too short will result in noisy results, and sections that are too long will give inaccurate results.

The statistical analysis can be taken further, and the data can be used to provide information on probability of event occurrence. To accomplish this with discrete data the most direct way is to create a histogram and probability mass function. If dealing with a continuous signal a probability density function is created.

3.2.2 Histogram

A histogram is typically shown as a bar graph with the resultant value along the x axis, and the number of occurrences along the y axis. The histogram typically takes on a bell shape, shown in Figure 19, and the results should become smoother as more data is collected. Data is shown as the number of samples that fall into each category (Lancaster, 1974).

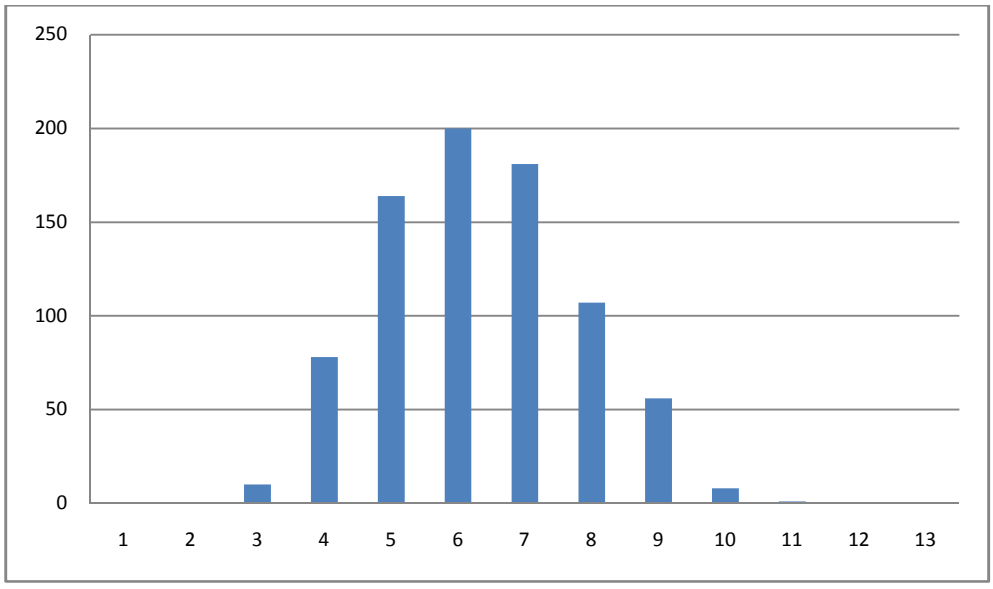

Figure 19: Sample histogram

The total of each bar in the histogram gives the total number of samples. Once the histogram is created, which is done using a sorting program, the histogram can give the mean and standard deviation of the signal. The mean is calculated by multiplying the number of samples in a range (H_i), by the signal it represents (i), doing a summation of all the ranges (0 to *M-1*), and dividing it by the total number of signals (N), as shown in equation (6). Standard deviation is calculated in a similar manner; first finding the variance and then determining the standard deviation, as shown in equation (7) (Smith, 2003). In the following equations, N represents the total number of points in the signal, M is the number of divisions in the histogram, and H_i is the number of points represented in the i^{th} division of the histogram.

$$\mu = \frac{1}{N}\sum_{i=0}^{M-1} i\,H_i \qquad (6)$$

$$\sigma^2 = \frac{1}{N-1}\sum_{i=0}^{M-1} (i-\mu)^2 H_i \qquad (7)$$

The histogram can also be used to form a probability mass function. The probability mass function is a function representing the shape of the histogram, with the y-axis representing the probability of each value occurring at any given point of time. Therefore, the sum of all the data points in the probability mass function should be equal to one (Smith, 2003).

3.2.3 Probability Density Function

In the case of continuous signals it is best to use a probability density function, also referred to as a probability distribution function. The probability density function is similar to the probability mass function, as it creates a bell shaped curve loosely representing probability of event occurrence; a visual comparison of the two functions is shown in Figure 20. Note the defined points versus the smooth line. Both of these visual samples have a mean of four and a standard deviation of one. A common problem with continuous signals is that the number of possible results is far greater than the number of samples. This problem can be solved through collecting data over an arbitrary range to give realistic results, a process called binning. Bin size should be chosen carefully to optimize results (Smith, 2003).

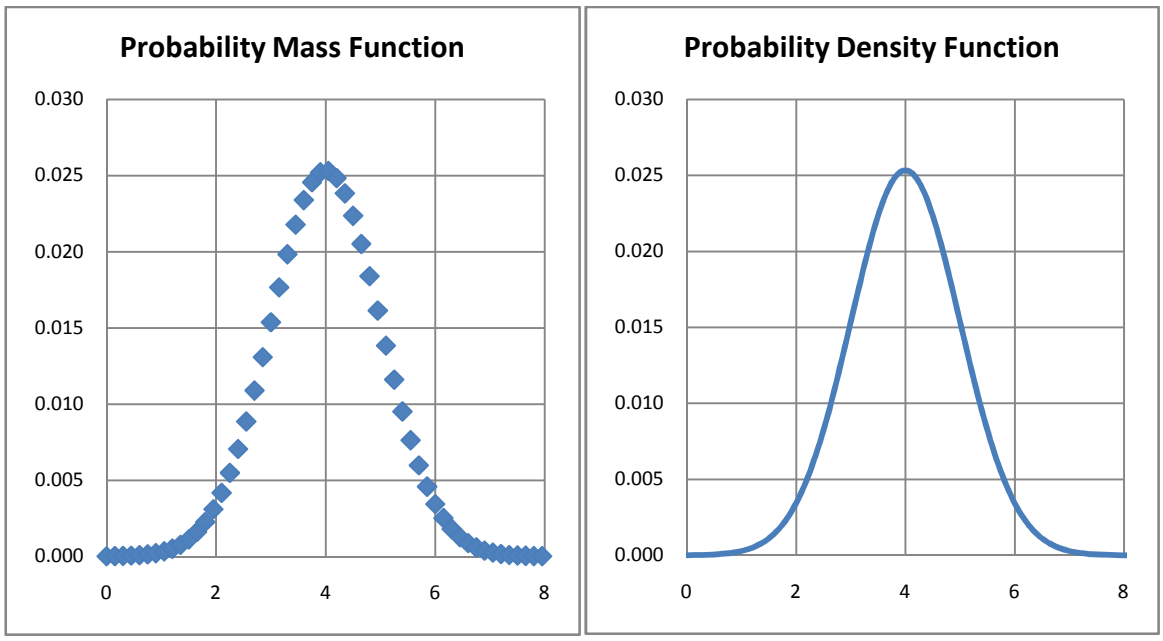

Figure 20: Probability Mass and Density Functions.

In most cases the bell shaped curve can be said to have a normal distribution, also termed a Gauss distribution, or as being Gaussian. The equation for a normal distribution can be written in terms of mean and standard deviation, where $P(x)$ is the resulting function (Smith, 2003).

$$P(x) = \frac{1}{\sqrt{2\pi}} \times \frac{1}{\sigma} \times e^{-(x-\mu)^2/2\sigma^2} \qquad (8)$$

To find the probability of a range of continuous data the integral of the probability density function is used to create the cumulative distribution function, represented by $\phi(x)$. The probability calculation is based on the fact that $\phi(2)$ is equal to the probability of the signal being between negative infinity and two. Therefore, to find the probability of the signal being between two and three, $\phi(3)$ minus $\phi(2)$ must be calculated. This should give results with sixty eight percent probability of the signal occurring within one standard deviation of the mean (Smith, 2003).

In statistical analysis the results may also be discussed in terms of accuracy and precision. Accuracy refers to how close the results are to the actual value, or how close the mean is to the actual value, and precision refers to how great is the standard deviation of the sample (Soong, 2004). In this way the testing can be analysed. Poor accuracy is an indicator of systematic errors while poor precision is an indicator of experimental errors (Smith, 2003).

Statistical analyses are also commonly used when testing materials (Wu & Knott, 2004). The ability of a statistical analysis to give clear results regarding mean, deviation from mean, and probability of occurrence, can be useful in almost any field.

3.3 Regression Analysis with Static Models

Regression analysis with static models finds the relation between two or more variables, for example environmental parameters and static movements. The ambient temperature is plotted against crack measurements, using time to correlate the two signals. This allows the user to see not only the range of motion, but also the effect of temperature on this motion. The resulting data will be a visual cloud of points roughly demonstrating the relationship. Using the regression analysis a formula relating the two variables can be created. The engineer must decide if the formula properly represents the data, or if the error, or residual, on the various points is excessively high.

Several types of regression analysis have the potential to be used with static models. These include linear regression models, polynomial regression models, logistic regression models, and logarithmic regression models. These models are best selected depending on the expected relation of variables and adjusted accordingly.

3.3.1 Linear Regression

Linear regression applies to models expected to be linear and to models that can be manipulated into being linear. Linear regression models are broken down into two types of modelling: simple linear regression modelling, used when a function only has one independent variable; and multiple linear regression modelling, used when a function has several independent variables. Both functions can be written in the same vector matrix notation, although for most simple linear regression analyses this is not required (Soong, 2004).

The standard mathematical expression of a simple linear regression model is shown in equation (9), where α and β are constants, and e represents the deviation from the mean.

$$y = \alpha + \beta x + e \qquad (9)$$

Here e will have a mean of zero and a standard deviation equal to the standard deviation of the function y. While the function will have upper and lower bounds based on the data analyzed, only α

and β require definition for the function. Using the least square method an approximate value for α and β can be found with equations (10) and (11) (Soong, 2004).

$$\hat{\alpha} = \bar{y} - \hat{\beta}\bar{x} \quad (10)$$

$$\hat{\beta} = \left[\sum_{i=0}^{n-1}(x_i - \bar{x})(y_i - \bar{y})\right]\left[\sum_{i=0}^{n-1}(x_i - \bar{x})^2\right]^{-1} \quad (11)$$

Where:

$$\bar{x} = \frac{1}{n}\sum_{i=0}^{n-1} x_i$$

$$\bar{y} = \frac{1}{n}\sum_{i=0}^{n-1} y_i$$

$$\alpha \approx \hat{\alpha}$$

$$\beta \approx \hat{\beta}$$

This method will create a linear equation for any set of data. Regardless of the actual relationship, this validity must be analyzed by the user. This simple linear regression equation can be converted into a matrix form, shown in equation (12), where e_i is the residual, or distance of point i from the mean.

$$\boldsymbol{y} = \boldsymbol{C\theta} + \boldsymbol{e} \quad (12)$$

Where:

$$\boldsymbol{C} = \begin{bmatrix} 1 & x_1 \\ 1 & x_2 \\ \vdots & \vdots \\ 1 & x_n \end{bmatrix}$$

$$\boldsymbol{y} = \begin{bmatrix} y_1 \\ y_2 \\ \vdots \\ y_n \end{bmatrix}$$

$$\boldsymbol{e} = \begin{bmatrix} e_1 \\ e_2 \\ \vdots \\ e_n \end{bmatrix}$$

$$\boldsymbol{\theta} = \begin{bmatrix} \alpha \\ \beta \end{bmatrix}$$

The matrix form also works for the multiple linear regression models. In the general equation, $\boldsymbol{y}$ and $\boldsymbol{e}$ remain the same, while $\boldsymbol{C}$ and $\boldsymbol{\theta}$ change to become the following, where m is the number of independent variables.

$$\boldsymbol{C} = \begin{bmatrix} 1 & x_{11} & x_{21} & \cdots & x_{m1} \\ 1 & x_{12} & x_{22} & \cdots & x_{m2} \\ \vdots & \vdots & \vdots & \ddots & \vdots \\ 1 & x_{1n} & x_{2n} & \cdots & x_{mn} \end{bmatrix}$$

$$\boldsymbol{\theta} = \begin{bmatrix} \beta_0 \\ \beta_1 \\ \vdots \\ \beta_m \end{bmatrix}$$

Where:

$$\boldsymbol{\theta} \approx \widehat{\boldsymbol{\theta}} = (\boldsymbol{C}^T\boldsymbol{C})^{-1}\boldsymbol{C}^T\boldsymbol{y}$$

This method works well for some non-linear cases where it is possible to set a non-linear variable equal to x_i. For example, the nonlinear equation $y = a + bx + cx^2$ could be adjusted to have $x_1 = x$ and $x_2 = x^2$ so that the linear regression formula can be applied. Significant detail on linear regression can be found from Green and Silverman (1995), Rao (1973), and Soong (2004).

3.3.2 Logistic Regression

Logistic regression models are better than linear regression models at modeling binary or dichotomous data. For data sets that are surveys of absolutes, with responses indicating either yes/no or 0/1, the logistic regression model is well suited. It creates an S shaped curve, demonstrated in Figure 21, leading gradually to zero and gradually to one in order to represent a situation where probability of an event increases over the sample, but is not always 0 or always 1 for any range (Hosmer & Lemeshow, 2000). The logistic regression model can also be expanded into the continuation ratio logistic regression model, as discussed by Peng and Zhang (2008). While these models are well suited to certain situations, they are not covered in detail as the structural sensors will produce data over a range of values.

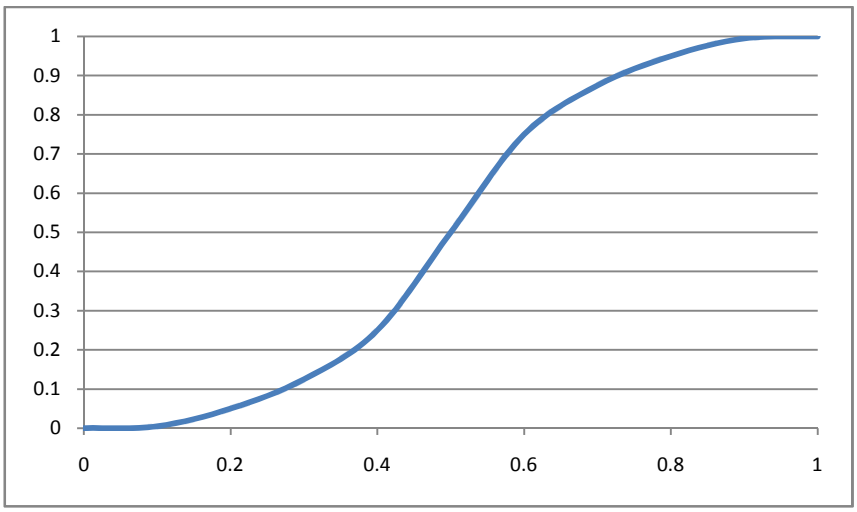

Figure 21: Sample logistic regression curve

3.3.3 Polynomial Regression

Polynomial regression is used for data that is not amenable to linear regression analysis. Instead, polynomial regression models aim to fit a curve to the data, based on the equation below, where $g(t)$ represents a curve, while e represents the error (Green & Silverman, 1995).

$$y = g(t) + e \qquad (13)$$

This technique is popular and widely used, but has several limitations such as single extraneous data points having a larger than appropriate effect on the final relation. Polynomial regression models use a multiple regression approach to the data analysis (Green & Silverman, 1995).

3.3.4 Logarithmic and Exponential Regression

Logarithmic and exponential regression are special case polynomial regression methods, where $g(t)$ in equation (13) represents a logarithmic or exponential equation. Equations (14) and (15) represent examples of logarithmic and exponential regression respectively.

$$y = \alpha + \beta \log(x) + e \qquad (14)$$

$$y = \alpha + \beta e^{-x} + e \qquad (15)$$

3.3.5 Normalized Regression Analysis

Running a regression analysis on actual data can provide unclear or misleading indicators on important variables of the equation. To avoid this it is possible to normalize the input and output data to provide a clearer understanding of the effect on each equation variable. Once the data is normalized the regression analysis is carried out in the same manner as the original data. Equation (16) and (17) show the calculations used to normalize output and input data respectively (Ramos L. F., 2007).

$$y_{k,\omega} = \frac{y_k^m - \overline{y}}{\sigma_y} \quad (16)$$

$$x_{k,\omega} = \frac{x_k^m - \overline{x}}{\sigma_x} \quad (17)$$

3.4 Regression Analysis with Dynamic Models

Regression analysis with dynamic models typically requires calculations that account for possible inertial relations between systems. The analysis may use differential relations to account for this. Therefore, dynamic models of regression analysis can consider the history of input and output signals in their final relations. In this sense dynamic models are not to be confused with the dynamic sensors, data, and data acquisition systems discussed in previous sections. Common regression analysis techniques used with dynamic models are the auto regressive moving average model and the auto regressive model with exogeneous inputs.

3.4.1 Auto Regressive Moving Average

The auto regressive moving average model can operate using the moving average method (described in section 3.1) in combination with an auto regressive function to give a comparison with some noise removed. On multiple degree of freedom systems a similar model, called the auto regressive moving average vector model, can be applied using matrices created from the existing data (Peeters, 2000). This method is simple and produces reliable results. The vector based model has been recently researched by Andresen (1997), Ljung (1999), and Peeters (2000).

The auto regressive moving average vector model is well suited to use with complex dynamic models. In cases where there are white noise stochastic processes the response vector can be simplified to the equation below, where y_k is a matrix with l column, e_k is a vector representing white noise, and A_i^{AR}

and C_i^{MA} are parameters matrices for the auto regression and moving average section of the function (Ramos L. F., 2007).

$$y_k = -A_1^{AR} y_{k-1} - A_2^{AR} y_{k-2} - \cdots - A_{na}^{AR} y_{k-na} + e_k + C_1^{MA} e_{k-1} + C_2^{MA} e_{k-2} + \cdots + C_{nc}^{MA} e_{k-nc} \quad (18)$$

3.4.2 Auto Regressive Models with Exogeneous Inputs

The auto regressive model with exogeneous inputs (ARX model) uses input in the period leading up to the calculation to produce an output that takes time delayed factors into account. This model permits a more accurate modeling of events such as thermal inertia (Ramos L. F., 2007). The basic equation, (19), shows the similarities between the ARX model and the auto regressive moving average equations. Here the A_i^{AR} values represent the auto regressive part of the function, and B_i^X represents the exogeneous part.

$$\hat{y}_k = -A_1^{AR} y_{k-1} - A_2^{AR} y_{k-2} - \cdots - A_{na}^{AR} y_{k-na} + B_1^X u_{k-nk}^{env} + B_2^X u_{k-nk-1}^{env} + \cdots + B_{nb}^X u_{k-nk-nb+1}^{env} + e_k \quad (19)$$

The ARX model theory can also be used for modeling of environmental effects and damage detection (Peeters, 2000). Through normalization of data, ARX model estimation, use of best fit models, re-simulation of model, as well as determining error and confidence intervals, the user is capable of detecting significant changes in natural frequency (Ramos L. F., 2007). Any significant change in natural frequency of a structure indicates the onset of damage.

3.5 Common Regression Quality Criteria

Quality criteria are best quantified using several measures. Four common calculations to quantify the accuracy of the regression model are:

- calculating the standard deviation of the error
- calculating the loss function
- calculating the final prediction error
- calculating the coefficient of determination (Ramos L. F., 2007)

The standard deviation of the error, or in shorter form the standard deviation error, uses the error values when comparing the model to the actual signal, and from these values calculates the standard deviation. This produces a result that should go progressively towards zero as the model improves.

The loss function, final predicted error, and coefficient of determination are the most commonly used quality criteria (Ramos L. F., 2007). The equations, (20) to (22), are based on the error between model and actual values, as well as the estimated covariance (Ljung, 1999), where *V* is the loss function, *FPE* is the final prediction error, and $\hat{r}_{xy}^2$ is the coefficient of determination. The loss function and final predication error show improvement by progressing towards zero, while the coefficient of determination has the optimal value of one (Ljung, 1999).

$$V = \frac{1}{N}\sum_{k=1}^{N} e_k^2 \qquad (20)$$

$$FPE = V\frac{1 + d/N}{1 - d/N} \qquad (21)$$

$$\hat{r}_{xy}^2 = \left(\frac{\hat{R}_{xy}}{\hat{\sigma}_x \hat{\sigma}_y}\right)^2 \qquad (22)$$

Where:

N is the number of samples

e is the error between model and actual signal

d is the number of estimated parameters

$\hat{R}_{xy} = \frac{1}{N-1}\sum_{k=1}^{N}(x_k - \bar{x})(y_k - \bar{y})$

$\hat{\sigma}_x = \sqrt{\frac{1}{N-1}\sum_{k=1}^{N}(x_k - \bar{x})^2}$

$\hat{\sigma}_y = \sqrt{\frac{1}{N-1}\sum_{k=1}^{N}(y_k - \bar{y})^2}$

Where:

$\bar{x}$ and $\bar{y}$ represent the mean values in each signal

x_k and y_k represent the values of *x* and *y* at value *k*

3.6 Analysis with Numerical Models

Numerical models have become useful tools in structural analysis. These models make it possible to digitally test a verified model with destructive forces to identify potential weaknesses. Finite element models have become the most dependable numerical models in determining structural behaviours, with several programs commercially available. Most modern finite element methods use the principle of the relations between displacement, strain, stress, and external forces. Therefore, if any of these values are known the others can be calculated, given a know stiffness matrix of the system (Shames & Dym, 1991). Figure 22 shows how an analyst can progress from the displacement to the external force. These relations do not take into account forces that are created internally, such as the structures self weight. The finite element method accounts for this by subdividing the structure, or surface, into many small units and analyzing all units plus their relation from one to the next.

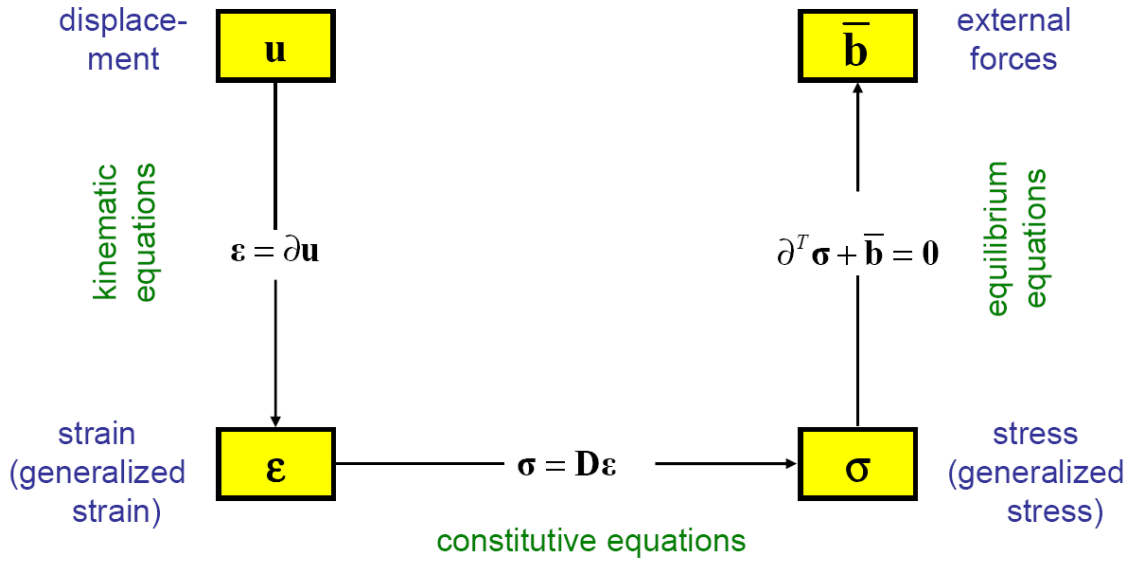

Figure 22: FEM Assumptions (Kabelle, 2007)

Finite Element Methods began development in 1858 and 1860, when the separate inventions of the mathematical matrix and discrete structural mechanics began. The first paper on matrix structural analysis was published in 1934 (Duncan & Collar, 1934), while the direct stiffness method, the direct predecessor of the finite element method, was first introduced in 1959. The first textbook on finite element method followed in 1967 (Felippa, 2001). While relatively new in terms of structural analysis, the process is based on basic material properties and tests that trace back to Newton's tests on cantilevers. Proper use of finite element methods in structural analysis requires well defined variable

input, including material properties, mesh sizing, nodal locations, external force application, potential restraints, and potential settlements to name a few. Such an analysis on an existing structure must be carefully designed.

Modern research on finite element methods covers a range of topics including improved model verification (Huiping, Guoqun, Shanting, & Chuanzhen, 2007). Structural health monitoring combines well with finite element models because structural monitoring is able to provide data to assist in model verification. The monitoring results give directly measured data, such as natural frequency. This data is compared to the numerical model which is adjusted to produce results as close to real life as possible. Static data, such as location and movements of cracks, should also be used to verify the numerical model.

3.7 Uncertainty Analysis

Unlike the previously discussed techniques, numerical analysis is the only technique that does not depend directly on the sensor data. Instead numerical analysis uses this data for verification purposes. The other techniques have error or uncertainty created by inadequate sensors (Garcia, Vehi, Matos, Henriques, & Casas, 2007), increasing the importance of proper sensor selection.

Given the increased risk of randomness, uncertainty, human mechanical and computational error, several techniques have been developed to assist in the verification of data. These techniques include the Monte Carlo Method, the First and Second Order Reliability Methods, Interval Analysis, and Perturbation Techniques (Coleman & Steele, 1999). Regression analysis also contains significant uncertainty in the coefficients, the function, the variables, and random sources. Due to these uncertainties, even if data has been verified before the regression analysis, uncertainty analysis should be carried out after the regression analysis is complete (Coleman & Steele, 1999).

The Monte Carlo Method is a dependable uncertainty analysis technique. The drawback to this method is its large computational demand (Henriques, Veiga, Matos, & Delgado, 2008). The Monte Carlo method uses the cumulative distribution function. This function represents the probability of an event based on past results and statistics, and can calculate uncertainty if required (Deutsch, et al., 2001). The Monte Carlo method demands great computational power due to the iterative technique used to obtain the results (Coleman & Steele, 1999).

First and Second Order Reliability Methods are useful in analysis of implicit functions, but are computationally difficult when used with finite element models (Henriques, Veiga, Matos, & Delgado, 2008). These analyses are able to quantify the probability of a given event, typically a failure event, to a higher degree of certainty than the Monte Carlo Method. Both first and second order reliability analysis techniques are for linear and non linear systems, with the second order reliability analysis giving better approximations of non linear systems. The reliability methods search the most likely location of failure using deterministic analysis tools amongst others (Allen & Maute, 2004).

Interval Analysis Techniques show promise, but at this time there is not enough research into the accuracy of this technique with finite element methods (Henriques, Veiga, Matos, & Delgado, 2008). With bridge monitoring this type of data analysis has gained popularity, as the technique is capable of dealing with large volumes of data using a methodology which considers the whole data set for uncertainty. There is some caution in interval analysis use because it has missed damage due to sensor tolerances (Garcia, Vehi, Matos, Henriques, & Casas, 2007).

Perturbation Techniques are also showing increasing promise. They are well suited for finite element modes, and show potential with detection of abnormal behaviour in monitoring systems. Perturbation techniques base the uncertainty analysis on the mean, standard deviation, and correlation coefficient. While the analysis is designed for linear, normally distributed functions, reliable results can also be produced for any system that can be manipulated into being linear (Henriques, Veiga, Matos, & Delgado, 2008). Further study into the perturbation technique has resulted in the functional perturbation method, and the optimal functional perturbation method. These methods are specifically for stochastically heterogeneous structures, and use $\theta(\boldsymbol{K})$ during computation to achieve faster convergence (Altus, Totry, & Givli, 2005).

3.8 Typical Monitoring Used with Structural Interventions

When conservation, restoration, renovation, or other major construction work is undertaken on or near a historical structure there is an increased need to have a structural monitoring system in place. In these cases some structural movement is expected, and various limits can be placed on acceptable rate of occurrence. Structural changes, such as crack widths, can be rated during construction work on a variety of scales.

Many industries use a simple three stage monitoring system during work; a sample system is outlined in Table 1. Depending on the thresholds observed by the sensors this system classifies problems as

green, yellow or red. A green classified problem should be monitored routinely, to ensure it remains stable. Some small variation in damage is allowable. A yellow problem is slightly more serious than the green problem. It has the potential to become worse, and is approaching the maximum amount of damage expected. Yellow problems are monitored daily to ensure the situation does not deteriorate. The red problem indicates a serious problem and that the structure has the potential of becoming unstable. In this case the monitoring should be at least twice a day; and all construction work should be halted until the problem can be properly analyzed. Monitoring should always take place at the same time in order to reduce environmental errors. If an automated system is in place the data collection frequency can be increased.

Table 1: Three stage monitoring system

	Green	Yellow	Red
Monitoring Frequency	Weekly	Daily	Twice or More Daily
Effect on Construction	None	Construction is undertaken with care in area	Construction is halted until proper analysis of situation is undertaken

Other evaluation methods used to assess structural problems include those proposed by Rankin (1988), and Boone (2001). The Rankin method used four classification categories based on the control parameters of maximum angular distortion (β_{max}) and maximum settlement (S_{max}) (Rankin, 1988). This method, outlined in Table 2, gives a category of damage, level of damage, and the two control parameters. The Boone classification goes into further detail, providing six classification levels, descriptions of damage, crack widths, strain limits, and an architectural damage limit, as well as containing damage category and type of damage (Boone, 2001).

Table 2: Rankin Damage Categories (Rankin, 1988)

Damage Category	Level of Damage	β_{max}	S_{max}
1: Aesthetic	Minor	<1/500	<10
2: Aesthetic	Light	1/500 – 1/200	10 – 50
3: Functional	Moderate	1/200 – 1/50	50 – 75
4: Structural	Sever	>1/50	>75

These kinds of clear indicators are valuable parts of monitoring systems in their ability to convey the importance of problems to individuals who may not have the experience in the field of damage classification.

3.9 General Remarks

This chapter has provided an overview of data analysis techniques which can be used to assist in understanding a set of data. Some of these data analysis techniques, such as logistic regression data analysis, are not likely to be useful in the structural analysis of historical structures. Depending on what data is being analyzed and what type of results are desired, different analysis systems can be implemented. Several of the data analysis techniques discussed in this chapter will be used in the numerical tool to provide a clear image of static and dynamic changes in the structure.

4 DEVELOPMENT OF MIROVY, THE NUMERICAL TOOL

As the cost of sensors and monitoring systems has been decreasing, there has been an increase in the use of these systems for structural health monitoring, and an increase in the amount of data produced by these systems. Large monitoring systems can produce more data than can feasibly be analyzed with present numerical tools. This results in excessive time requirements for interpretation of data, and increases the risk of important data going unnoticed.

The goal of MIROVY, the numerical tool, is to assist the user in the analysis of large quantities of data. MIROVY accomplishes this analysis by providing the user with a variety of options by which the data can be analyzed, correlated, compared, and plotted. These capabilities will assist the user in determining probable causes for deterioration, detecting damage, and alarming serious damage potential. The numerical tool is designed to minimize the amount of pre-processing from the users.

MIROVY will use the input of sensors and data acquisition systems discussed in chapter 2. With the assistance of the various analysis techniques discussed in chapter 3, the tool provides the user with the most comprehensive data analysis possible. Matlab will be the programming language and computational base for MIROVY. As MIROVY is a starting base for an automated structural monitoring system, the simplest applicable functions will be selected for the testing.

4.1 Architectural Description

A general overview of the numerical tool is provided in this section, which consists of a basic description of the program architecture. A more detailed description will be provided in section 4.2, and a user's manual for the numerical tool is provided in the appendix. The architecture of MIROVY will illustrate its ability to analyse data from any monitoring system though a review of the processes conducted.

4.1.1 Model Skeleton

The numerical tool will be developed in a linear methodology, as shown in Table 3. It is assumed that the user has an understanding of programming language and will be able to adjust and make demands of the program as required. MIROVY is not a finished commercial product.

Each section of the program, with the exception of Data Input, can be skipped when running the numerical tool, and each section requires specific user input. The actually programming for each section takes place in sub-programs and functions.

Table 3: Operating Process of MIROVY

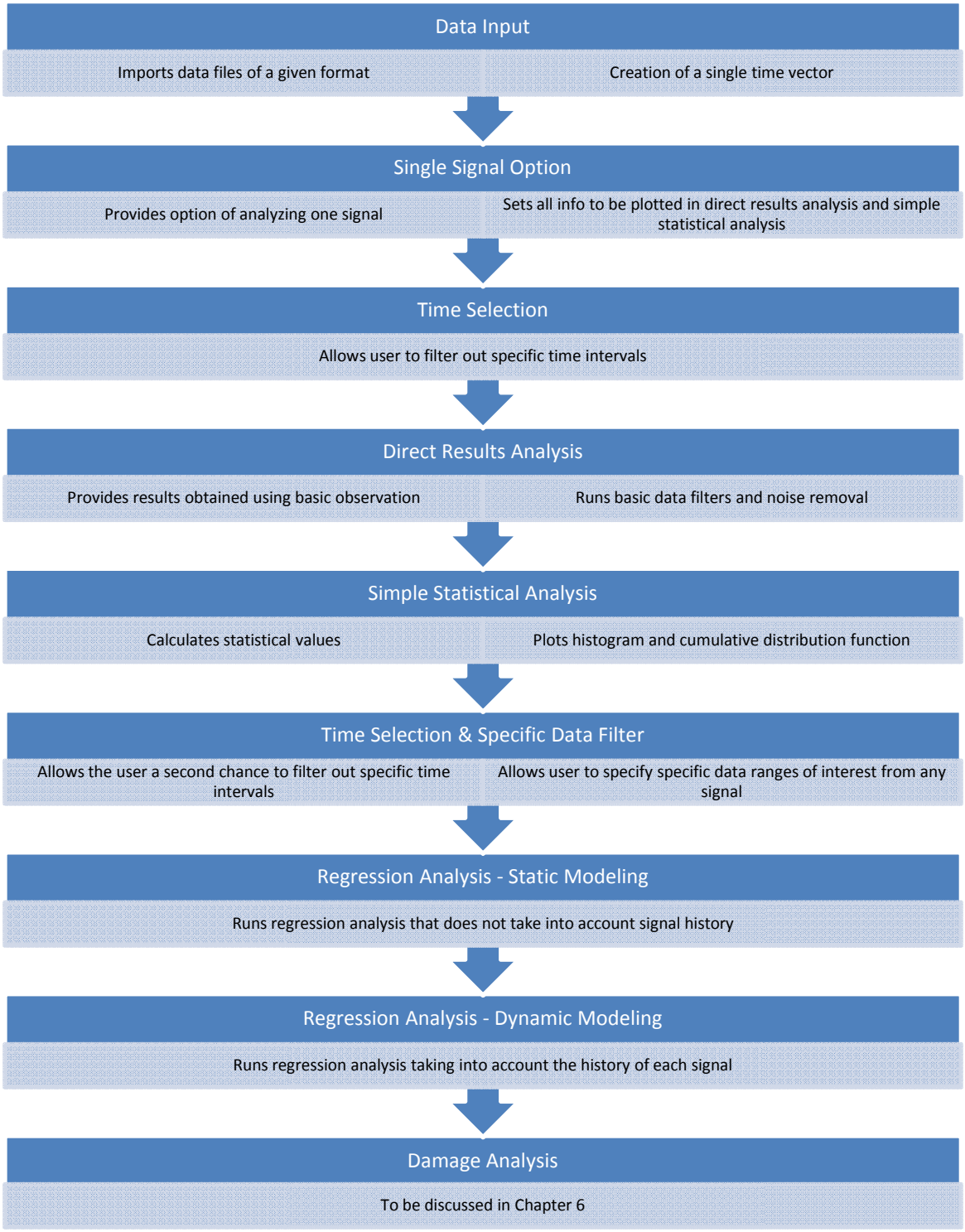
Data Input
Imports data files of a given format
Creation of a single time vector
Single Signal Option
Provides option of analyzing one signal
Sets all info to be plotted in direct results analysis and simple statistical analysis
Time Selection
Allows user to filter out specific time intervals
Direct Results Analysis
Provides results obtained using basic observation
Runs basic data filters and noise removal
Simple Statistical Analysis
Calculates statistical values
Plots histogram and cumulative distribution function
Time Selection & Specific Data Filter
Allows the user a second chance to filter out specific time intervals
Allows user to specify specific data ranges of interest from any signal
Regression Analysis - Static Modeling
Runs regression analysis that does not take into account signal history
Regression Analysis - Dynamic Modeling
Runs regression analysis taking into account the history of each signal
Damage Analysis
To be discussed in Chapter 6

4.1.2 Data Input

The data input is simple in architecture. The user enters the file name of the data into the main program, ensuring that the file is in the proper format and saved in the proper location. This information is sent to a sub-program which imports the data and formats it for working with Matlab. An outline of this program is shown in Table 4.

Table 4: Architectural outline of data input sub-program

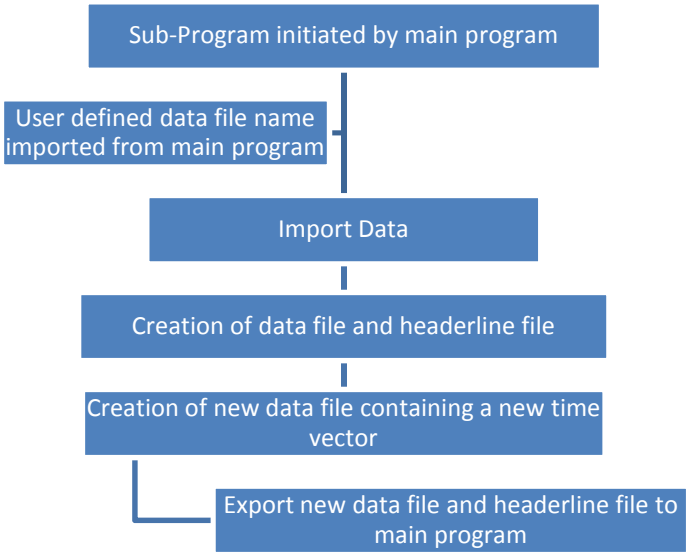
Sub-Program initiated by main program
User defined data file name imported from main program
Import Data
Creation of data file and headerline file
Creation of new data file containing a new time vector
Export new data file and headerline file to main program

4.1.3 Single Signal Option

This sub-program provides the user with the option of displaying all results from the direct results analysis and simple statistical analysis on one signal, thus enabling the user to focus on one data set at a time.

4.1.4 Time Selection

The time selection sub-program is offered twice in the numerical tool. The first opportunity for the user to make time selections is placed early in the analysis so that if sensors are producing errors during certain times of the day, due to extreme conditions or unrelated loading, signals during these time intervals can be ignored and without affecting the filtering process.

4.1.5 Direct Results Analysis

Direct results analysis is run as the second major sub-program, with the architectural outline shown in Table 5. These topics do not require statistical or advanced mathematical analysis. They include: plotting unfiltered data, locating maximum and minimum data points, locating outlyers, plotting unfiltered data with upper and lower bounds shown, removing outlyers, plotting data without outlyers, running a moving average filter, plotting filtered signal and comparing filtered and unfiltered signals. The program architecture makes it possible for the sub-program to provide any, all, or none of this information. The two filters, the removal of outlyers, and the moving average, can be turned on or off, depending on the amount of noise reduction required for the following analysis programs.

Table 5: Architectural Outline of the Direct Results Analysis

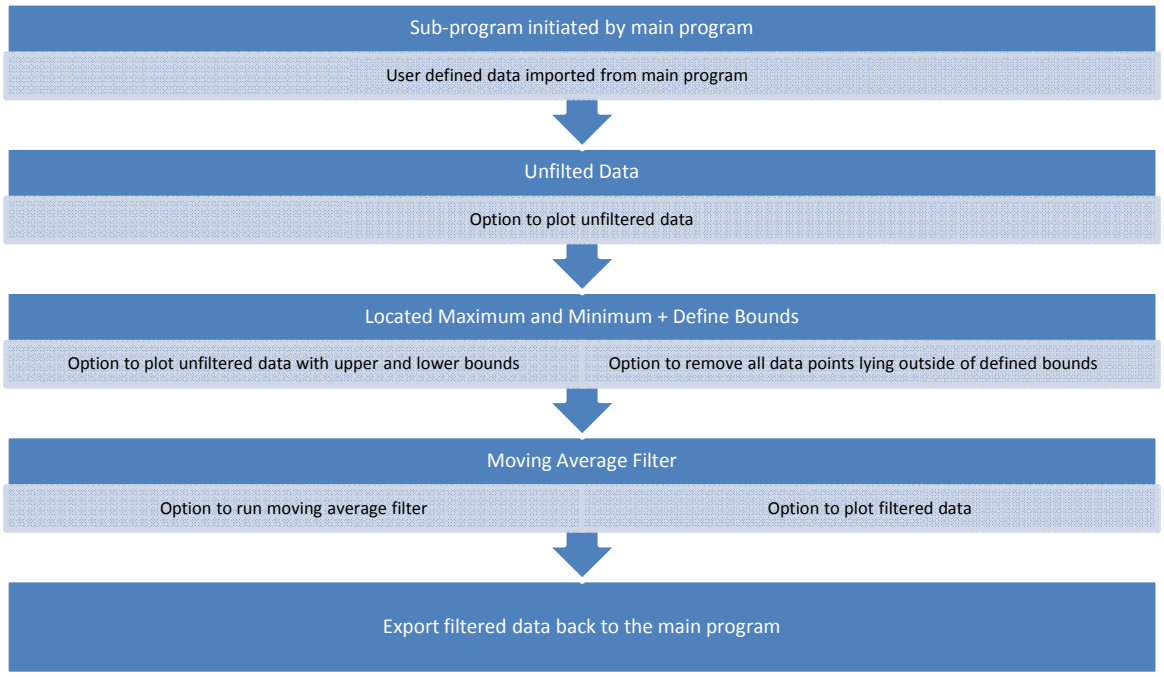
Sub-program initiated by main program
User defined data imported from main program
Unfilted Data
Option to plot unfiltered data
Located Maximum and Minimum + Define Bounds
Option to plot unfiltered data with upper and lower bounds
Option to remove all data points lying outside of defined bounds
Moving Average Filter
Option to run moving average filter
Option to plot filtered data
Export filtered data back to the main program

User input in the filtering process is further improved by options given in the user interface program. The main program gives the user several options for both the outlyer removal and moving average filter. Filtering data based on outlyer removal depends on the number of standard deviations the user selects as upper or lower boundaries; the user can then remove any data points on either side of these boundaries. The moving average filter is discussed in section 3.1 of this thesis. In the numerical tool, this filter allows the user to define the window size and the program removes the erroneous data to produce better results.

4.1.6 Simple Statistical Analysis

Simple statistical analysis is run as a sub-program, and while this provides no filtering, it does provide information on each of the data signals. The sub-program provides mean standard deviation, maximum and minimum values for each signal, coefficient of variation, signal to noise ratio, a binned histogram, and a binned cumulative distribution function. Table 3 shows the architectural outline of the sub-program.

Table 6: Architectural Outline of the Simple Statistical Analysis

Sub-program initiated by main program	
Data, Header lines, and user defined data is received by the sub-program	
Basic statistical data	
Sub-program calculates and displays mean, standard deviation, maximum and minimun values. This data can be used to find coefficient of variation and signal to noise ratio.	
Histogram	
Using number of bins defined by the user the sub-program creates the histogram. Results are displayed visually	Data from the histogram is used to create the cumulative distribution function, which is plotted

This sub-program provides the user with many options to run or display different data. Particular attention should be given to the selection of the number of bins used for the histogram and cumulative distribution function. The main program offers a suggestion of 50 bins to give good visual results.

4.1.7 Time Selection and Specific Data Filters

Time selection and specific data filters are offered just before the regression analysis occurs. These two additional filters are provided at this point in the program to assist the user in getting clean relations in the regression analysis. The time selection sub-program is run in the same manner as the earlier time selection sub-program and requires the same input. The specific data filter permits the user to decide the signal they wish to filter, the signal range (upper, middle or lower) of interest, and the appropriate bounds. This sub-program will then remove the undesirable data.

4.1.8 Regression Analysis – Static Modeling

The data has now gone through various sub-programs, as selected by the user, where the data may have been filtered for noise and had specific intervals selected. Static modelling of the regression analysis, meaning a regression analysis of the signals not considering signal history, is dealt with by a sub-program at this point in the numerical tool. In this sub-program the correlation coefficient between signals is checked, the user selects signals of interest, while single and multiple regression analysis is carried out and plotted on both actual and normalized data. These calculations are carried out much faster than the dynamic modelling regression analysis, and in some cases can provide more reliable results. It is also possible to run the regression analysis on normalized data, in order to better assess the effect each environmental input has on the structural output. The architectural outline of the sub-program is given in Table 7.

Table 7: Architectural Outline of Static Regression Analysis Sub-program

Sub-program initilized by main program	
Data, header lines, and user selections are received by the sub-program	
Coefficient of Determination	
Coefficients of determination are output, both in matrix format displaying all signals, and correlations of signals selected for regression analysis	
Single static regression analysis	
Regression analysis run on normalized data, displaying relation constants	Regression analysis run on actual data, displaying relation constants and error, plotting data and residuals
Multiple static regression analysis	
Regression analysis run on normalized data, displaying relation constants	Regression analysis run on actual data, displaying relation constants and error, plotting data and residuals

4.1.9 Regression Analysis – Dynamic Modeling

Dynamic modeling of the regression analysis is the final regression sub-program. This sub-program uses the ARX methods mentioned in section 3.4.2 to find the relations between different signals. Here the user must select which signals to compare as well as their respective polynomial representation of transfer functions. The polynomial representation of transfer functions include: order of structural

response, order of environmental input, and the number of delays from input to output respectively. The architectural outline of the sub-program is given in Table 8.

Table 8: Architectural Outline of Dynamic Regression Analysis

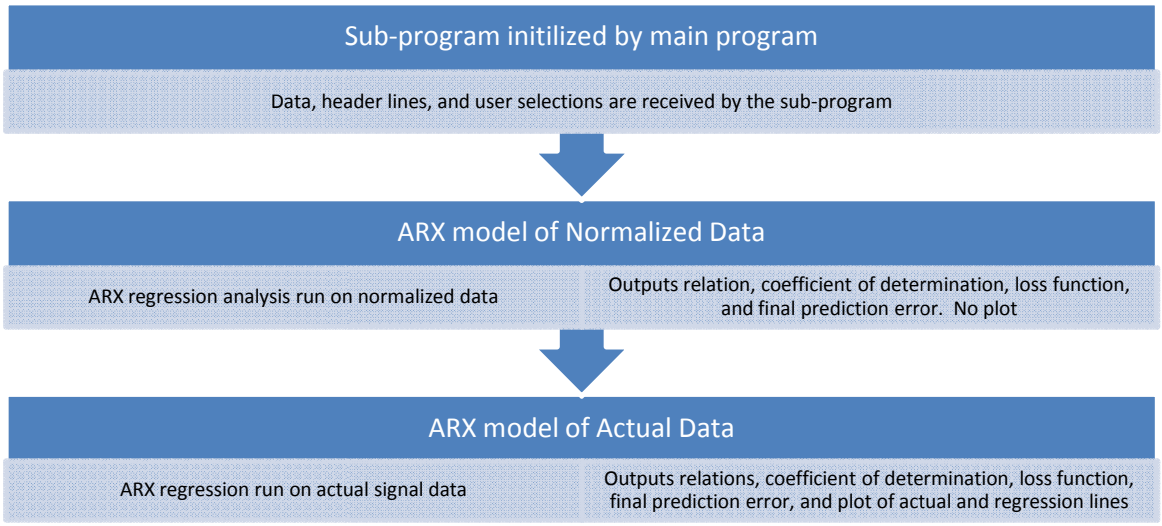
Sub-program initilized by main program
Data, header lines, and user selections are received by the sub-program
ARX model of Normalized Data
ARX regression analysis run on normalized data
Outputs relation, coefficient of determination, loss function, and final prediction error. No plot
ARX model of Actual Data
ARX regression run on actual signal data
Outputs relations, coefficient of determination, loss function, final prediction error, and plot of actual and regression lines

4.2 Detailed Description of the Features

This prototype numerical tool will be created in MATLAB. MATLAB was selected as an operating program because of its ability to manipulate matrices with simple user input. Specifically the program is being created in MATLAB Version 7.3. It is expected that the user has a basic understanding of the MATLAB program, and has access to all required toolboxes. In this section a more detailed account of each sub-program is given.

With the exception of the data input sub-program it is possible to skip or turn off any sub-programs the user is not using, or does not want to use. It is suggested to start with all sub-programs off, and confirm that the data from the initial programs is desirable before starting the next sub-program. This methodology will reduce the amount of output information to be reviewed each time the program is run.

4.2.1 Data Input

The user is required to put the filename into the main program. This information will then be transferred to the sub-program. The second and final user requirement is that the data file is in the proper format.

The proper data format is a matrix of data where the first row is column titles, and all other rows are data, with no empty fields. Each column title should have no spaces, since the sub-program will read the entire line into Matlab as a string, and then break it into matrix cells based on the location of white space. All other data must be numeric and tab separated. In the numeric data the first three columns should represent time as recorded by the data acquisition system; first column should be year, second column should be the day (from 1 to 365 or 366), and the third column should be the time of day with no punctuation between hours and minutes. The sub-program sends the data to a function that converts these three columns into a one column standard Matlab time vector.

The function used to change the three columns into the standard Matlab time vector reads methodically through the data, initially changing the day of the year data into month and day of the month data; while doing this it also ensures that leap years are taken into account. A similar procedure is used to separate the data by hour, minute, and second. Once the data has been formatted into year, month, day, hour, minute, and second values; it can be evaluated used an internal Matlab function which creates the Matlab time vector. The Matlab time vector is a number, where the base value is days, the first day being January first, year 0000. Hours, minutes, and seconds are the appropriate fractions of the day, where 12h00 would be .5 of the day. For example, 18:00 on November 24th, 2005, would be translated into 732640.75. This data is then sent back to the sub-program.

The sub-program returns the data file with the new Matlab time vector to the data file. As a final procedure the sub-program displays "→ DATA HAS BEEN SUCCESSFULLY IMPORTED←".

4.2.2 Single Signal Option

The single signal option is initialized by the user in the main numerical tool program. The main program then sends the data and header line matrices along with the selected column to the sub-program. When the sub-program starts it displays the message "→ SINGLE SIGNAL OPTION HAS BEEN SELECTED←" in the command window.

Programming required in the sub-program is short, the program creates a new data matrix containing only two columns, that of the time and that of the selected signal. The new data matrix is then returned to the program.

In the main program, when the single signal option is selected, the program has been designed to turn on the direct and statistical analyses, while turning off both regression analysis sub-programs. This also initiates the output and plotting of all data from the direct and statistical analysis sub-programs.

4.2.3 Time Selection

The time selection sub-program appears twice during the main numerical tool program. The first occurrence is directly after the data import function allowing the user to discard time intervals that could be erroneous before the signals filters run to reduce signal noise. The main program sends the current data file, as well as start and stop times for the desired time interval. This means that if the user wishes to discard the daytime data, keeping the night time data, they would enter a start time greater than the stop time, and the sub-program would be able to analyze this. When this sub-program begins to run it displays the message "→ START OF TIME SELECTION FUNCTION←".

The sub-program turns the time vector into a vector representing the time of day, and uses this to locate all signal readings that the user wishes to keep. All rows in the time vector that represent unwanted times are set equal to zero, and through several calculations are removed. This removal process will select any data equal to zero in the first two columns and remove the rows. It is statistically unlikely this will cause many rows to be removed accidentally, so long as there is real data for all signal points in the first two rows and no zeros used to fill in lack of data.

The sub-program returns the smaller data file, containing only the desired times. The sub-program will also display " → TIME SELECTION FUNCTION SUCCESSFULLY COMPLETED←" when it is completed.

4.2.4 Direct Results Analysis

The direct results analysis sub-program is initiated by the numerical tools main program. When the sub-program is initialized it is sent the data file, the header line file, and several files informing the sub-program of what calculations are to be run, what values are to be shown, and what graphs should be plotted. Also coming from the main program is information on where the upper and lower bounds will be located, as well as the window size of the moving average filter. When this sub-program starts it displays the message "→ START OF DIRECT RESULTS ANALYSIS←".

If it was chosen by the user, the first thing the direct results analysis sub-program does is plot the unfiltered data. This is done through a function created for this purpose, where the data, header lines, and the name of the plot is sent and the function creates a standard figure displaying the required information, as shown in Figure 23. This is followed by a display of the minimum and maximum values for each unfiltered signal, presented in the command window.

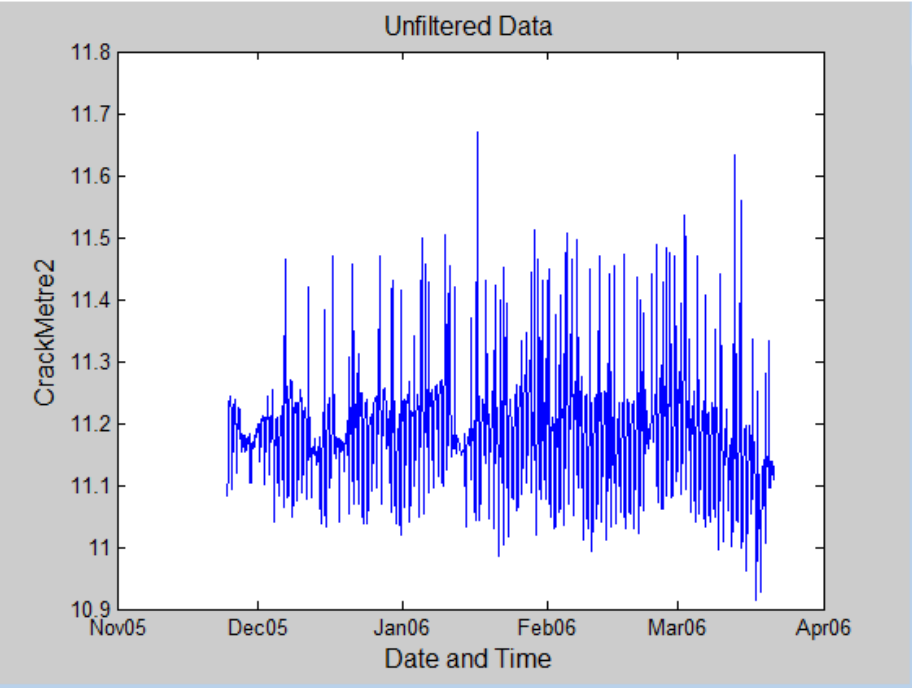

Figure 23: Plot of unfiltered data

The first filter in the direct results analysis sub-program removes signal outlyers. The sub-program receives input from the main program indicating how many standard deviations are acceptable. The suggested number of acceptable standard deviations is three, because for a normally distributed function this will contain 99.73 % of the data points. The outlyers section of the sub-program has three steps, plotting the data with the upper and lower bounds shown, removal of the outlyers, and plotting the data without outlyers. The most significant of these steps is the removal of the outlyers, and is conducted in a separate function where the data rows of the matrix with outlyers are removed. Removal of these rows can creates some gaps in the signal timeline, and this may cause slight inaccuracy when reaching the dynamic modeling of regression analysis, however for large amounts of data it should be insignificant.

A moving average function provides the second noise filter of the direct results analysis sub-program. This part of the sub-program is also in three sections: first, the moving average filter is run using a predefined window size; second, the filtered data can be plotted; and third, the output of the moving average filter can be plotted against the input of the moving average filter. Running the moving average filter is the longest of these steps, using a small function and an internal Matlab function. The moving average filter takes the average of neighbouring points, number of points used dependant on user input, and outputs a new averaged value. The first point contains significant error as the

nonexistent values are set equal to zero in the Matlab function. This error is corrected in the sub-program function by removing the first m rows from the data file, where m is the assigned window size. Window size is selected based on number of data points in the file. Common practices by those working in the field include using the number of points in a day or a week for the window size. If the data is recoded every hour, this would result in a window size of 24 or 168 points. Figure 24, an example of the third part of moving average section of the sub-program, shows the data before the moving average filter is run in red and the data after a moving average filter of window size twenty four has been run in blue.

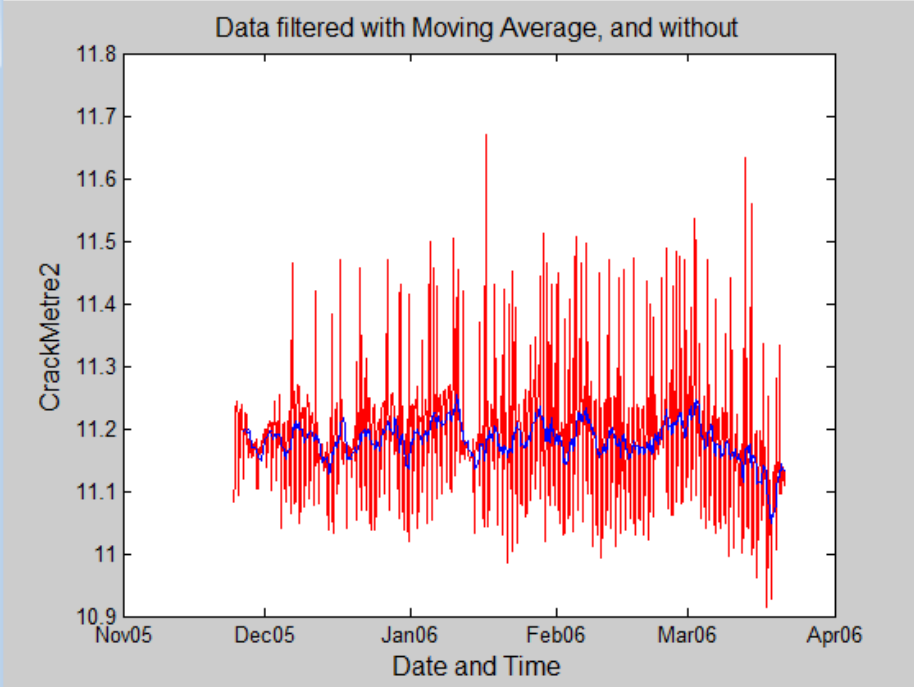

Figure 24: Data before and after moving average filter

The direct results analysis sub-program returns the filtered data matrix to the main program, and displays "→ DIRECT RESULTS ANALYSIS SUCCESSFULLY COMPLETED←" upon program completion.

4.2.5 Simple Statistical Analysis

The simple statistical analysis sub-program is initialized by the main numerical tool program. The main numerical tool program sends: filtered data, the header line file, several options informing the sub-program what to print and what to plot, as well as a selection of the number of bins to be used in

the histogram and cumulative distribution function to the simple statistics sub-program. At the start of the sub-program it displays "→ START OF SIMPLE STATISTICAL ANALYSIS←".

Simple statistical analysis sub-program produces four important pieces of information.

- The sub-program can output a grouping of post filter mean, standard deviation, maximum and minimum values.
- The sub-program can output the coefficient of variation and signal to noise ratio.
- The sub-program can create the histogram, based on the number of bins.
- The sub-program can produce a cumulative distribution function based on the number of bins selected by the user.

Of these four outputs, the simple statistical analysis creates the first two in the main sub-program, while the last two are created in a separate function. The displaying of the mean, standard deviation, maximum and minimum values are all done using existing Matlab functions. Results are shown in the command window. Both the coefficient of variation and the signal to noise ratio are simple calculations dependant on the standard deviation and the mean values. Results from these calculations are displayed in the command window.

Plotting the histogram is done in the created function, referred to by the sub-program. This is done using an existing Matlab plot designed specifically to produce histogram plots, shown in Figure 25. The number of bins is selected by the user in the main numerical tool program, fifty being suggested as the most visually appealing. The actual histogram data is also calculated using an existing Matlab function and stored for use both with the cumulated distribution function, and with the future idea that this could be desired for output. The cumulative distribution function is created using the binned data from the histogram; therefore the number of bins selected will affect the smoothness of the function. A created formula, taking each bin and adding the total value to the sum of all previous bins, then dividing the total by the number of sample, gives the resulting cumulative distribution values. The resulting cumulative distribution function plot is shown in Figure 25.

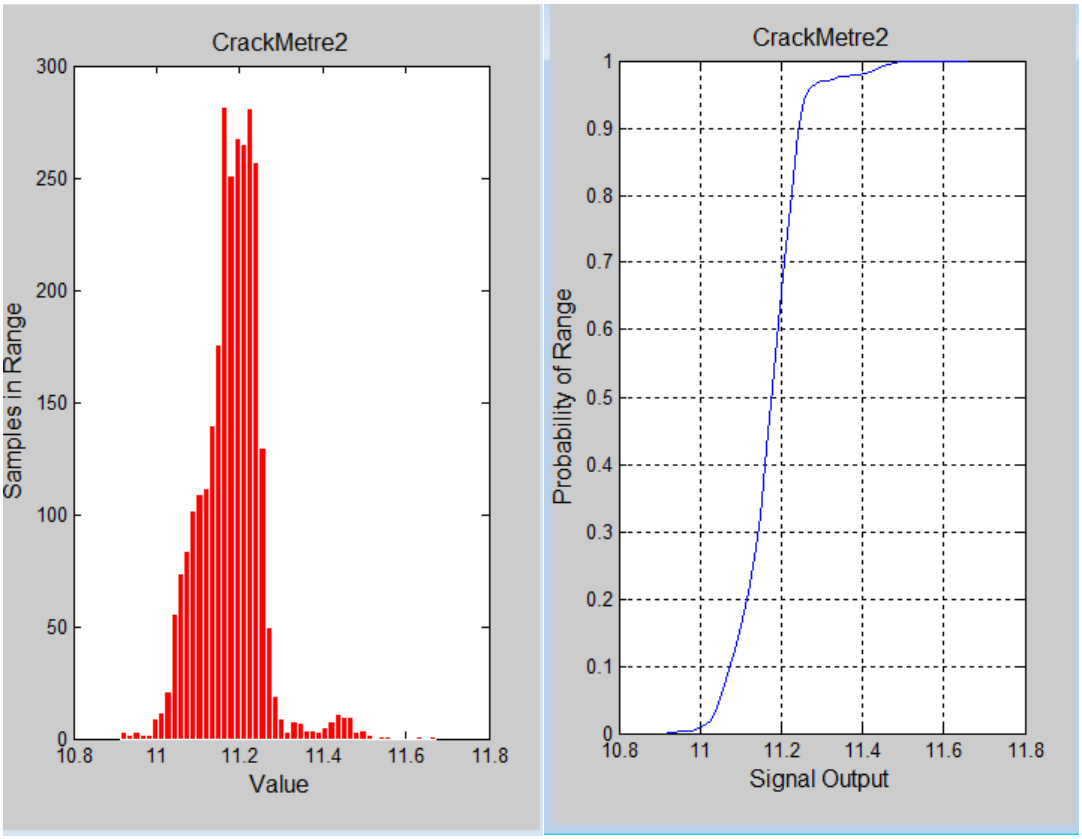

Figure 25: Sample of Histogram and Cumulative Distribution Function created by the Numerical Tool

The simple statistical analysis is designed to provide output data, and accomplishes this inside the sub-program and related functions; therefore there is not meaningful data to be returned to the main numerical tool program. A user would gather the statistical data from what has been displayed in the command window or by plot. Upon completion of the tasks the simple statistical analysis displays the message "→ SIMPLE STATISTICAL ANALYSIS SUCCESSFULLY COMPLETED←" in the command window.

4.2.6 Time Selection and Specific Data Filter

Before regression modeling the user is given a second chance to make a time selection, and a first opportunity to use the specific data filter. This filter is run as separate sub-programs, the time selection filter being the same sub-program as was used earlier. These sub-programs are selected for use based on visual inspection of the signal, prior knowledge of sensor problems, or interest in investigating specific phenomena.

The specific data filter sub-program is based on the time selection sub-program. The user decides in the main program if they would like to run the program, what signal the filter would be based on, weather upper data, lower data, or both are to be removed, and what the upper and lower bounds will be. All of this information is sent to the sub-program. The sub-program displays the message "→ START OF SPECIFIC DATA FILTER←" in the command window upon initializations. Following that it displays the header line the program associates with the selected column, informing the user what parameter they are basing the filter on.

Using a similar method as the time selection sub-program, the specific data filter sub-program first creates a column matrix indicating which rows will be removed and which rows will remain. The sub-program locates and matrix cells with a value of zero, and removes the corresponding row. A new, further filtered, data matrix is returned to the main program, and "→ SPECIFIC DATA FILTER SUCCESSFULLY COMPLETED←" is displayed in the command window. Users should beware of data columns that contain a significant number of zeros, as this may cause false positives when the program is removing rows with the value zero.

4.2.7 Regression Analysis – Static Modeling

The regression analysis, static modeling, sub-program is initialized by the main numerical tool program. The main program provides the filtered data matrix, the header line matrix, selection of signals to model, various option on type of static regression analysis to be run and option of plotting of resulting information. When the program is initialized it begins by displaying "→ START OF REGRESSION ANALYSIS – STATIC MODELING←" in the command window.

Regression analysis, static modeling, sub-program is the first regression analysis undertaken in the numerical tool, and is its self divided into six parts. Calculation of correlation coefficients, normalized regression analysis, linear regression analysis, polynomial regression analysis, exponential regression analysis, and multiple regression analysis can all be carried out by this sub-program if the user selects them. Calculation of correlation coefficients can either be done as a matrix representing correlation between each separate data signal, or as one value showing correlation between two data signals.

Normalized data can be used in a regression analysis in order to judge the importance of each variable in a resulting equation. This is carried out in a function that is combined with the linear, polynomial, exponential, and multiple regression analysis. When the user selects the normalized regression analysis option this function is initialized alongside each of the regular regression analysis functions. The function initially creates the normalized data, then sends this data to the corresponding regression

function for analysis, and displays the coefficients. Therefore the resulting data is displayed in the command window just above the actual regression analysis. The normalized analysis data is separated from the other data with ">>>>>>>>>>>>>>>>>" symbolizing the beginning of data, and "<<<<<<<<<<<<<<<" symbolizing end of normalized data.

Linear regression analysis, polynomial regression analysis, and exponential regression analysis are all processed by the same created function in the sub-program. Each analysis is identified separately, initiated separately, and computed separately. The created function uses existing Matlab computational programming to find the relations, after having first created data sets for x axis, y axis, and time. The resulting data relation can then be plotted, as shown in Figure 26, where the o represents the shared data points, and the blue line represents the function used. The representative data are shown in the command window, including signal names, the regression relations, and the numerical values of constants. Since these are all static regression analyzes, signal history is not important, and it is not important if time intervals are regular or irregular.

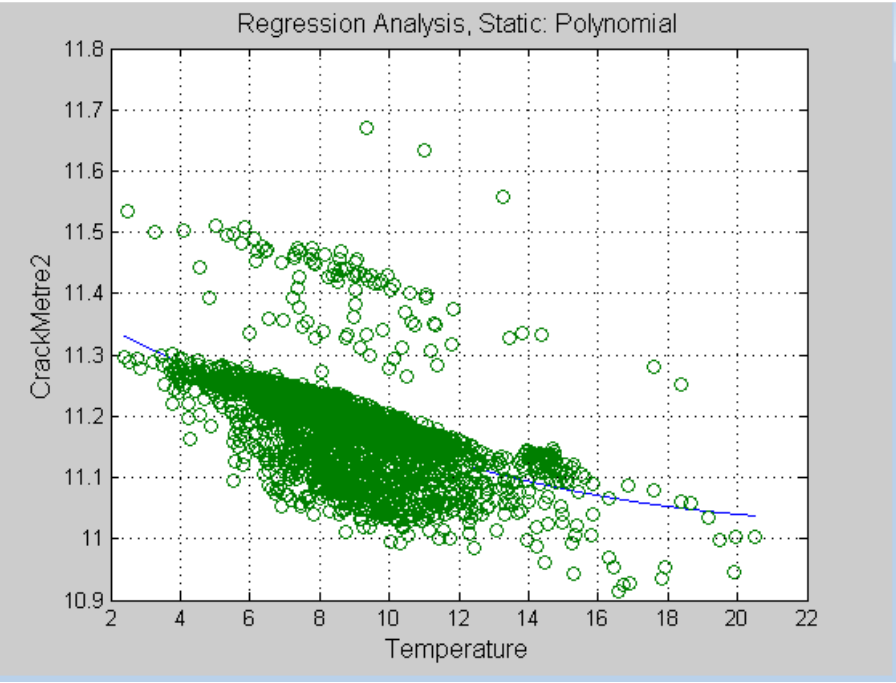

Figure 26: Plotted Polynomial Regression Analysis relations.

Multiple regression analysis is run in a separate created function, using a similar principal as the one input one output regression analysis methods. The multiple regression analysis can consider up to three environmental inputs, and one structural response. It will be displayed in the command window what the structural response, and environmental inputs are, as well as the constants and relations.

When the results are plotted, as seen in Figure 27, the signal on which the regression analysis is being run is shown, and the predicted signal based on the regression analysis. In Figure 27 a signal is shown that has not had any previous filtering, the graph has also been magnified in order to give a clearer demonstration.

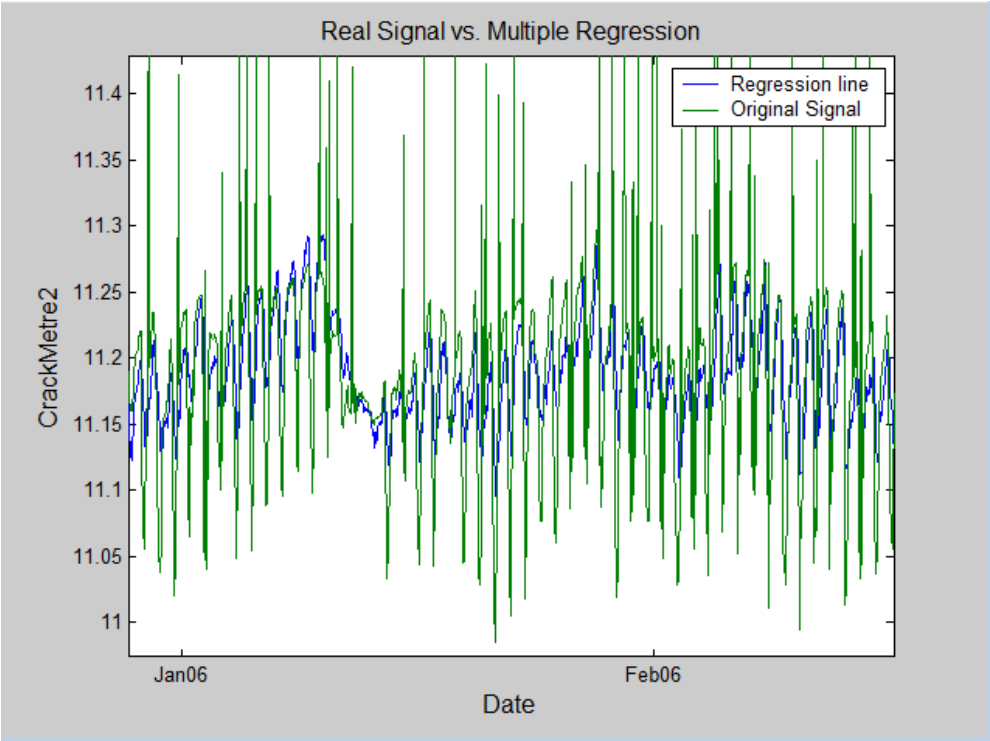

Figure 27: Static, Multiple Regression Analysis results

For all of the static regression analyzes, the numerical tool will provide the equation constants and their order in the command window, as well as provide the option of plotting the residuals, and displaying the mean and standard deviation of the error. In order to better compare regression models the user can also have this section of the numerical tool calculate regression quality criteria, including, the standard deviation of the residuals, loss function, final prediction error, and coefficient of determination.

This sub-program conducts all analysis, including display of information and plots, in the sub-program and associated functions; therefore, there is no data being returned to the main numerical tool program. Upon completion of its assigned tasks, the regression analysis, static modeling, displays the message "→ STATIC REGRESSION ANALYSIS SUCCESSFULLY COMPLETED←" in the command window.

4.2.8 Regression Analysis – Dynamic Modeling

The regression analysis dynamic modelling sub-program is initialized by the main numerical tool program. The user enters information into the main program indicating what signals are to be analyzed, maximum of one structural response and four environmental inputs, the model orders, and if the results should be plotted. Model orders specify the number of input channels for each signal, and the delays for each of the environmental inputs. All of this data is forwarded to the sub-program. When the dynamic regression analysis modelling sub-program initializes, "→ START OF REGRESSION ANALYSIS – DYNAMIC MODELING←" is displayed in the command window.

The dynamic regression modeling sub-program uses the existing Matlab auto regressive model with exogeneous inputs (ARX) to find history dependant relations. An auto regressive moving average model (ARMA) was decided against due to multiple programming difficulties. This sub-program, as well as the created function used by the sub-program, and the Matlab ARX function, carry out the calculation and display of the results shown in Figure 28. In the command window the sub-program will display information on the signals being analyzed, and the basic data resulting from the ARX model.

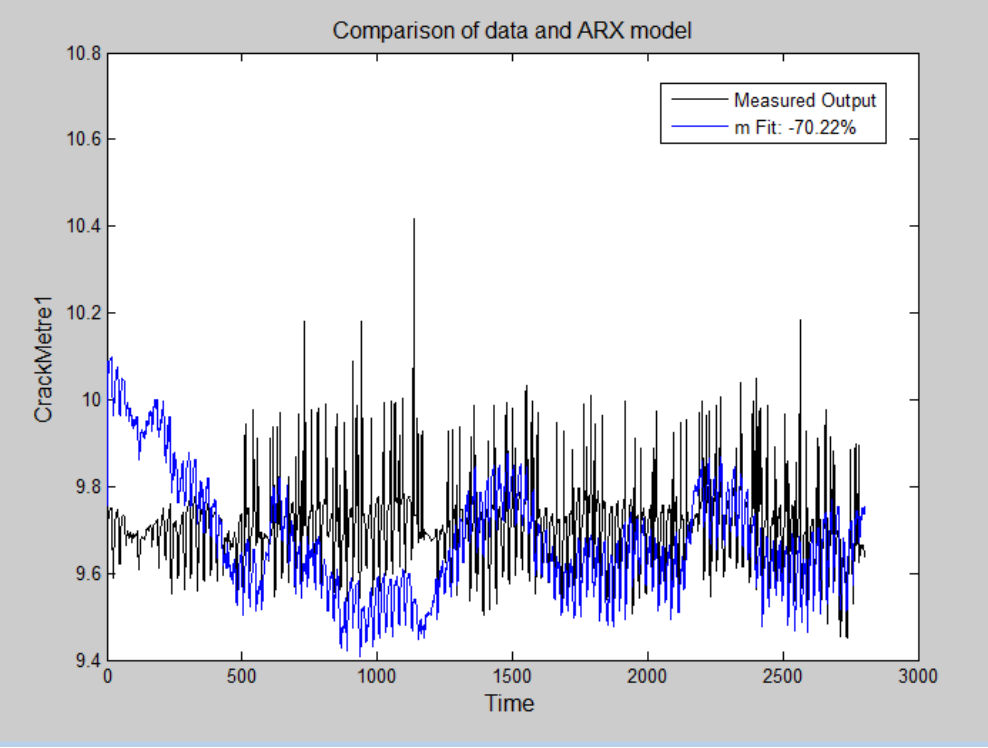

Figure 28: Comparison of data and ARX model

Matlab's internal ARX function assumes that each signal reading comes at a regular time interval. This is needed as the ARX model considers historic signal data and non-regular intervals will affect the accuracy of the results. When the ARX function completes, it will display the loss function and final prediction error in the command window.

If the normalized data option is activates a separate function receives the data, normalizes the data, and sends the normalized data to be ARX created function for the analysis and display of results. The plot option has been turned off in the normalized data function as the plot created by the non normalized data should be more useful in analysis. The normalized data section in the command window will start with ">>>>>>>>>>>>>>>", and finish with "<<<<<<<<<<<<<<<". The normalized data function relies on functions used by the actual signal data, and the results should be displayed first.

In order to best compare various model results, the numerical tool can provide regression analysis quality criteria. These criteria include the standard deviation of the residuals, loss function, final prediction error, and coefficient of determination.

This sub-program conducts all analysis, including display of information and plots, in the sub-program and associated functions; therefore, there is no data being returned to the main numerical tool program. Upon completion of its assigned tasks, the regression analysis, static modeling, displays the message "→ DYNAMIC REGRESSION ANALYSIS SUCCESSFULLY COMPLETED←" in the command window.

4.3 General Remarks

MIROVY is capable of importing the data, with minimal organization, from the data acquisition system and running a basic analysis. While many of these functions can be programmed on other systems, such as Microsoft Excel, this numerical tool aims to be faster and easier to use. Layout of the main program of the advanced numerical tool is designed to facilitate the creation of a graphical user interface, which will make MIROVY more user-friendly.

5 APPLICATIONS TO TWO CASE STUDIES

Two case studies are considered to demonstrate the capabilities of MIROVY and how it can assist the user in determining structural stability. These case studies are not intended to be reports on the structural stability of these structures, and should not be used in any structural analysis. For a proper report the user of the numerical tool should, at a minimum, have full knowledge of the structure, and its history. The author claims no such knowledge of these structures.

5.1 Oporto Cathedral

Oporto Cathedral is located in Porto, Portugal. The structure is Romanesque, and the initial building phase took place in the middle of the twelfth century (Azevedo, 2001). Construction continued into the thirteenth century, with significant changes being made in the seventeenth and eighteenth centuries (Azevedo, 2001). The main facade of the cathedral is shown in Figure 29, including the two bell towers. The Cathedral continues to be in use as a Catholic church, and the seat of the Porto Bishop.

Figure 29: Oporto Cathedral (Virtual Porugal, 2008)

During its lifespan the Oporto Cathedral has undergone previous structural interventions. The most recent structural intervention of the Oporto Cathedral took place at the start of the twenty first century, while earlier reconstruction dates back to the seventeenth century (Lourenco, Melo, & Carneiro, 2005). The most recent intervention was focused on the southern tower, addressing problems such as: poor connection between the leaves in the masonry wall, severe water infiltration into walls, and the outwards bulging of the tower (Lourenco, Melo, & Carneiro, 2005). The main strengthening consisted of using a confining steel ring to create a rigid frame that connected the interior and exterior using large anchorages, while some several locations also required ties (Lourenco, Melo, & Carneiro, 2005). Upon completion of the structural strengthening a monitoring system was installed to ensure the improved state of the tower was maintained.

5.1.1 Sensors

Sensors used in the Porto Cathedral are located in the southern tower. A rough schematic of the sensors locations is provided in Figure 30, (Ramos & Lourenco, 2007), while Table 9 provides more details on the sensors ID in the schematic. Three kinds of monitors are used to measure the structural response. Crack meters, Figure 31 (a), are installed on both exterior and interior cracks, located on what appear to have been the worse structural cracking. The bar extensometers, Figure 31 (b), are installed in the interior monitoring movement between the two walls. The tilt Meters, Figure 31 (c), are installed in two exterior perpendicular walls, shown here with a neighbouring surface temperature monitor.

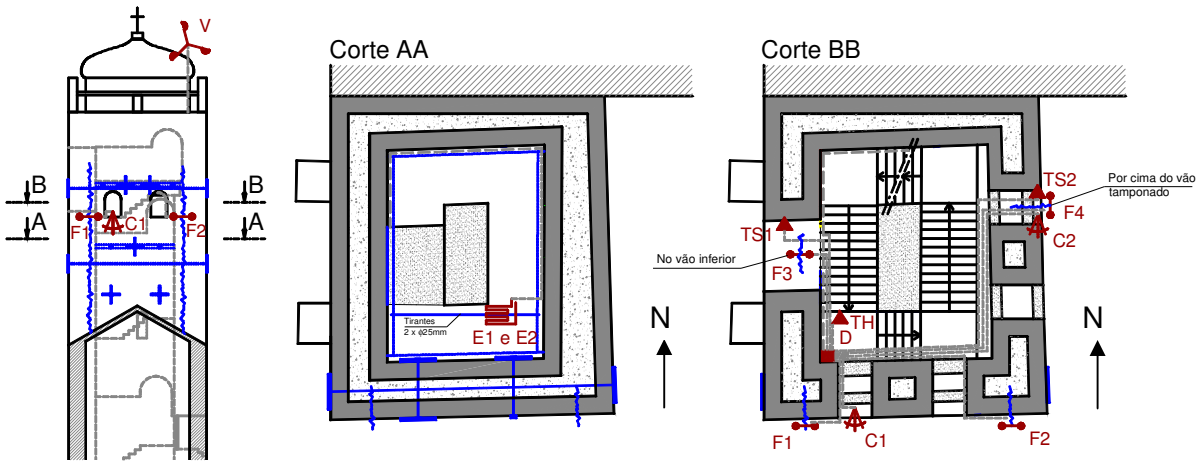

Figure 30: Location of Sensors in Oporto Cathedral (Ramos & Lourenco, 2007)

Table 9: Oporto sensor type and ID

Sensor ID	Sensor Type	Range	Resolution	Notes
F1 – F4	Crack Meters	± 30 mm	0.015 mm	-45 to 100ºC
E1 – E2	Extensometers	8 mm	0.001 mm	-45 to 100ºC
TS1 – TS2	Surface Temperature Sensors	-45 to 100ºC	0.05 ºC	-45 to 100ºC
TH	Combined Temperature Humidity Sensor	-30 to 70ºC 0 to 100%	±2%	-30 to 70ºC
C1 – C2	Tilt Meters	± 10º	$2.78x10^{-4}$ degrees	
V	Anemometer	0 to 60 m/s 0 to 360º	0.01 m/s 1º	
D	Data Logger (Data Acquisition System)	Max 32 Sensors		

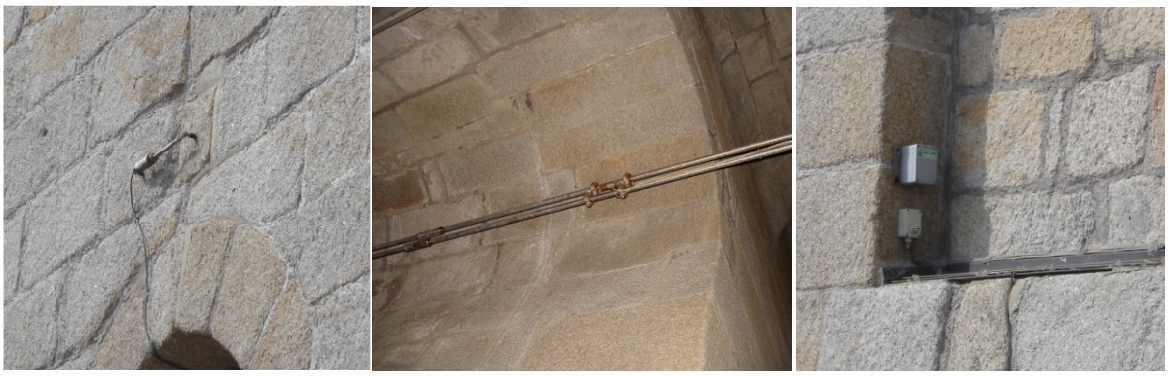

(a) (b) (c)

Figure 31: Oporto Cathedral (a) Crack Meter (b) Extensometer (c) Tilt Meter

The environmental input on the structure is monitored by temperature, relative air humidity, and wind velocity and direction. Relative air temperature and air humidity are measured with a combined sensor, Figure 32 (a), which is located in an interior corner. This type of location is preferable as it avoids direct sunlight, which can affect the quality of the results. Other temperature sensors are located in different positions around the structure, as shown in Figure 31 (c), where a surface temperature meter is installed with the tilt meter. The wind sensor, Figure 32 (b), records two channels of data, one corresponding to wind direction, and a second providing wind speed. This sensor is located at the top of the south tower, with the bottom of the cross in the left of the picture.

(a) (b)

Figure 32: Oporto Cathedral (a) Temperature Humidity Sensor (b) Wind Velocity Sensor

5.1.2 Creation of Data Files

Sensor data are collected from the data acquisition at regular intervals, and recorded as an ASCII file. Other than the sensor data, including time of each data entry, the data file contains a first column containing a marker number and a first row containing data acquisition identification information. No text is given in the file. In the case of Porto Cathedral thirteen text files were combined to give a file covering over three years of data. These files had an average sampling rate of one reading per hour, and the files were downloaded using a remote connection.

These files were uploaded into an Excel worksheet, and reviewed to verify that no duplicate data remained. The first column, containing a marker number, was removed, and the first row was replaced with the name of each signal. These names have no spaces so that the numerical tool is able to manipulate them properly. The data are then copied and pasted into a text file, with tab spacing.

Oporto Cathedral has two new signals added to the system after the first year. The numerical tool is not able to import data with rows of varying lengths, and filling the empty space with zeros could have an effect of the analysis of the signal as well as the proper functioning of the filters. Therefore, two text files are created, the first containing all signals but the recently added, the second file containing all signals, but no data points before the final two signals are added. Therefore for most analyses the first file is best used, having the longest history, but for any analysis requiring the final two signals the second file can be used.

5.1.3 Direct Results Analysis

The direct results analysis provides us with the maximum and minimum signal values. In Table 10 the maximum and minimum values are shown before and after the outlyers have been removed. For this analysis the outlyers are set as any value greater than three standard deviations from the mean. This becomes the confidence interval for our analysis, any data inside this interval is considered to be 'good' data. Figure 33 shows two sample signals with upper and lower bounds. The first of these samples is an example of a signal that will lose data that is potentially valuable. The second sample shows a signal that has three clearly erroneous data points that will be removed as outlyers. These two figures demonstrate the importance of selecting the acceptable range. With the Oporto Cathedral a range of three standard deviations is selected as it removes most clearly erroneous data, while minimizing the loss of potentially useful data. The first sample signal in Figure 33 is one of the few plotted signals to lose many data points.

Table 10: Maximum and Minimum Signal Values before and after Outlier Removal

Signal	Maximum Value with Outliers	Minimum Value with Outliers	Outlier Removed Maximum	Outlier Removed Minimum
Crack Meter 2 (mm)	12.5740	-11.3910	11.4250	10.8040
Crack Meter 1 (mm)	10.1480	9.2654	9.8616	9.3502
Crack Meter 3 (mm)	8.6542	-15.8470	8.6542	7.6518
Crack Meter 4 (mm)	10.2810	-17.1410	10.0790	9.1924
Bar Extensometer Upper (KHz)	2.6539	-0.0388	2.6508	2.6383
Bar Extensometer Lower (KHz)	2.6827	2.6294	2.6689	2.6349
Tilt Meter 1, Direction A	-6.5686	-8.1746	-6.5686	-7.5701
Tilt Meter 1, Direction B	-9.5726	-11.2540	-9.8823	-11.0870
Tilt Meter 2, Direction A	-3.9240	-5.8848	-4.5260	-5.3434

Table 10: Maximum and Minimum Signal Values before and after Outlier Removal (continued)

Signal	Maximum Value with Outliers	Minimum Value with Outliers	Outlier Removed Maximum	Outlier Removed Minimum
Tilt Meter 2, Direction B	-1.8720	-3.4980	-2.0320	-3.0365
Relative Humidity (%)	104.7800	14.7170	104.7800	26.0670
Relative Temperature (ºC)	30.6950	2.9520	27.0820	2.9520
Wind Direction (º)	360.5800	-2.3739	360.5800	-2.1475
Wind Velocity	25.5030	-13.0340	15.4090	-9.6171
Surface Temperature 1 (ºC)	44.8520	0.5952	38.4210	0.5952
Surface Temperature 2 (ºC)	40.9730	2.3467	31.0570	2.3467

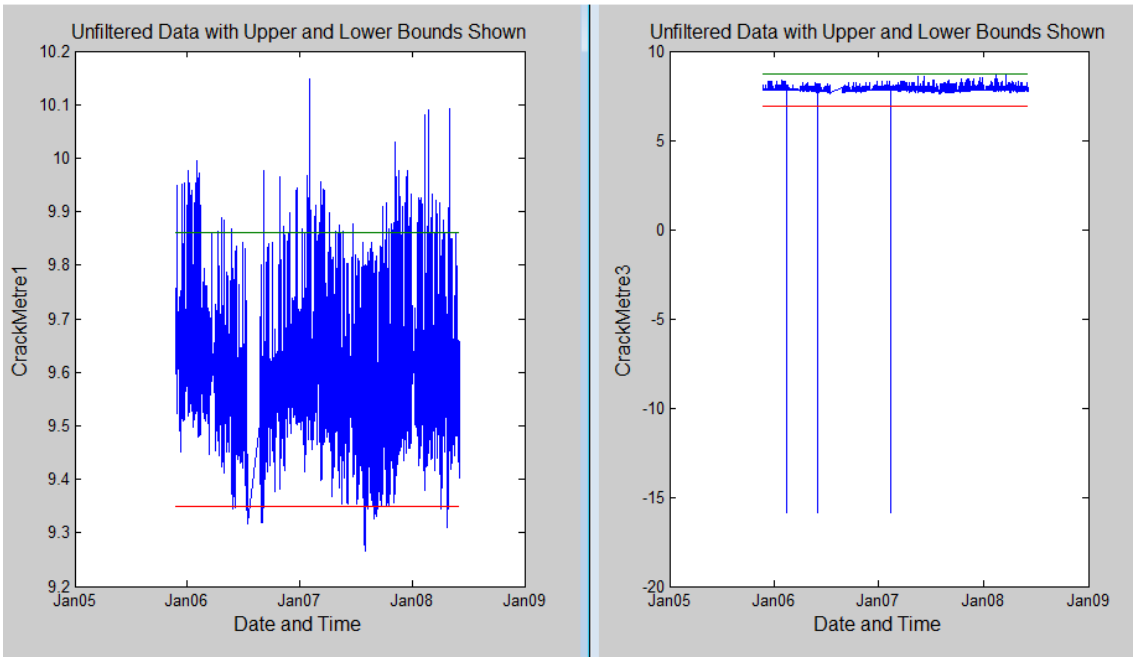

Figure 33: Sample unfiltered plots with upper and lower bounds at three standard deviations

Direct results analysis allows us to run a moving average filter to reduce the noise contained in the signal. The window size is set to fifty, decided by visual inspection. A larger window size provides a

smoother result, but has the potential to miss important data points; therefore fifty was selected. Figure 34 shows the data filtered with the moving average filtered line is shown in black, and in red is the data before the moving average filter is applied. Figure 35 shows a section of the signal zoomed in for clarity. Note the gap showing in Figure 34, this is caused by a jump in available data.

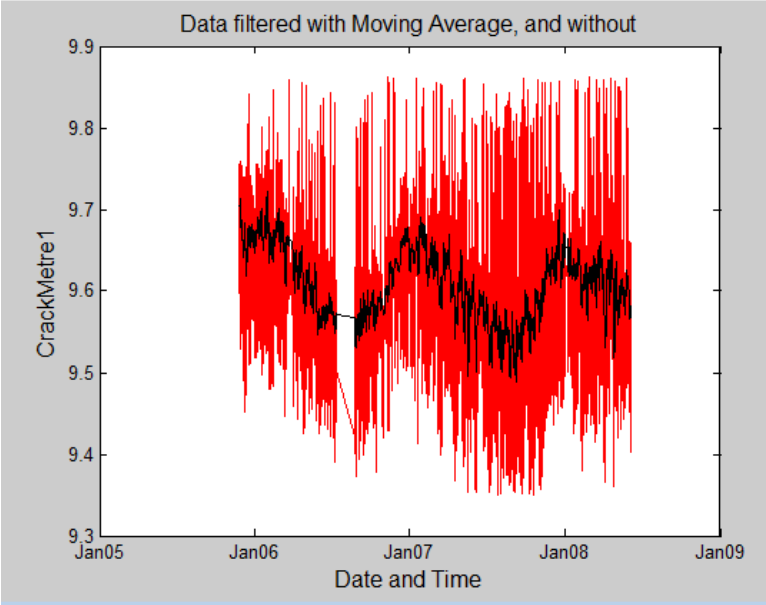

Figure 34: Data filtered with moving average filter compared to unfiltered

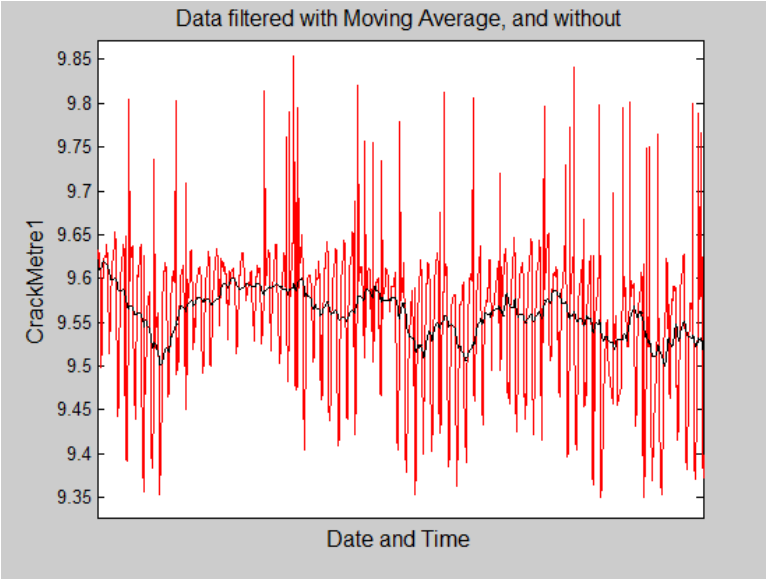

Figure 35: Close up on Data filtered with moving average compared to unfiltered

5.1.4 Simple Statistical Analysis

The simple statistical analysis is run on data provided by the direct results analysis, therefore, filtered data. Table 11 displays the resulting mean, standard deviation, coefficient of variation, and signal to noise ratio as calculated by the numerical tool. The crack Meters and extensometers have high signal to noise ratios when compared to the tilt meters. The signal to noise ratio is the lowest among the environmental signals.

Table 11: Simple statistical analysis by signal

Signal	Mean	Standard Deviation	Coefficient of Variation	Signal to Noise Ratio
Crack Meter 2 (mm)	11.0632	0.0466	0.4216	237.2
Crack Meter 1 (mm)	9.6080	0.0434	0.4517	221.4
Crack Meter 3 (mm)	7.8191	0.0373	0.4773	209.5
Crack Meter 4 (mm)	9.4571	0.0530	0.5609	178.3
Bar Extensometer Upper (KHz)	2.6442	0.0019	0.0706	1416.5
Bar Extensometer Lower (KHz)	2.6508	0.0061	0.2309	433.1
Tilt Meter 1 Direction A	-6.9893	0.1636	2.3404	42.7
Tilt Meter 1 Direction B	-10.6010	0.1740	1.6409	60.9
Tilt Meter 2 Direction A	-5.0144	0.1539	3.0688	32.6
Tilt Meter 2 Direction B	-2.4719	0.1909	7.7221	12.9
Relative Humidity (%)	74.0759	12.5285	16.9131	5.9
Relative Temperature (ºC)	13.9208	3.9293	28.2263	3.5
Wind Direction	172.8054	49.0553	28.3876	3.5
Wind Velocity	3.2519	2.8392	87.3094	1.1

Table 11: Simple statistical analysis by signal (continued)

Signal	Mean	Standard Deviation	Coefficient of Variation	Signal to Noise Ratio
Surface Temperature 1 (ºC)	18.2452	5.5289	30.3034	3.3
Surface Temperature 2 (ºC)	15.3095	3.9961	26.1021	3.8

For the creation of histogram and cumulative distribution function one hundred bins were selected. There are around twenty thousand samples; therefore one hundred bins should give acceptable results, while the number remains small enough to give a clear plot. Figure 36 show the almost normally distributed results for crack meter 4.

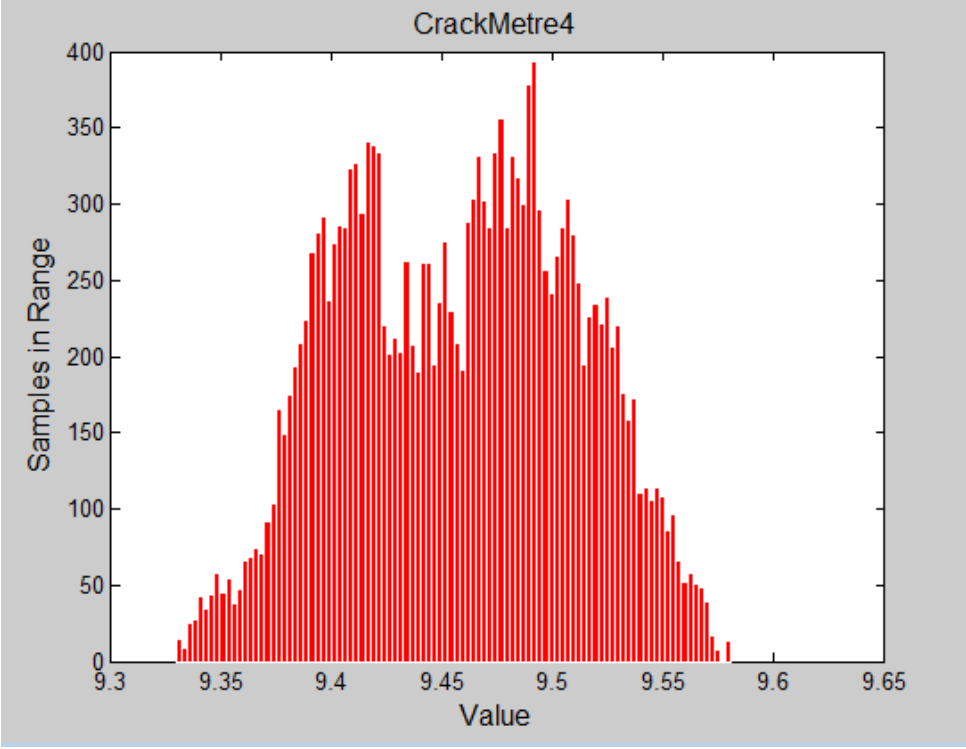

Figure 36: Histogram sample from Oporto Cathedral

5.1.5 Regression Analysis

The coefficient of determination (r^2) value for all signals, representing the correlation between signals, is shown in matrix format in Table 12. Using this data it is possible to select the signals to run the regression analysis on. The higher the value the more likely there is a relation between the two

signals. The first signal, representative of time, has been removed; therefore, no row one and no column one. On Table 12 it can be seen that there is a good correlation between the surface temperature 2 and the crack meter 2 sensors, while the relative humidity has poor correlation with all signals.

Table 12: Matrix of the Oporto Cathedral Coefficients of Determination

	Crack Meter 2	Crack Meter 1	Crack Meter 3	Crack Meter 4	Tilt Meter 1, Direction A	Tilt Meter 1, Direction B	Tilt Meter 2, Direction A	Tilt Meter 2, Direction B	Relative Humidity	Relative Temperature	Wind Direction	Wind Speed	Surface Temperature 1	Surface Temperature 2
Crack Meter 2	-													
Crack Meter 1	0.97	-												
Crack Meter 3	0.85	0.84	-											
Crack Meter 4	0.93	0.92	0.87	-										
Tilt Meter 1, Direction A	0.53	0.51	0.43	0.43	-									
Tilt Meter 1, Direction B	0.13	0.13	0.14	0.2	0.05	-								
Tilt Meter 2, Direction A	0.32	0.35	0.26	0.28	0.71	0.16	-							
Tilt Meter 2, Direction B	0.65	0.62	0.66	0.7	0.49	0.12	0.26	-						
Relative Humidity	0.06	0.05	0	0.02	0.04	0.02	0.01	0.01	-					
Relative Temperature	0.91	0.88	0.9	0.93	0.41	0.24	0.2	0.74	0.02	-				
Wind Direction	0.07	0.09	0.16	0.15	0.01	0.05	0.04	0.13	0.22	0.13	-			
Wind Speed	0	0	0	0	0.02	0	0	0.02	0.04	0	0	-		
Surface Temperature 1	0.82	0.84	0.76	0.82	0.42	0.06	0.38	0.46	0.02	0.77	0.15	0.01	-	
Surface Temperature 2	0.93	0.91	0.89	0.94	0.38	0.25	0.2	0.69	0.03	0.99	0.11	0	0.78	-
Extensometer Above	0.58	0.63	0.57	0.65	0.21	0.62	0.24	0.41	0.01	0.63	0.10	0.01	0.45	0.66
Extensometer Below	0.30	0.29	0.43	0.37	0.20	0.46	0.00	0.53	0.02	0.45	0.04	0.11	0.07	0.45

5.1.6 Enhanced Analysis with the Advanced Numerical Tool

In the following sections a more detailed analysis of each signal group will be provided.

5.1.6.1 Crack Meters

Crack Meter two is hooked into the data acquisition system as the first incoming signal; therefore, it will be used to demonstrate general findings for all crack meters. For three of the four crack meters obvious outlyers existed, cause of which is unknown. However, judging the data based on Figure 37 the data appears to be an error, and will be removed.

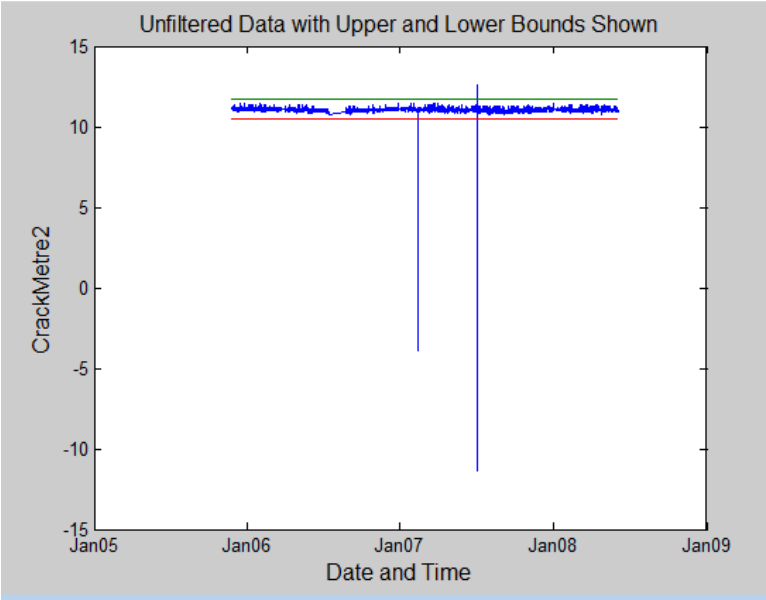

Figure 37: Crack Meter 2 Signal, Unfiltered with Upper and Lower Bounds

Figure 38 shows the filtered signal. The filtered signal follows the expected seasonal oscillation, indicating likely relation to temperature. First impression with regard to the crack stability is that the crack movement is reducing over time. This may be due to the previous conservation work undertaken at the site. It is interesting to note that while the standard deviation appears to be reducing, the mean crack size appears to remain the same.

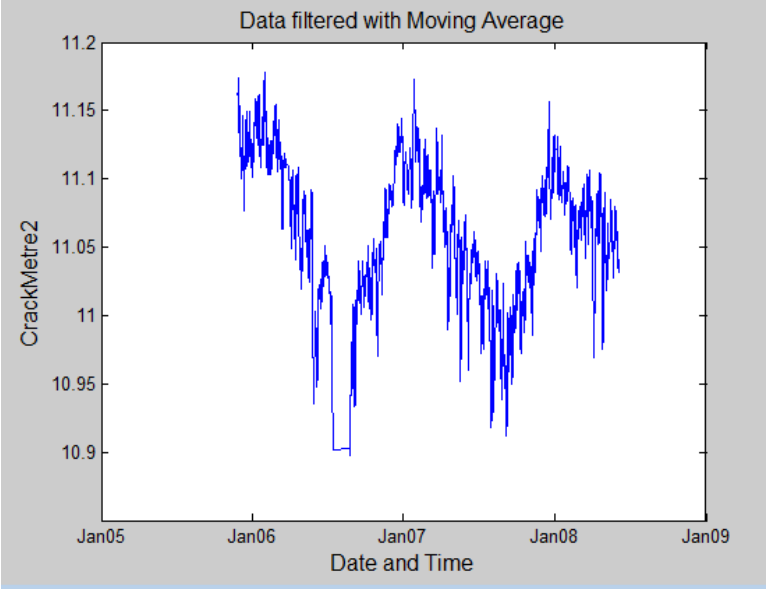

Figure 38: Crack Meter 2 Signal, After Filtering

The histogram created using crack meter two data, Figure 39, shows a normally distributed function. This is shown as it is the expected result for a crack Meter.

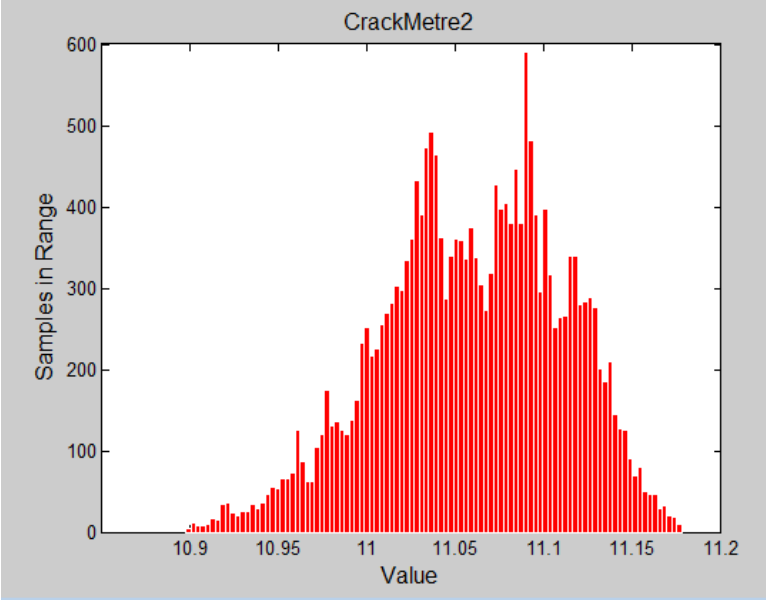

Figure 39: Crack Meter 2, Histogram

The polynomial regression analysis comparing the crack meter 2 to the surface temperature 2, which was chosen because of the high value of correlation, shows a clear linear relation in Figure 40. An equation representing the relationship as calculated by Matlab is given in equation (23). Where y

represents the crack meter 2 readings, x represents the surface temperature 2 readings. Figure 40 clearly shows that with an increase in temperature will cause a decrease in crack width, and a decrease in temperature will cause further opening of the crack.

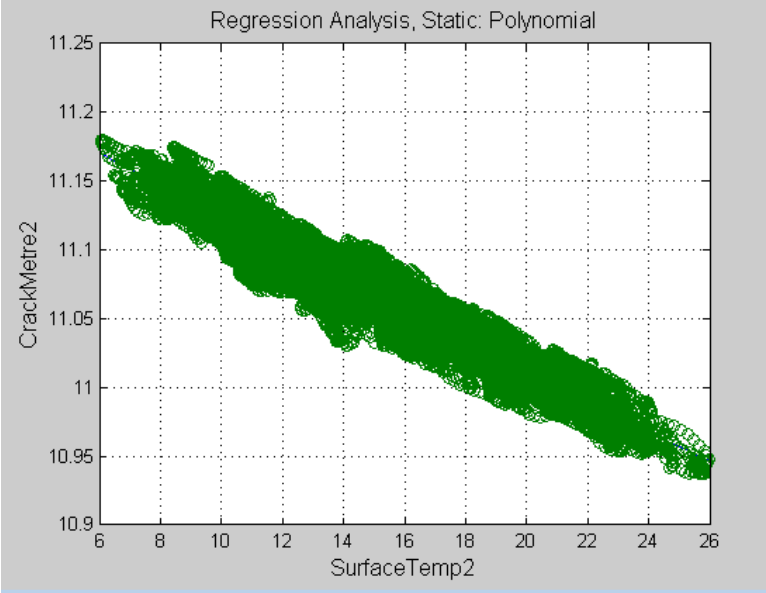

Figure 40: Relation between Crack Meter 2 and Surface Temperature 2

$$y = 11.2444 - 0.0125 * x \qquad (23)$$

Various error indicators and their results from crack meter 2 are shown in Table 13.

Table 13: Crack Meter 2, Single Regression Error Indicators

Error indicator:	Crack Meter 2
Standard Deviation of Error	0.0126
Loss Function	1.5920×10^{-4}
Final Prediction Error	1.5925×10^{-4}
Coefficient of Determination	6.8967×10^{-8}

For the multiple regression analysis, one output is crack meter 2; the two inputs are surface temperature 2 and tilt meter 2 direction B. The resulting regression line is shown and compares to the original signal in Figure 41. Results appear to have good correlation to the original signal. The resulting equation, equation (24), is shown below; where y represents the crack meter response, x

and z represent surface temperature 2 and tilt meter 2 direction B structural input respectively. If the data were to be normalized it would give the equation (25), which clearly shows that the surface temperature sensor 2 has the greatest effect on the data.

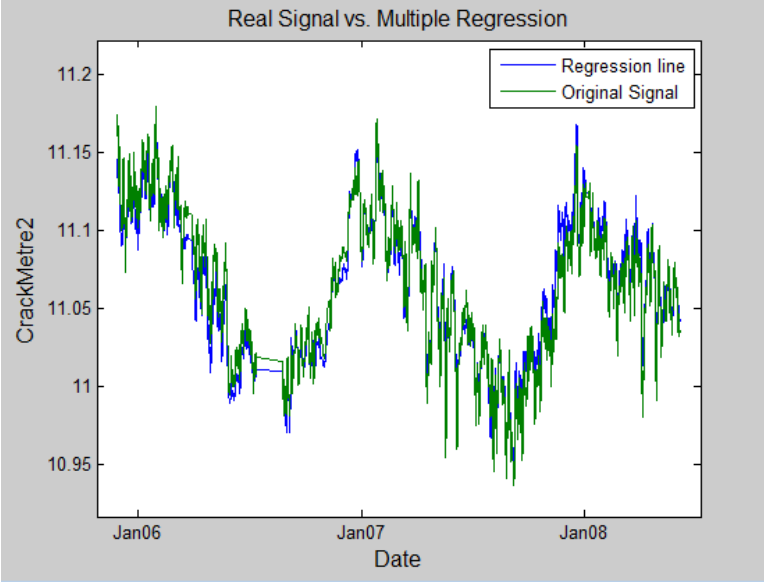

Figure 41: Crack Meter 2, Multiple Regression Analysis Results

$$y = 11.6812 + 0.0108 * x + 0.4963 * z + 0.0129 * x * z + 0.0003 * x^2 + 0.1396 * z^2 \quad (24)$$

$$y = -0.9724 * x + 0.0088 * z + 0.2092 * x * z + 0.1054 * x^2 + 0.1090 * z^2 \quad (25)$$

Error of the multiple regression analysis is shown in Table 14. A plot of the residuals gives Figure 42, which appears to show that the regression analysis becomes less accurate at the signal ends.

Table 14: Crack Meter 2, Multiple Regression Error Indicators

Multiple Regression Error indicator:	Crack Meter 2
Standard Deviation of Error	0.0124
Loss Function	1.5362×10^{-4}
Final Prediction Error	1.5371×10^{-4}
Coefficient of Determination	0.9294

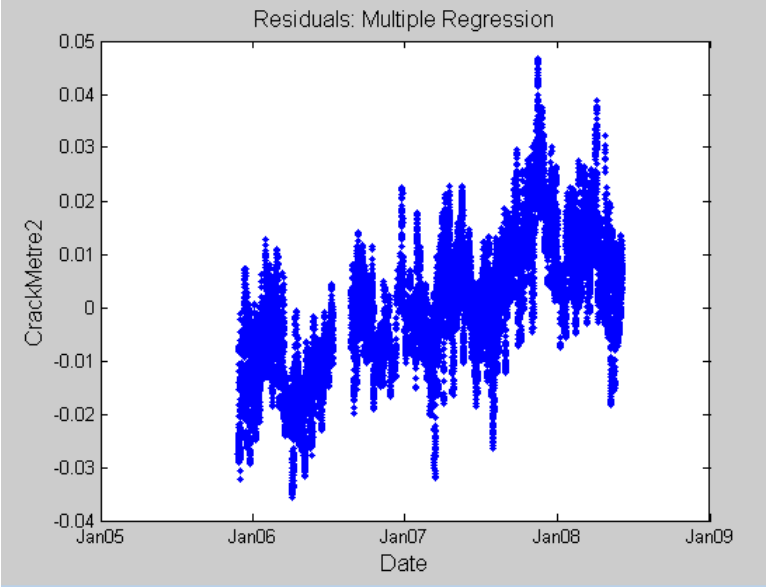

Figure 42: Crack Meter 2, Multiple Regression Residuals

Several ARX analyzes of the crack meter 2 signal were also run, the analysis with lowest final prediction error is shown in Figure 43. The two environmental inputs were relative temperature and relative humidity, while all *na* and *nb* values were set equal to 4, all *nk* values set equal to zero. Resulting relation has error shown in Table 15. These results give mixed information. The loss function and final prediction error suggest that the ARX model is more accurate, however the standard deviation of error is much higher and coefficient of determination much lower than in the static regression analysis, suggesting that the analysis is less accurate. A general conclusion that can be drawn from the quality criteria is that even though the correlation of the two signals may not be as strong, the seasonal variation can be reproduced with some confidence.

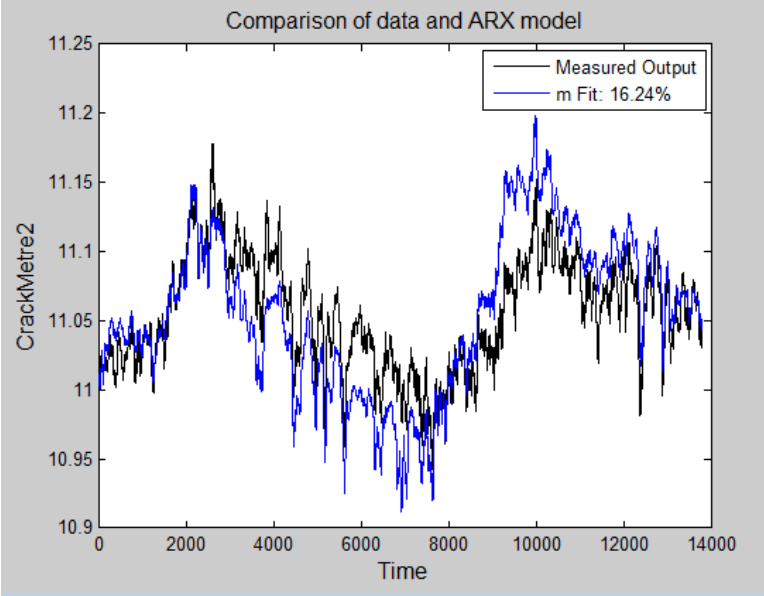

Figure 43: Crack Meter 2, ARX Model Results

Table 15: Crack Meter 2, ARX Regression Error Indicators

ARX Regression Error indicator:	Crack Meter 2
Standard Deviation Error	1.0945
Loss Function	1.0339×10^{-6}
Final Prediction Error	1.0357×10^{-6}
Coefficient of Determination	0.1255

5.1.6.2 Extensometers

The upper and low extensometers were installed after the rest of the system was in place. Previously in place were two extensometers that used vibration to determine the elongation; however, since these were installed on metals bars that vibrated the data was unusable. The new extensometers work on a different principle and supply good data. The gathered data is similar, and as the upper extensometer has a lower coefficient of variation it will be investigated.

Figure 44 shows the first two years of data for the upper extensometer, and while this is not enough time to draw any conclusions with regard to long term structural stability, the signal will be analyzed. The structural movement is not the smooth curve expected, containing seasonal points which appear to occur in December each year. It is possible this is related to the function of the structure at this time of

year, but requires further study. However, Figure 44 does appear to show that the extensometer is under less stress, and therefore, that the walls of the structure are gradually coming closer together.

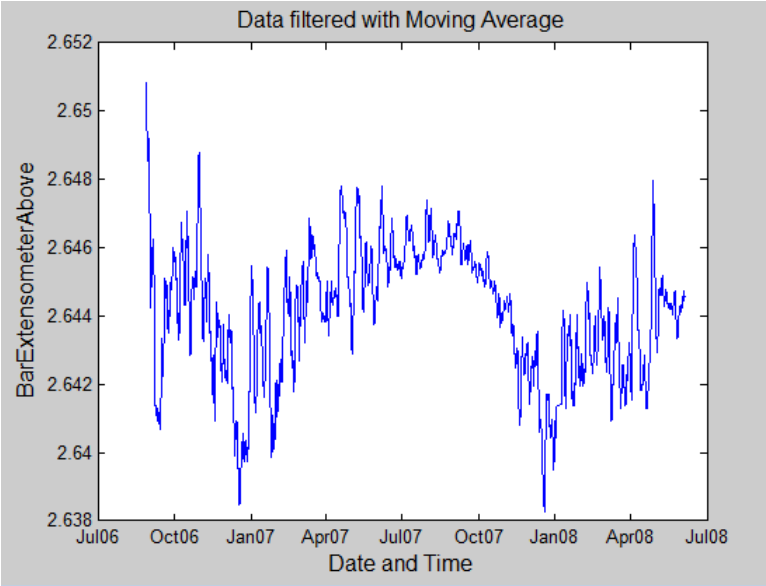

Figure 44: Extensometer Above, Filtered Data

The histogram created by the extensometer, shown in Figure 45, demonstrates the Gaussian distribution of the data and low signal variation.

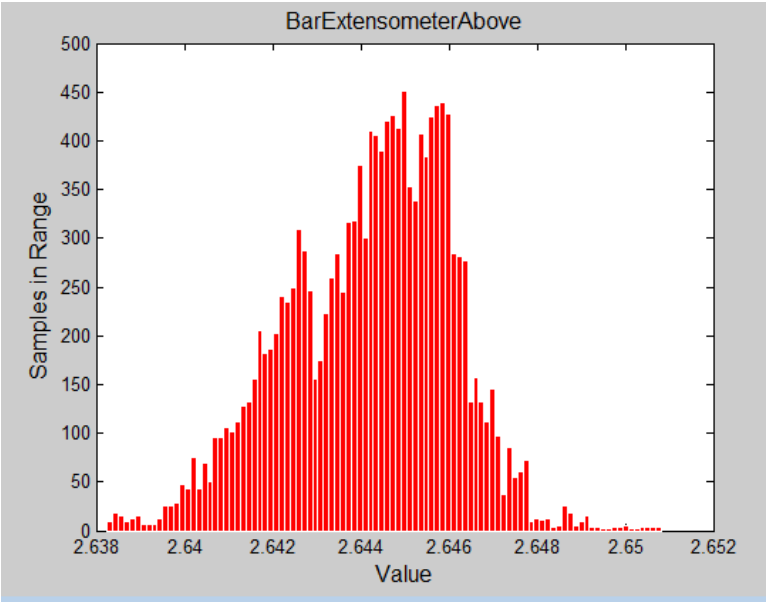

Figure 45: Extensometer Above, Histogram

The static regression analysis first compared the extensometer results to the relative temperature, then using the multiple regression compared the extensometer to relative temperature, tilt meter 1 direction b, and crack meter 4. There appears a noticeable correlation, although not as strong as was discovered between crack meter 2 and surface temperature 2. Results and residual plots of these regression analyzes are shown in Figure 46, while Table 16 displays standard deviation of error, loss function and final predicted error for each value.

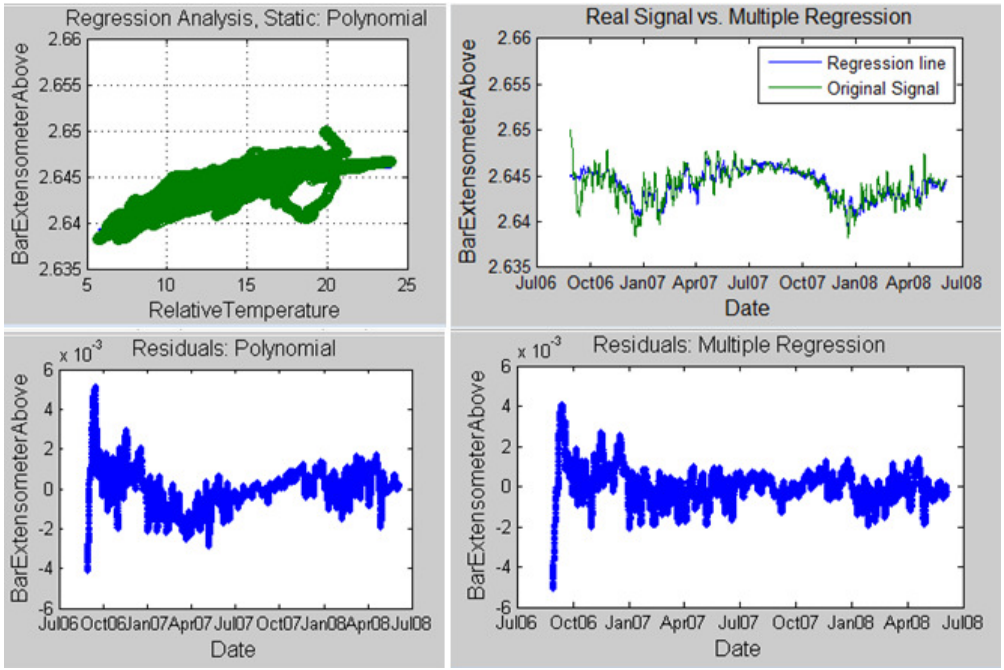

Figure 46: Extensometer Above, Static Regression

Table 16: Extensometer Above, Static Regression Error Summary

	Standard Deviation of Error	Loss Function	Final Prediction Error	Coefficient of Determination
Single Regression	0.0010	1.0548×10^{-6}	1.0553×10^{-6}	0.6326
Multiple Regress.	0.0009	7.2707×10^{-7}	7.2812×10^{-7}	0.7711

Equations (26) through (29) provide, in the following order: the polynomial regression equation based on normalized data, the polynomial regression equation based on actual data, the multiple regression equation based on normalized data, the multiple regression equation based on actual data. In the following equations y represents the upper extensometer, x the relative temperature, z the tilt

meter 1, direction B data, and w represents the readings obtained from crack meter 4. No strong relations appear in the regression analysis results.

Polynomial Regression: Normalized Data

$$y = 0.8061 * x - 0.1708 * x^2 \quad (26)$$

Polynomial Regression: Actual Data

$$y = 2.6341 + 0.0010 * x - 0.0000 * x^2 \quad (27)$$

Multiple Regression: Normalized Data

$$y = 0.12x + 0.47z - 0.34w - 0.05xz + 0.56xw + 0.20zw + 0.18x^2 + 0.08z^2 + 0.32w^2 \quad (28)$$

Multiple Regression: Actual Data

$$y = 22.51x - 0.058z - 0.330w - 4.470xz + 0.052zw + 0.007z^2 + 0.260w^2 \quad (29)$$

5.1.6.3 Tilt Meters

The second tilt meter will be analyzed as representative of both tilt meters. Each tilt meter provides data on two perpendicular directions, and provides this data as two inputs for the data acquisition system. In order to review the data we will investigate both of these signals. Figure 48 shows the filtered data from directions A and B respectively, while Figure 47 shows the tilt meter location and directions. Direction A, North, appears to show that the tower is leaning further than before, while direction B, South, shows a stepped leaning.

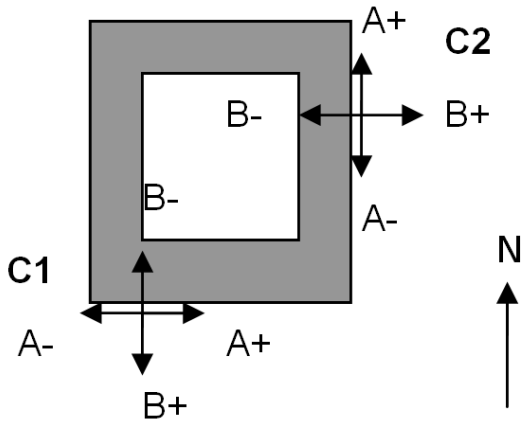

Figure 47: Oporto Cathedral Tilt Meter Directions (Ramos & Lourenco, 2007)

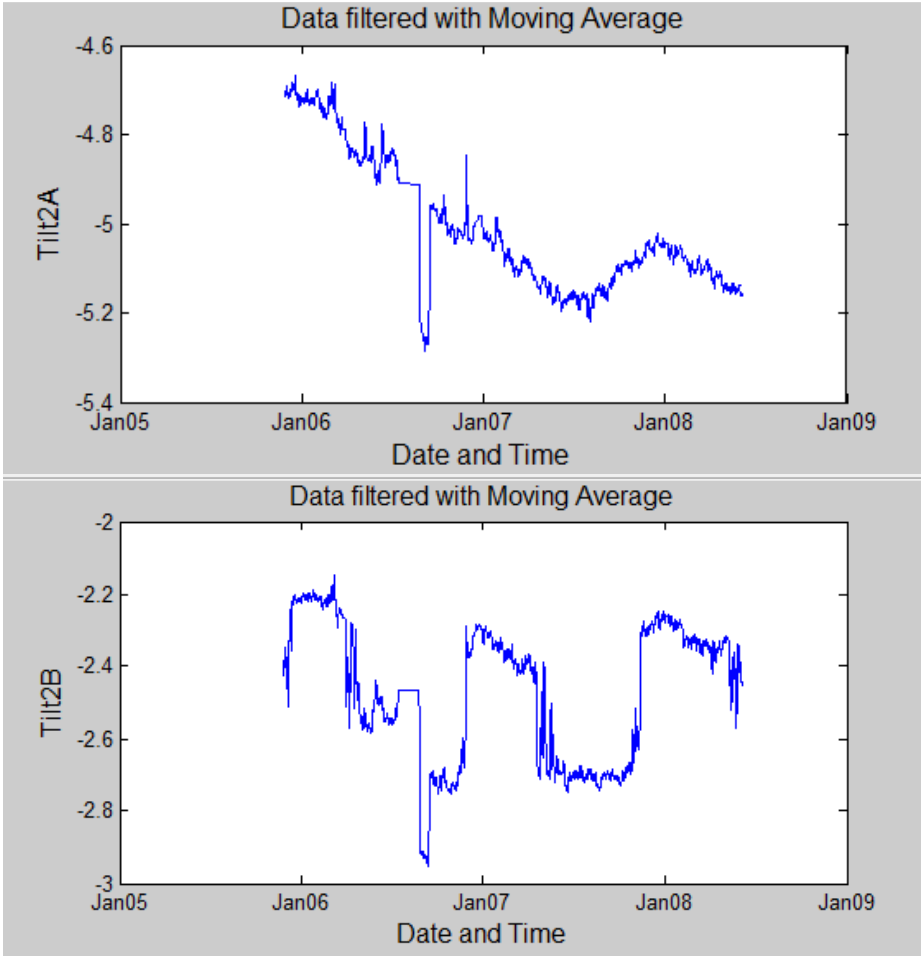

Figure 48: Tilt Meter 2, Filtered Data

It is unknown if the tilt meter was zeroed, as described by manufacturer information (Durham Geo, 2008); however, if this was the case conclusions can be drawn on the direction of tilt. Figure 48 also

shows that both direction A and B of tilt meter 2 are negative, indicating that this part of the tower is tilting in the South West direction, with direction A, South, being the more inclined. A review of Table 11 shows that tilt meter 1 is also negative in both directions, in that case indicating tilt in the North West direction. From this the conclusion can be drawn that the tower is tilting West, and undergoing twist.

The histograms shown in Figure 49 tell us that in direction A the tower is often at the greater degree in its tilt range, while direction B does not have this lopsided tendency. Therefore we can draw the conclusion that the tower is more vulnerable in the A direction, and extrapolate that to indicate that the twisting phenomena is more likely to cause serious damage than the Westward tilt.

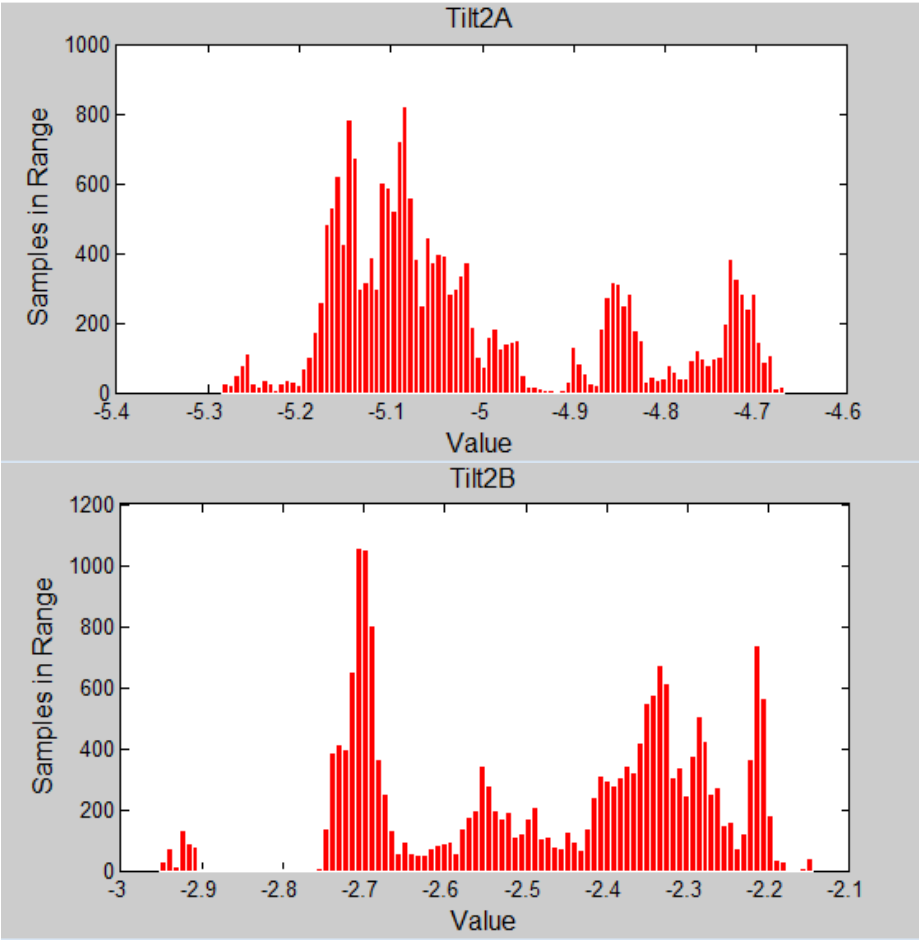

Figure 49: Tilt Meter 2, Histogram

The static, single regression analysis of the tilt meter, direction B, related to the relative temperature, shows some relation between data sets, but contains significant error, as seen in Figure 50. From this it can be decided that the relative temperature relates to the tilt, higher temperature causing greater

tilting, but this correlation is not strong enough to make predictions of any accuracy. Some tilt meters are sensitive to direct sunlight; therefore the daytime data is removed, providing Figure 51. In order to remove the daytime data the time selection sub-program is used. Table 17 shows the quality criteria of each regression analysis, that containing daytime data and that without daytime data. It can be clearly seen that the daytime signal is just as good as or better than the night time only signal.

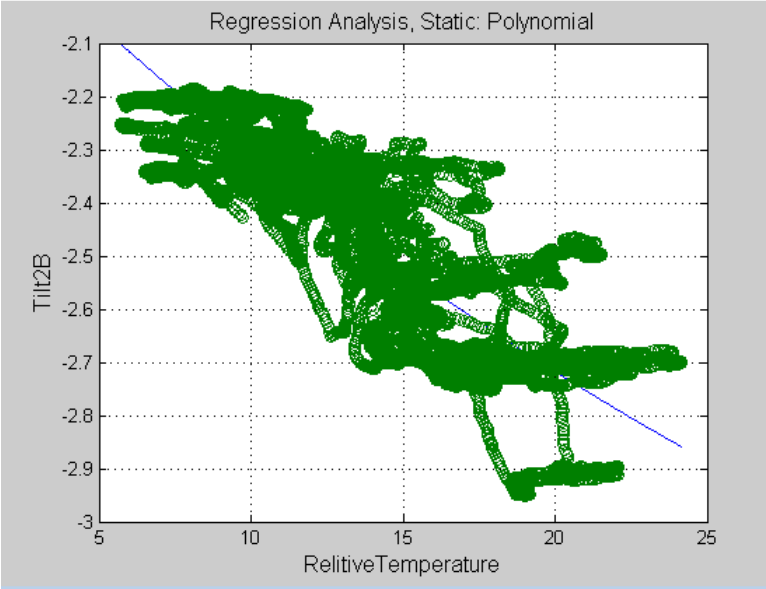

Figure 50: Tilt Meter 2, Relation to Temperature

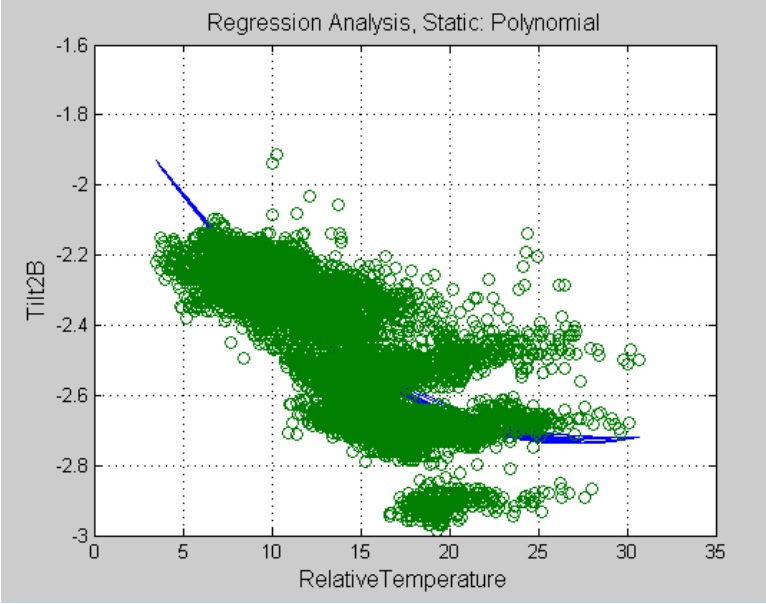

Figure 51: Tilt Meter 2, Night time Relation to Temperature

Table 17: Tilt Meter 2, Compared Quality Criteria

	Standard Deviation of Error	Loss Function	Final Prediction Error	Coefficient of Determination
All Data	0.0972	0.0094	0.0095	0.7389
Night Only	0.1180	0.0139	0.0139	0.6082

A multiple regression analysis is carried out on the tilt meter 2, direction B signal, and is shown in Figure 52. The analysis inputs are relative air temperature and surface temperature 2. The resulting loss function and final prediction error are equal to 0.0072. Equations (30) and (31) show the normalized and actual relations respectively. It appear that the relative temperature, x, has a greater effect than the surface temperature, y.

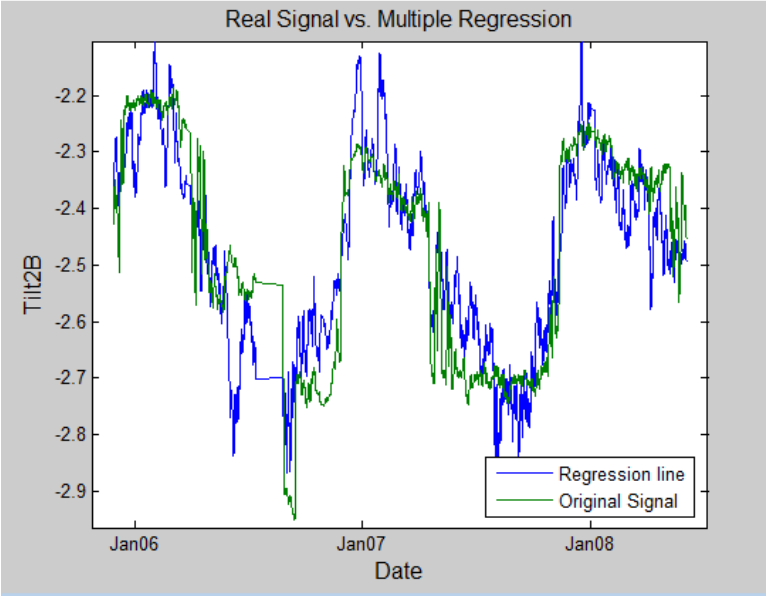

Figure 52: Tilt Meter 2, Multiple Regression Analysis

$$y = -2.3186x + 1.4714z - 1.1170xz + 0.2686x^2 + 0.8714z^2 \quad (30)$$

$$y = -1.7573 + 0.0163x - 0.0779z - 0.0153xz + 0.0037x^2 + 0.0118z^2 \quad (31)$$

5.1.6.4 Relative Humidity

Relative humidity is an environmental input that may affect the structure. It is interesting to note, as shown in Figure 53, that the relative humidity is often in the range of eighty percent.

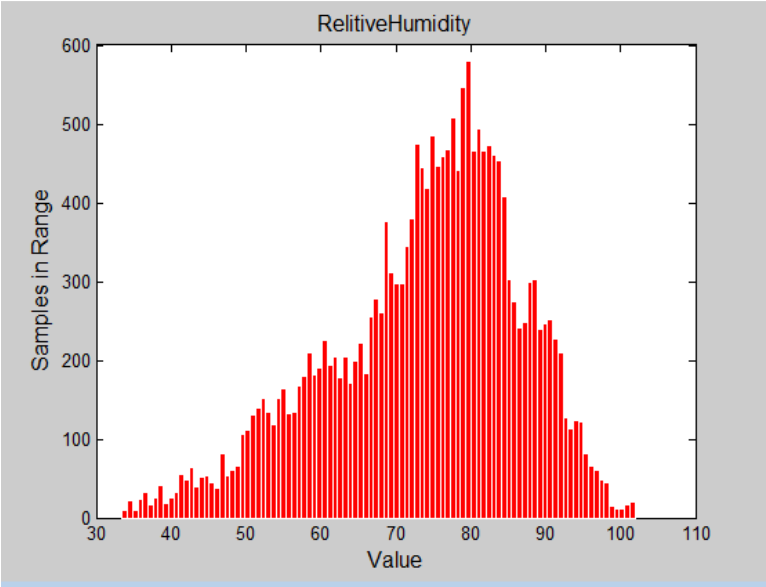

Figure 53: Relative Humidity, Histogram

5.1.6.5 Relative Air Temperature

Temperature is the environmental parameter that most often has a high coefficient of determination in relation to structural reactions. Figure 54 shows that the temperature follows the predicted oscillation between summer heat and winter cool; this is the most likely cause for the structural response signals having similar seasonal oscillations.

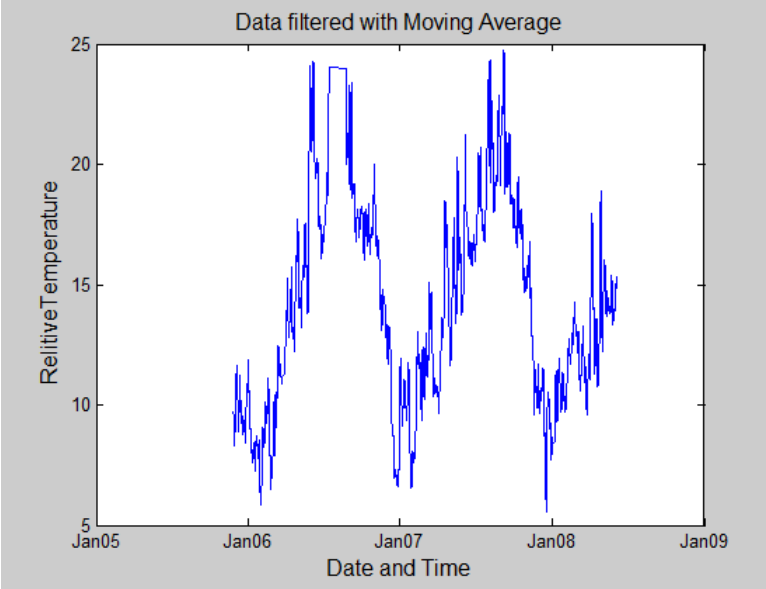

Figure 54: Relative Temperature, Filtered Data

5.1.6.6 Wind Direction and Speed

Wind velocity is provided by the sensors in two channels, one providing wind direction, and a second providing wind velocity. The resulting histograms, shown in Figure 55, show us that the wind is typically blowing in the one hundred to two hundred and fifty degree range, has a mean speed of four, and standard deviation of approximately two. The filtered data does not appear to show any seasonal trends and therefore are not shown. According to the wind velocity signal, there are several negative wind velocities recorded, which could not exist. The sensor was not designed for negative wind velocity input, and its existence indicates possible errors in the sensor, either the signal should actually be the absolute value of the number, or the errors are more complex in nature. Presently the numerical tool does not have the ability to remove these values before the histogram is created. Fortunately, there are relatively few negative samples and the effect will be minimal.

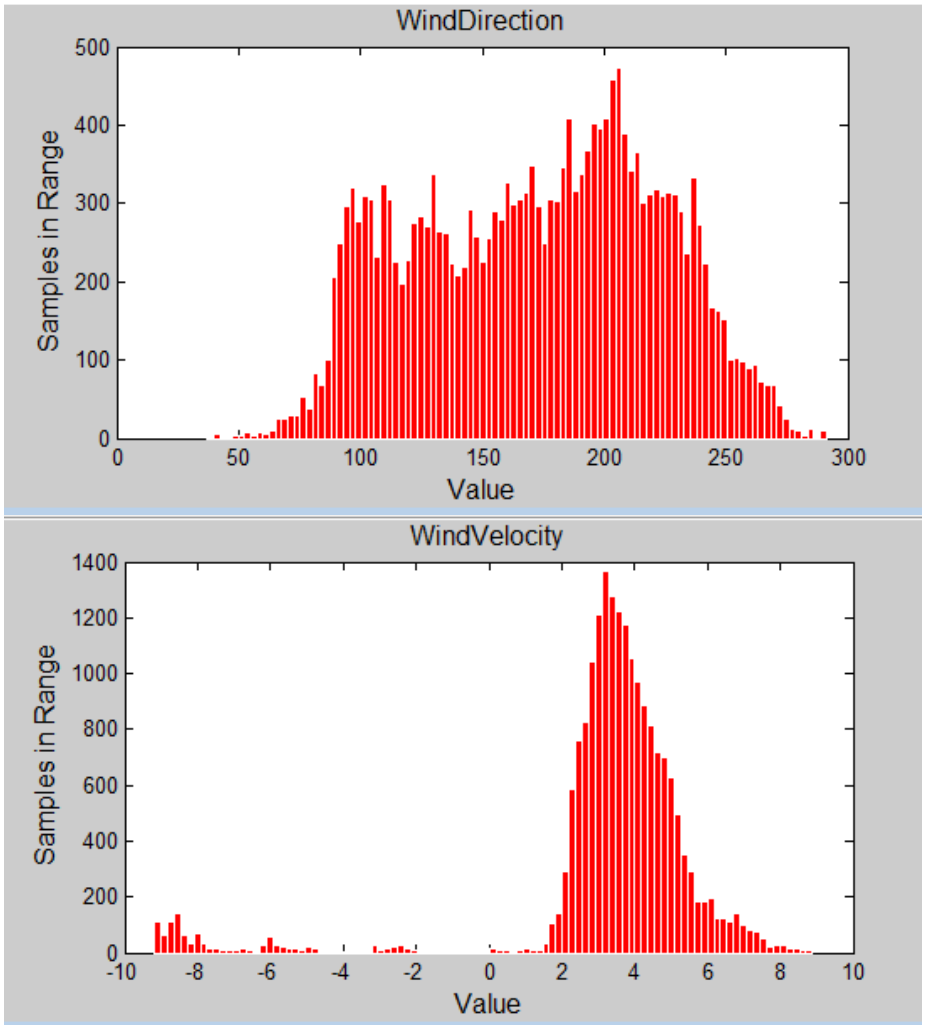

Figure 55: Wind Direction and Speed, Histogram

5.1.6.7 Surface Temperature

The filtered surface temperature data, shown in Figure 56, are similar to the relative temperature signal, with higher maximum values. This is no surprise as the surface temperature probes could be in sunlight, and do not have the surrounding stone temperature buffer.

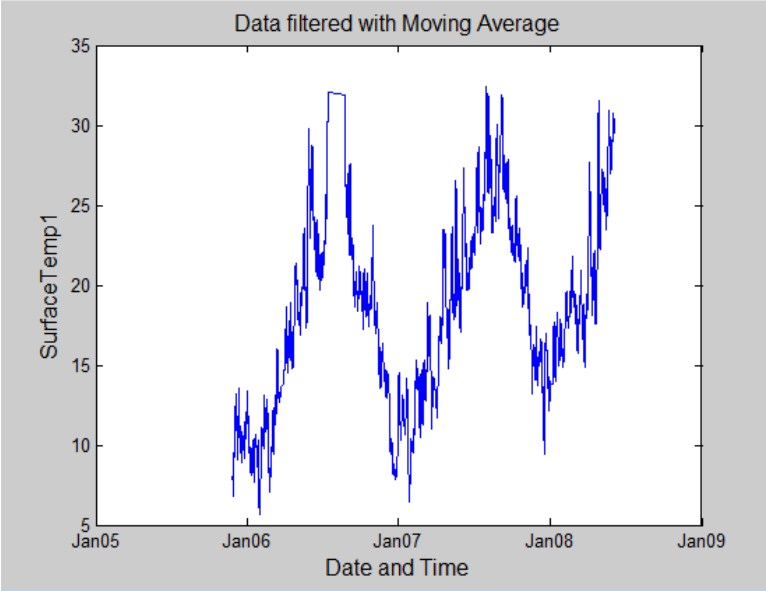

Figure 56: Surface Temperature 1, Filtered Data

5.1.7 General Notes on Oporto Cathedral

The analysis results suggest that the cracks are becoming less active, which is a positive indicator for the structure. However, the tilt in one direction appears to be getting worse, and this would have a negative impact on the structure. Further analysis would be beneficial. This investigation, however, falls outside the scope of this thesis.

5.2 Monastery of Jerónimos

Monastery of Jerónimos, Lisbon, dates back to the sixteenth century, and has become one of the most famous pieces of built heritage in Portugal (Ramos L. F., 2007). Figure 57 shows the Monastery of Jerónimos. The monastery compound covers an area of over fifteen thousand square Meters, evolving around two courts (Ramos L. F., 2007).

Figure 57: Monastery of Jerónimos (Freire, 2008)

5.2.1 Sensor Locations

All sensors at the Monastery of Jerónimos are located in the church. Previous structural studies have identified four key structural issues (Mourao, 2002) (Oliveira D. V., 2003) (Oliveira, Ramos, Lourenco, & Roque, 2005) (Lanco, 2006) (Lourenco, Krakowiak, Fernandes, & Ramos, 2007) (Ramos L. F., 2007). First issue is a possible failure mechanism involving columns and vaults, and could cause the collapse of the church nave. Second issue is a possible failure mechanism involving the external walls and vaults, and could cause the collapse of the church transept. Third issue is the compressive strength of the masonry, and its effect on the structural response. And the fourth issue is excessive slenderness of nave columns. Study of these issues and a detailed modal identification of the church, undertaken by Ramos (Ramos L. F., 2007), determined the best locations for the monitoring system. Figure 58 shows the location of each sensor, while Table 18 provides a legend providing details on each sensor. The two uniaxial tilt meters provide the structural response, while the remaining sensors provide environmental input information and distributions.

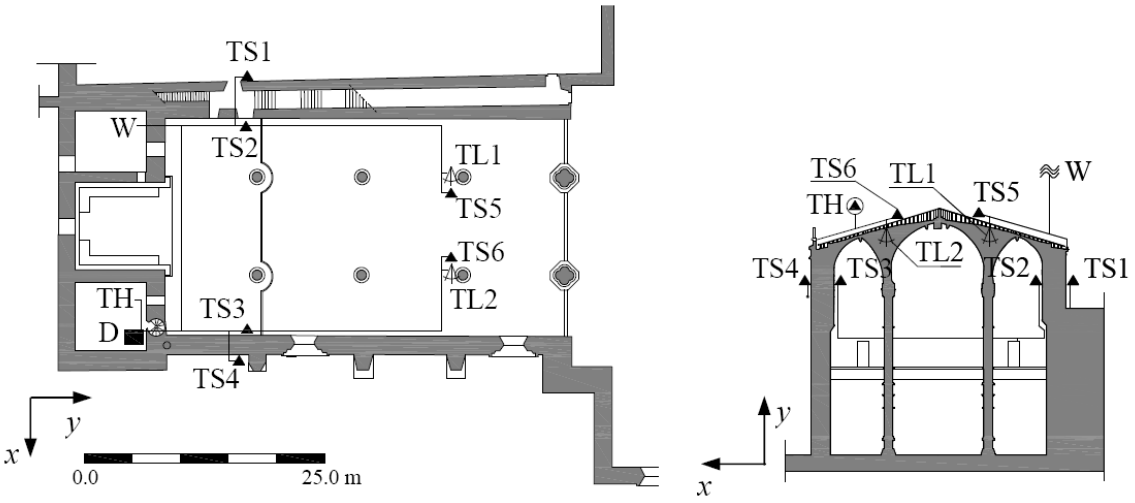

Figure 58: Sensor Locations in the Monastery of Jerónimos (courtesy of Prof. Ramos, University of Minho)

Table 18: Monastery of Jerónimos Sensor Types

Sensor ID	Sensor Type	Range	Resolution	Notes
TS1 – TS6	Temperature Sensors	-20 to 100ºC	0.2ºC	
TL1 – TL2	Uniaxial Tilt Meters	± 1.5º	0.03º	North=Positive South=Negative
TH	Combined Temperature Humidity Sensor	-20 to 70ºC 0 to 100%	0.2ºC 2%	
W	Anemometer	0 to 60m/s 360º	0.01m/s 1º	Operating range -35 to 70ºC 5 to 100% RH
D	Data logger (Data Acquisition)			

The data entered into the numerical tool did not contain these sensor ID numbers as column headers, and therefore return another set of names for each sensor. A conversion chart between the sensor ID numbers and the names used in the numerical tool is provided in Table 19.

Table 19: Jerónimos Monastery, sensor name conversion chart

Sensor ID	Numerical Tool Name
TS1	Temp. Ext. North
TS2	Temp. Int. North

Table 19: Jerónimos Monastery, sensor name conversion chart (continued)

TS3	Temp. Int. South
TS4	Temp. Ext. South
TS5	Temp. Tilt North
TS6	Temp. Tilt South
TL1	Tilt Meter North
TL2	Tilt Meter South
TH (Temperature Record)	Relative Temp.
TH (Humidity Record)	Rel. Humidity
W (Speed)	Wind Speed
W (Direction)	Wind Direction

5.2.2 Creation of Data File

In order to create an ASCII file for the numerical tool the same methodology was followed as the Oporto Cathedral outlined in 5.1.2. One additional step taken was to remove an initial section of data, where it could be seen that several adjustments to the system were made. It would also be possible to adjust this data in pre-processing, thus removing the large step present, and giving a slightly longer data history.

5.2.3 Direct Results Analysis

The direct results analysis provides maximum and minimum signal values, an outlyer filter based on upper and lower bounds, and a moving average filter. Table 20 displays the maximum and minimum signals values before and after the outlying values were removed. The outlyers were defined as any value greater than three standard deviations from the mean. As can be seen in the table there were several signals, such as the south interior temperature that had obvious erroneous results providing a maximum temperature of almost seven thousand degrees centigrade, where removal of outlyers was required before further analysis.

Table 20: Jerónimos Monastery: Maximum and Minimum Signal Values before and after Outlier Removal

Signal	Maximum Value with Outliers	Minimum Value with Outliers	Outlier Removed Maximum	Outlier Removed Minimum
Tilt Meter North	0.2251	-0.1803	0.1714	-0.1373
Tilt Meter South	0.2935	-0.1560	0.2251	-0.1560
Temp. Tilt North	35.9900	6.8650	34.8000	6.8650
Temp. Tilt South	35.1300	7.6600	34.3200	7.6600
Temp Ext North	475.1000	4.6830	32.3500	4.6830
Temp Int. North	6999	14.4300	27.8500	14.4300
Temp Ext South	6999	3.1730	37.4200	3.1730
Temp Int. South	6999	13.6200	37.4300	13.6200
Relative Temp.	34.9400	-73.8000	32.4900	7.4000
Rel. Humidity	98.6000	-52.1700	98.6000	24.2000
Wind Speed	7.5700	-26.1800	7.5700	0.1890
Wind Direction	360	-190.1000	360	0.0480

When visually inspecting many of the results, such as the north exterior temperature shown in Figure 59, the upper and lower bounds show how far the outliers are from the normal signal. The first outlier removal filter removes all points outside of the bounds.

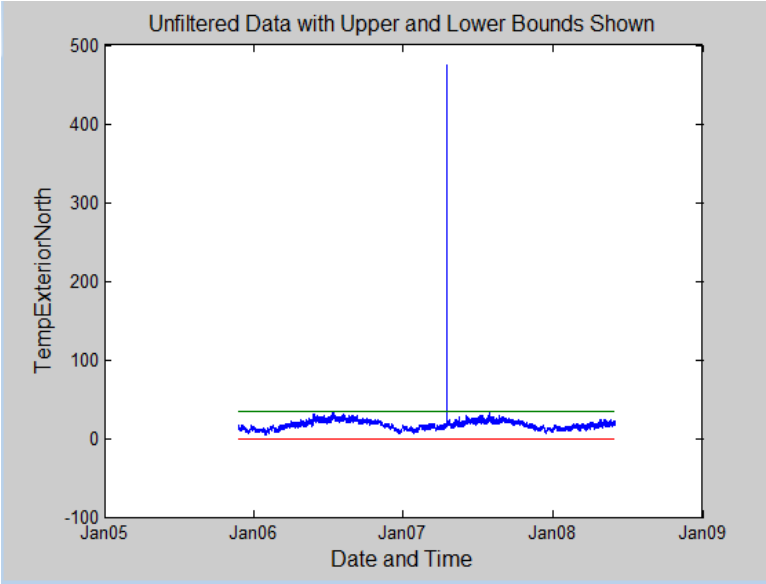

Figure 59: Jerónimos Monastery, unfiltered data with upper and lower bounds

The direct results analysis also runs a moving average filter. The moving average reduces noise to create a smoother signal. For the Jerónimos Monastery data a moving average window size was set at fifty samples. Figure 60 shows the moving average filter in black compared to the unfiltered data shown in red; Figure 61 shows a close up view on Figure 60. Figure 61 gives a clear view of how the filtered signal follows the trend of what is happening, while removing sudden changes that are caused by noise.

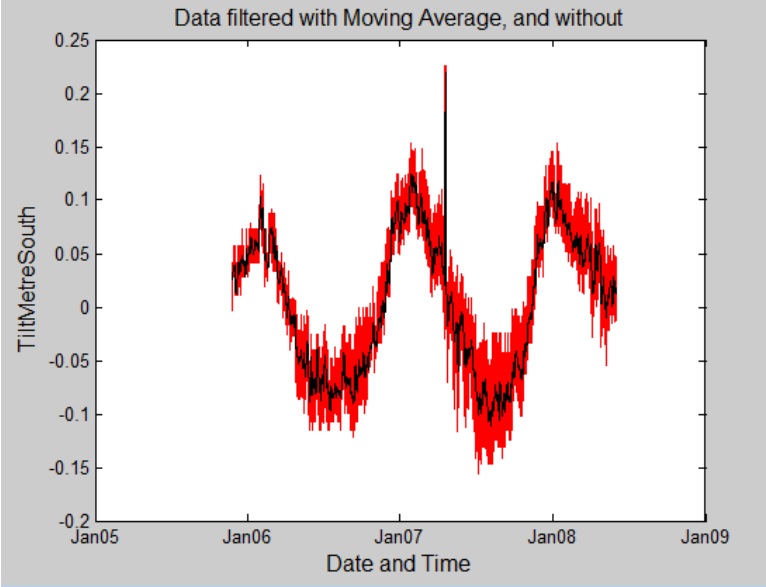

Figure 60: Jerónimos Monastery, data filtered with moving average compared to unfiltered data

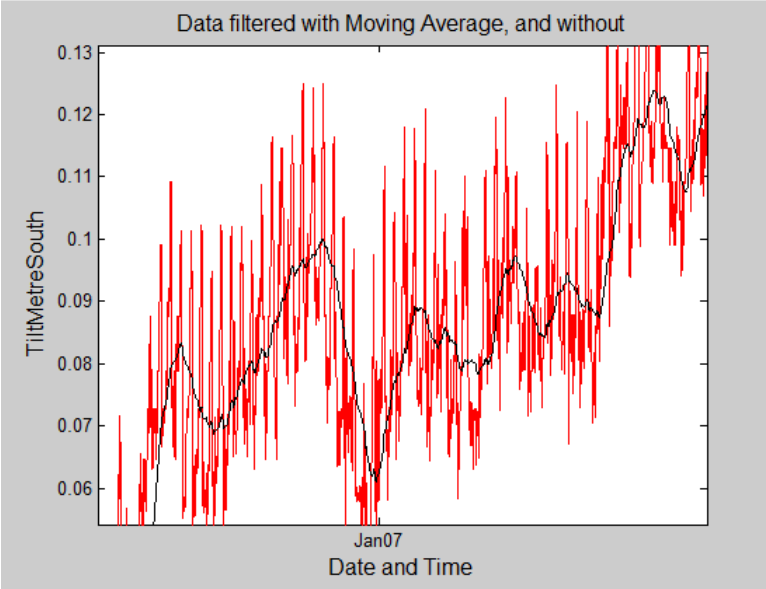

Figure 61: Jerónimos Monastery, close up view of filtered and unfiltered data

5.2.4 Simple Statistical Analysis

The simple statistical analysis is conducted on the filtered data provided by the direct results analysis. Table 21 provides the resulting mean, standard deviation, coefficient of variation, and signal to noise ratio for each of the sensors.

Table 21: Jerónimos Monastery, Simple Statistical Analysis by Signal

Signal	Mean	Standard Deviation	Coefficient of Variation	Signal to Noise Ratio
Tilt Meter North	0.0160	0.0440	274.8	0.3639
Tilt Meter South	0.0048	0.0638	1330.8	0.0751
Temp. Tilt North	18.7447	4.9969	26.7	3.7512
Temp. Tilt South	19.5872	5.0153	25.6	3.9055
Temp Ext North	16.9626	4.8079	28.3	3.5280
Temp Int. North	20.6545	3.5468	17.2	5.8234
Temp Ext South	18.7427	4.4277	23.6	4.2331
Temp Int. South	20.1808	3.7118	18.4	5.4370
Relative Temp.	17.9169	3.3866	18.9	5.2905
Rel. Humidity	65.9111	11.3427	17.2	5.8109
Wind Speed	2.1280	0.7029	33.0	3.0275
Wind Direction	202.4127	69.6732	34.4	2.9052

A sample histogram is shown in Figure 62, showing the almost normal distribution of the North tilt meter. For the Jerónimos Monastery data a bin number of one hundred had been selected. One hundred bins appear to provide clear visual results for the histogram, and will provide smoother results for the cumulative distribution function. A sample of the cumulative distribution function is shown in Figure 63.

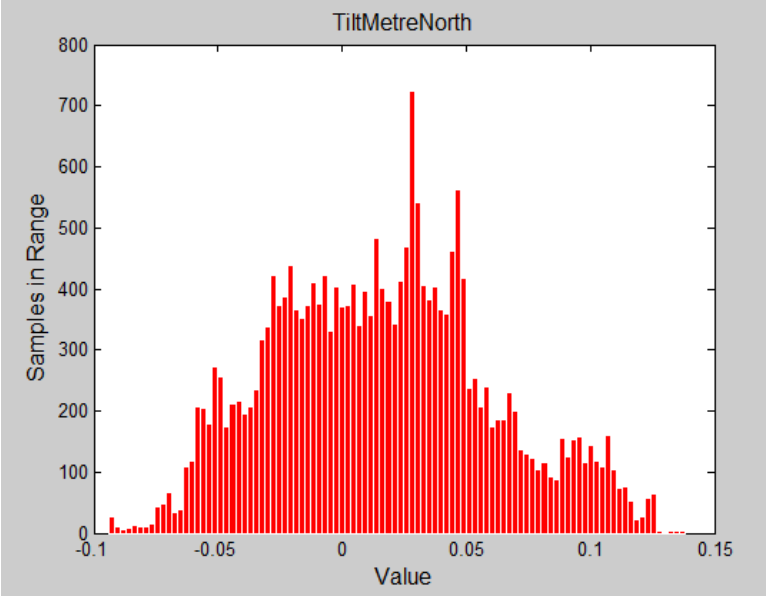

Figure 62: Jerónimos Monastery, histogram sample

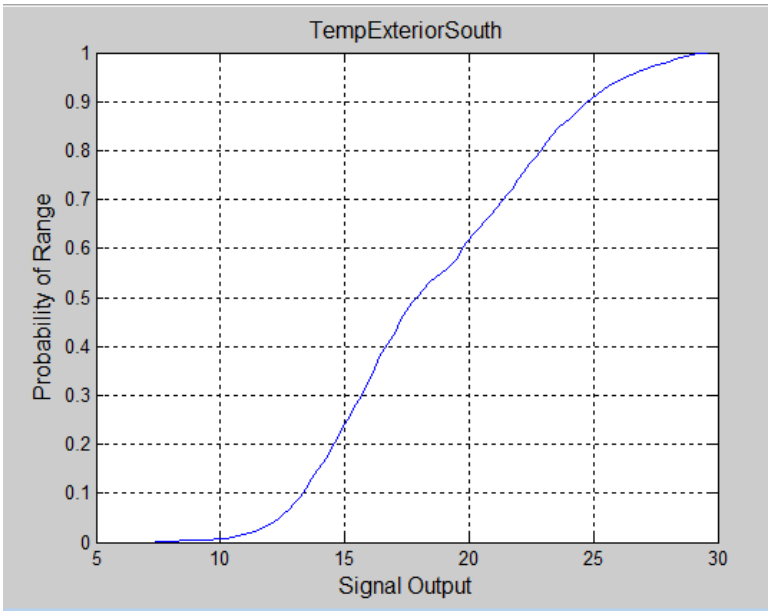

Figure 63: Jerónimos Monastery, cumulative distribution function sample

5.2.5 Regression Analysis

The coefficient of determination (r^2) values for the tilt meters compared to the environmental inputs are displayed as a bar chart in Table 22. Since the regression analysis is interested in the relation between structural responses and environmental inputs only the tilt meters have all of their coefficients of determination displayed. The higher the coefficient of determination value the stronger the relation

between the variables, with a direct relation returning a value of one, as seen when a tilt meter is compared to itself. From Table 22 it appears that the South tilt meter has a closer temperature relation than the North tilt meter. It is interesting to note that the expected correlation between the two tilt meters is not very high. Detailed regression analysis of the structural responses will be done in Section 5.2.6.

Table 22: Jerónimos Monastery, Coefficients of Determination

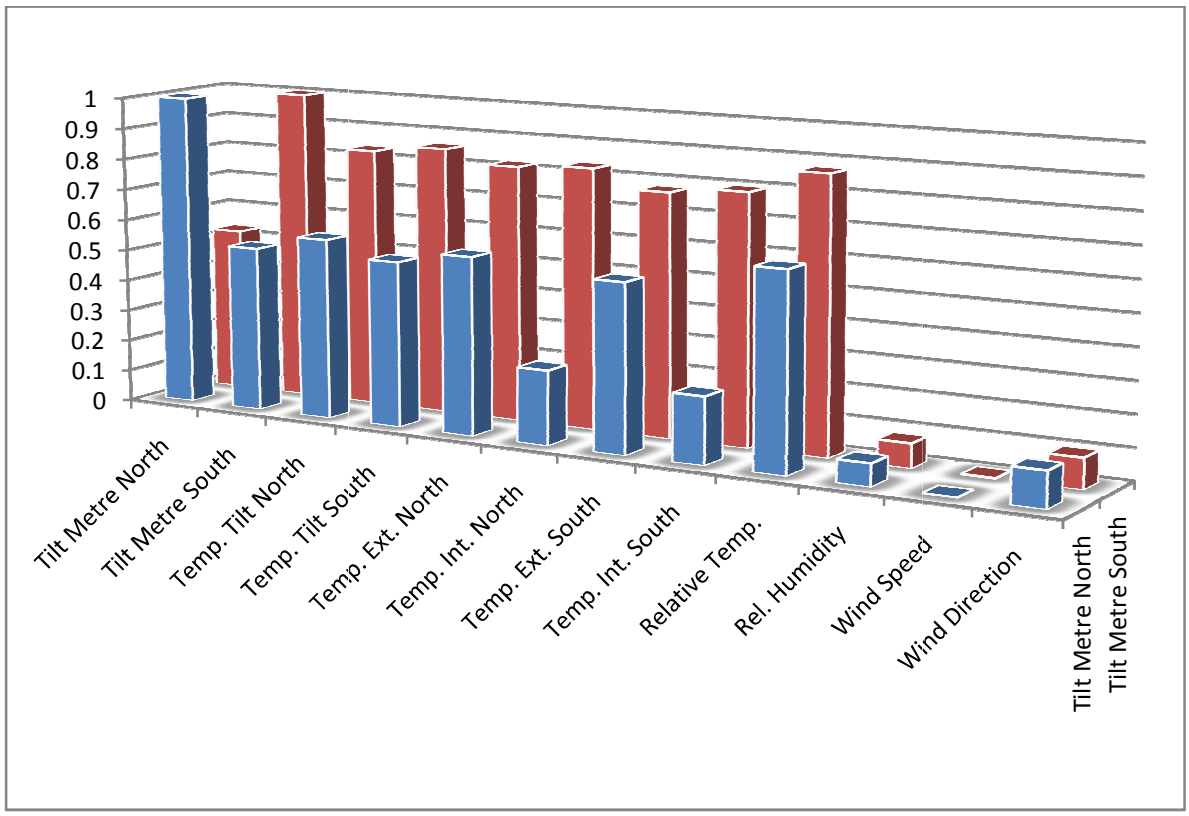

5.2.6 Enhanced Analysis with the Advanced Numerical Tool

This section will go into further analysis of each signal group from the Jerónimos Monastery data.

5.2.6.1 Tilt Meters

The two tilt meters represent only two sensors monitoring structural response in the Jerónimos Monastery structural health monitoring system. A visual review of the filtered data from the north and south tilt meters, shown in Figure 64 and Figure 65 respectively, provides us with some preliminary information. Both sensors are recoding a southward tilt during the summer and a northern tilt during the winter, suggesting that the movement is related to temperature, or perhaps temperature variation in

the masonry. One noticeable difference is that with the same filtering applied the north tilt meter has a signal containing more noise than the south tilt meter. Upon closer examination it appears that while movements occur at similar seasons, this movement does not happen at the same time in both sensors.

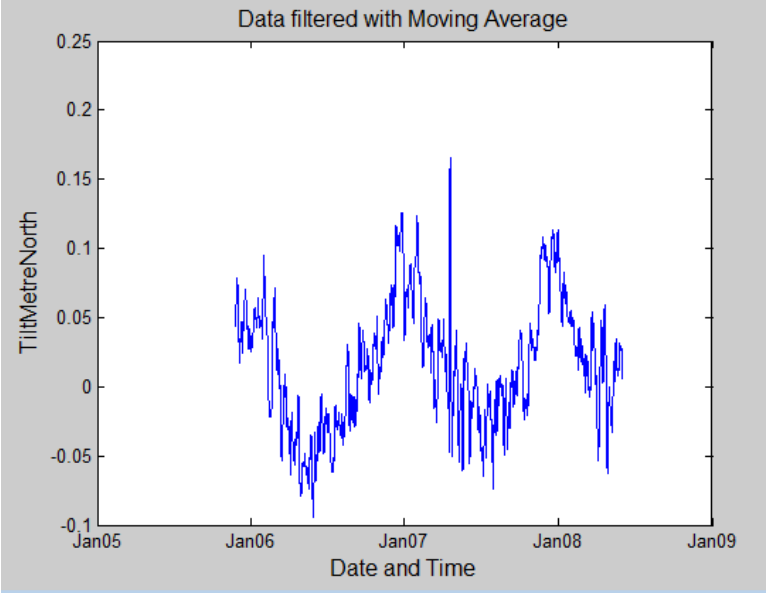

Figure 64: Jerónimos Monastery, Tilt Meter North filtered data

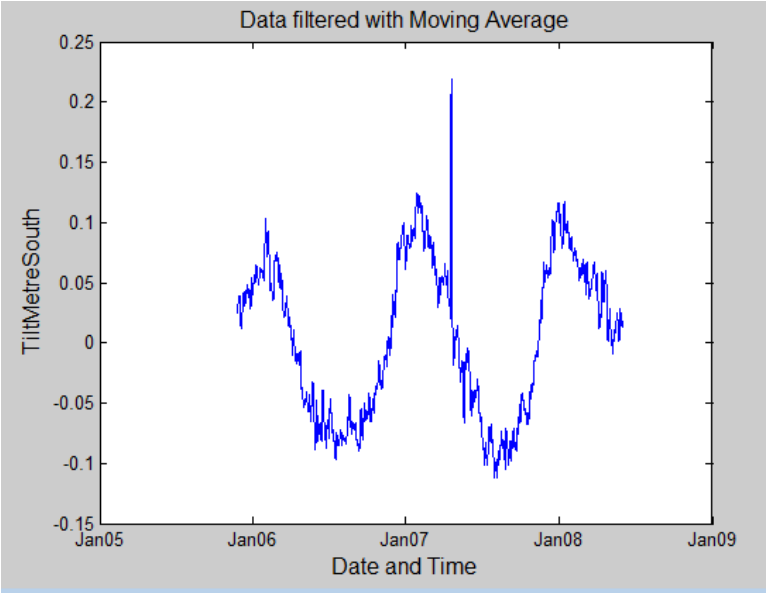

Figure 65: Jerónimos Monastery, Tilt Meter South filtered data

Review of the histograms from the north and south tilt meters, shown in Figure 66 and Figure 67 respectively, further demonstrates the differences at each location. The location of the north tilt meter

has more normally distributed data, while the south tilt meter provided data with two clear densities of samples at its location. To determine what, if any, effect this would have on the structure would require further study. Potentially a finite element model of the arch connecting points would provide further insight into the results. As expected the cumulative distribution function results reflect what is seen in the histogram.

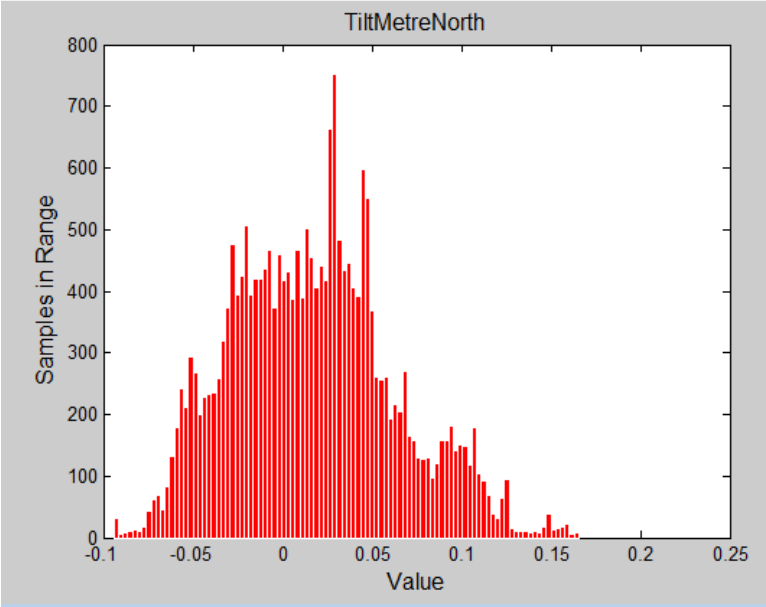

Figure 66: Jerónimos Monastery, Tilt Meter North histogram

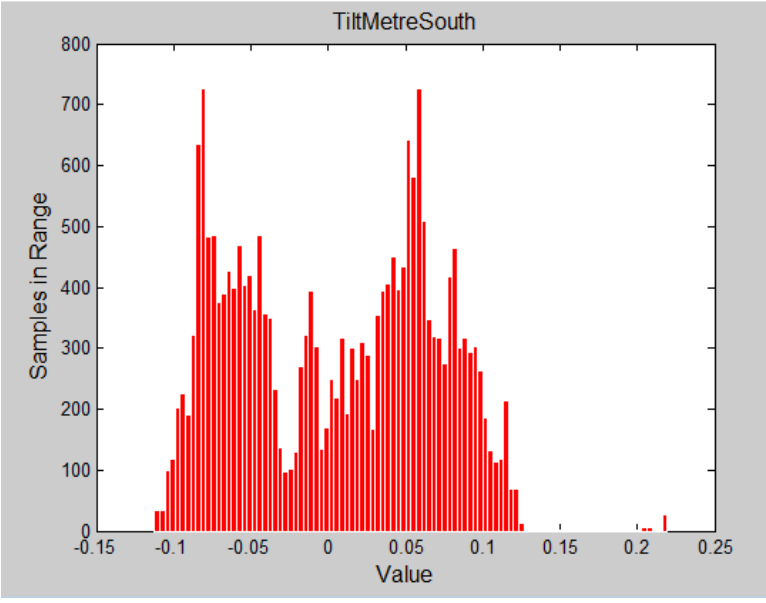

Figure 67: Jerónimos Monastery, Tilt Meter South histogram

For the regression analysis signals with a history over two years are considered first. Table 22 is used in determining which sensors are selected for comparison. First, single regression analyses were run to compare the tilt meters to the temperature sensors at the same location. The multiple regression analysis compared the tilt meters to the three temperature sensors with the highest coefficient of determination, excluding relative air temperature since it has a shorter history. The resulting plots of the regression and residuals are displayed in Figure 68 and Figure 69, showing results for North and South tilt meters respectively. Both single and multiple static regression analyses appear to have better correlation, and smaller residuals, for the South tilt meter, this is confirmed by the data in Table 23.

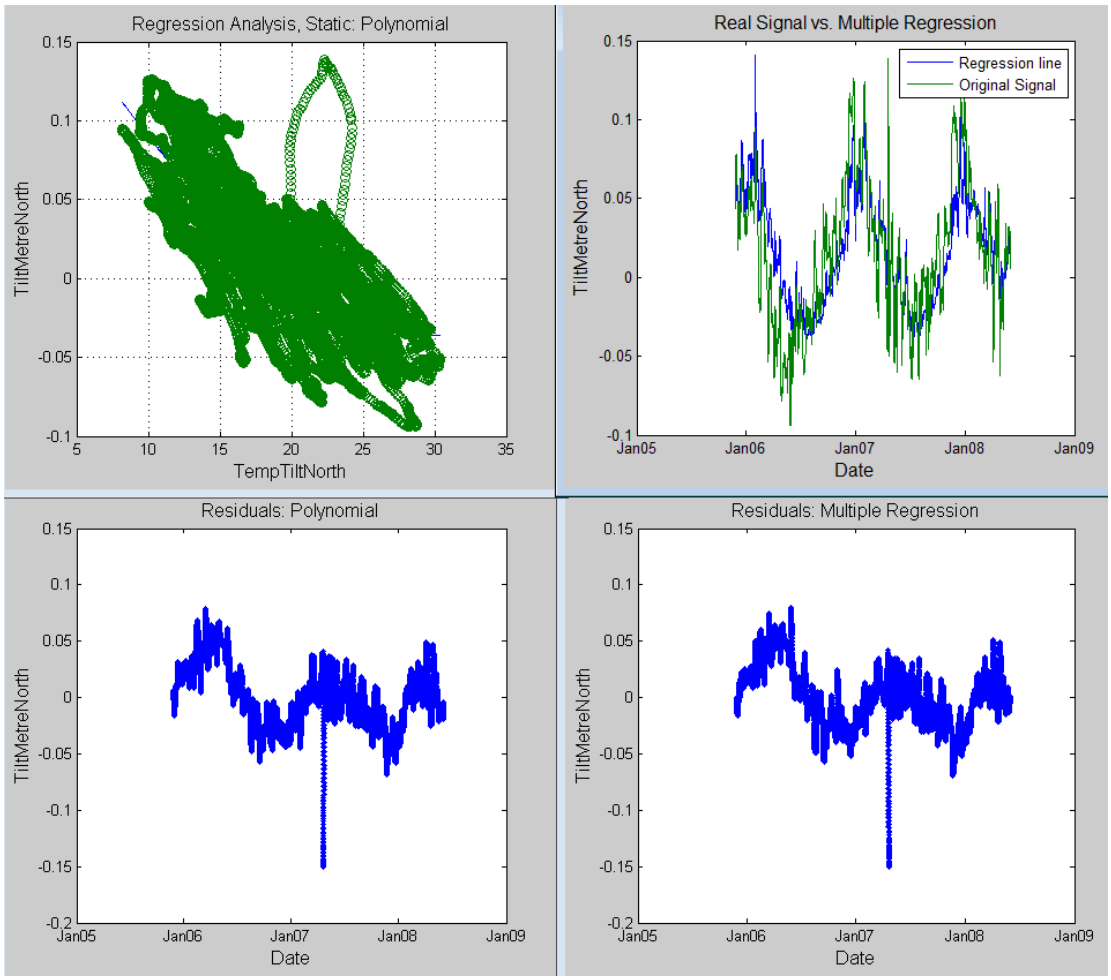

Figure 68: Jerónimos Monastery, Tilt Meter North Static Regression

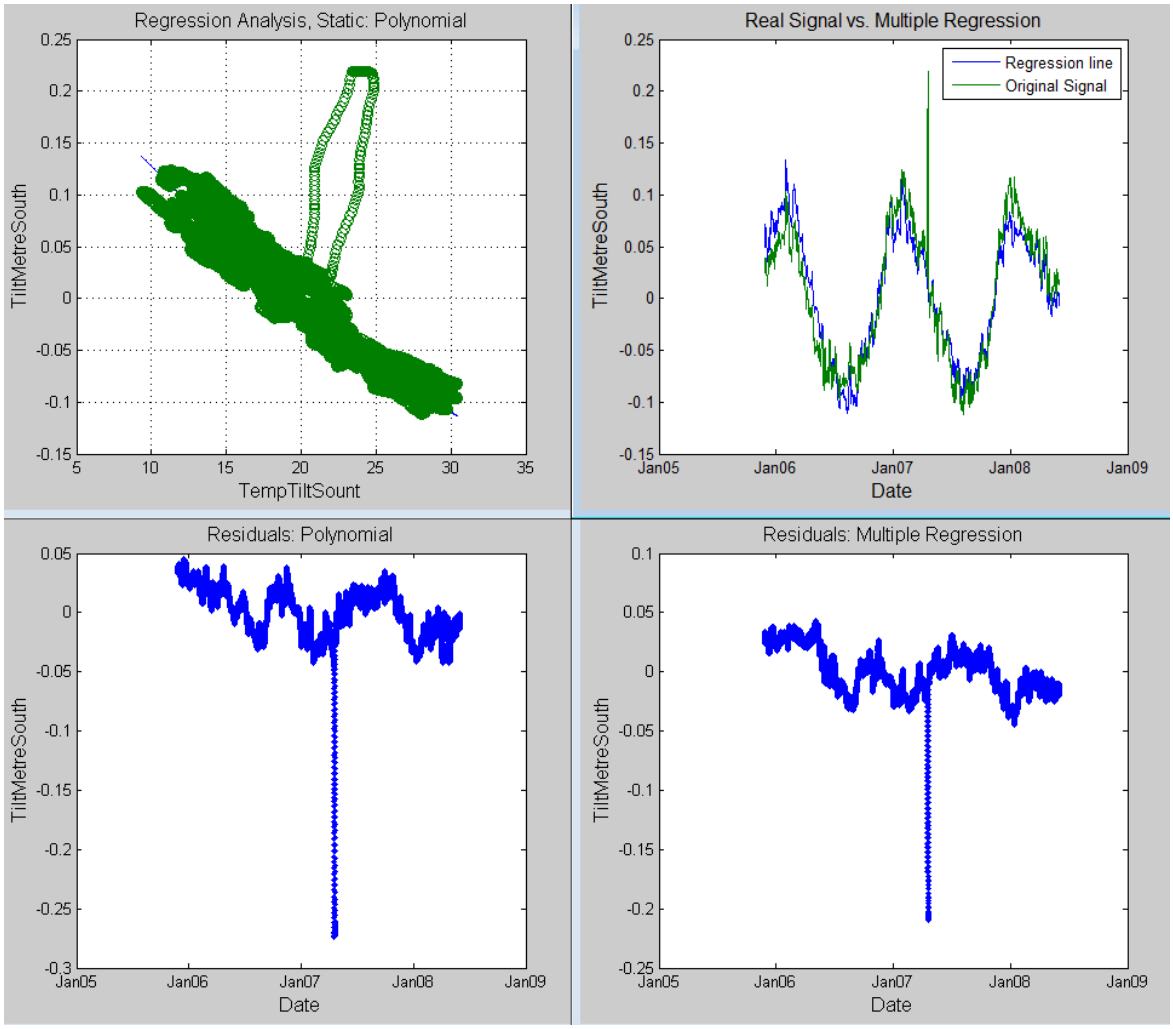

Figure 69: Jerónimos Monastery, Tilt Meter South Static Regression

Table 23: Jerónimos Monastery, Static Regression

	Tilt Meter North	Tilt Meter South
Single Regression:		
Environmental Inputs	Temp. Tilt Meter North	Temp. Tilt Meter South
Standard Deviation of Error	0.0279	0.0240
Loss Function	0.000778	0.000576
Final Prediction Error	0.000778	0.000576
Coefficient of Determination	0.5785	0.8566

Table 23: Jerónimos Monastery, Static Regression (continued)

	Tilt Meter North	Tilt Meter South
Multiple Regression:		
Environmental Inputs	Temp. Tilt Meter North Temp. Exterior North Temp. Exterior South	Temp. Tilt Meter South Temp. Exterior North Temp. Interior North
Standard Deviation of Error	0.0273	0.0218
Loss Function	0.000747	0.000473
Final Prediction Error	0.000748	0.000474
Coefficient of Determination	0.6148	0.8837

Dynamic regression analysis, using ARX models, provides a better model according to the loss function and the final prediction error, found in Table 24. It is interesting to note that the visual results do not lead the analyst to the same conclusions that the calculated accuracy does. Figure 70 and Figure 71 show the measured output and the modeled fit for both the North and South tilt meters, respectively, and the South tilt meter appears to have a more accurate model of the results. Table 24 confirms better signal correlation for the South tilt meter, while the ability to reproduce the signal, quantified by the loss function and final prediction error, shows both models to be of a similar quality.

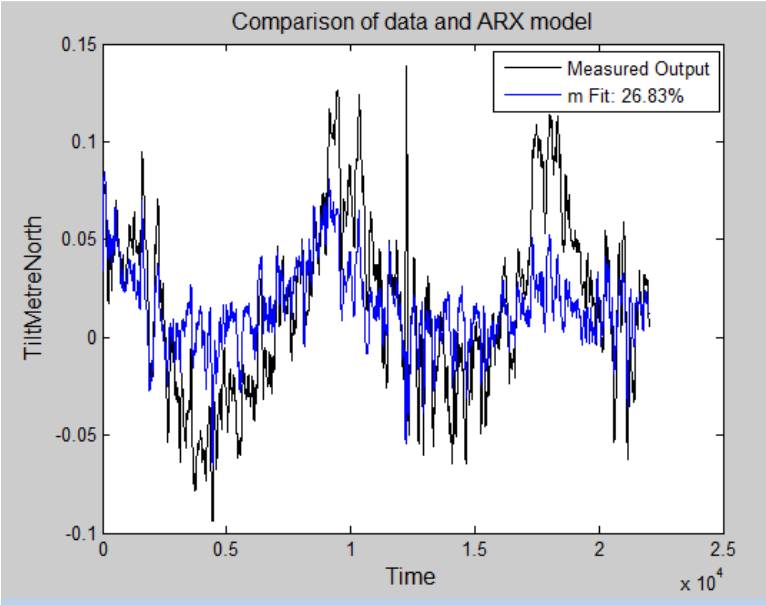

Figure 70: Jerónimos Monastery, ARX model of North Tilt Meter

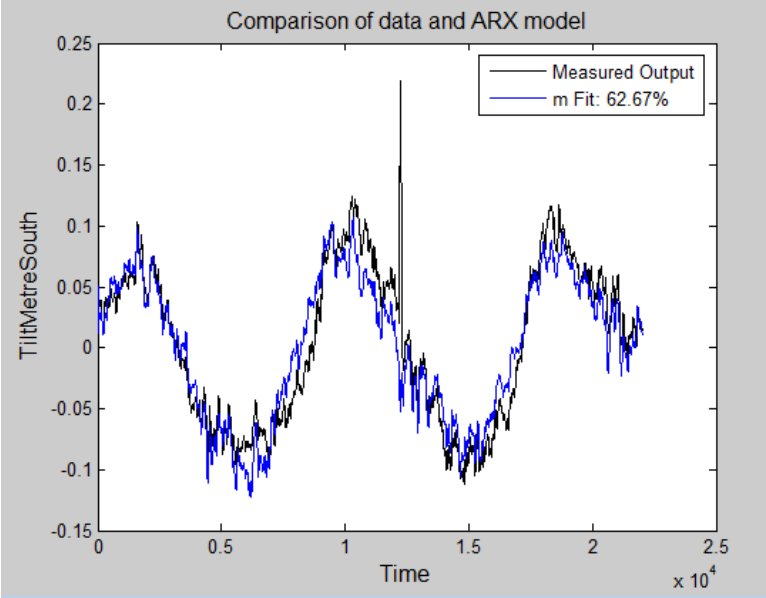

Figure 71: Jerónimos Monastery, ARX model of South Tilt Meter

Table 24: Jerónimos Monastery, ARX model

	Tilt Meter North	Tilt Meter South
Environmental Input	Temp. Tilt Meter North Temp. Tilt Meter South Temp. Exterior North Temp. Exterior South	Temp. Tilt Meter South Temp. Interior North Temp. Exterior South Temp. Interior South
Orders	[4,4,4,4,4,1,1,1,1]	[4,4,4,4,4,1,1,1,1]
Standard Deviation Error	0.0447	0.0244
Loss Function	3.57857×10^{-8}	6.27298×10^{-8}
Final Prediction Error	3.58507×10^{-8}	6.28438×10^{-8}
Coefficient of Determination	0.1164	0.8544

A general conclusion to be drawn from the tilt meters is that the structure appears stable. There is no excessive lean at either location, and the annual variation does not appear to be changing in any significant manner. There are several curious points, such as the differences in cycles and the lack of a normal distribution on the south tilt meter, but nothing indicating the structure is anything other than stable. The coefficient of determination for the North tile meter, on Table 24, appears much lower than expected, and does not appear to agree with the other quality checks. Further investigation is required to determine the cause of this phenomenon.

5.2.6.2 Temperature Sensors

The temperature sensors all record similar seasonal variations, as seen in Figure 72, where the viewer can clearly see higher summer temperatures and lower winter temperature. The location of the sensors will have an effect on how warm or cool the seasonal variation is, since an interior sensor will not be exposed to as extreme temperatures as an exterior sensor. There are also some slight phase shifts between sensors. These variances were expected, and the data from each temperature sensor appears to be the true environmental input for each location.

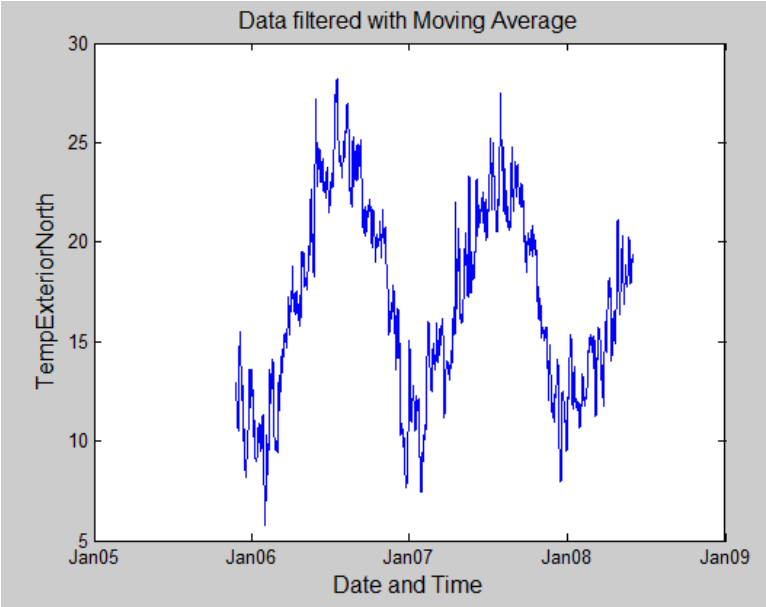

Figure 72: Jerónimos Monastery Temperature Sensor

5.2.6.3 Humidity

Relative humidity has a chaotic filtered signal, as expected. The histogram and cumulative distribution function, shown in Figure 73, also produce the expected results, showing normally distributed data. The sensor data appears to be representative of the true environmental input. The humidity was not entered into the regression models due to the low coefficient of determination and short data history.

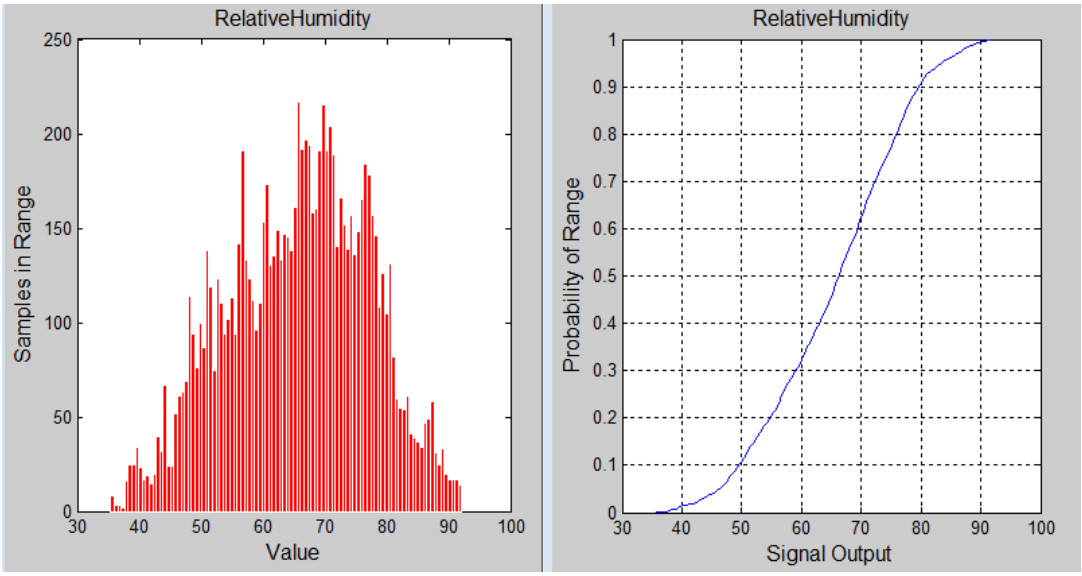

Figure 73: Jerónimos Monastery, Humidity Data

5.2.6.4 Wind Sensors

The anemometer provides the results on wind velocity and wind direction, shown in Figure 74. Results indicate that wind velocity is occasionally high, and direction always between forty and three hundred and forty degrees. The wind direction appears most often around two hundred and thirty degrees, plus or minus twenty. Future analysis could investigate if the high velocity wind also has such a wide distribution of direction, and if not, how specifically that data relates to structural movements. The wind was not entered into the regression models due to the low coefficient of determination and short data history.

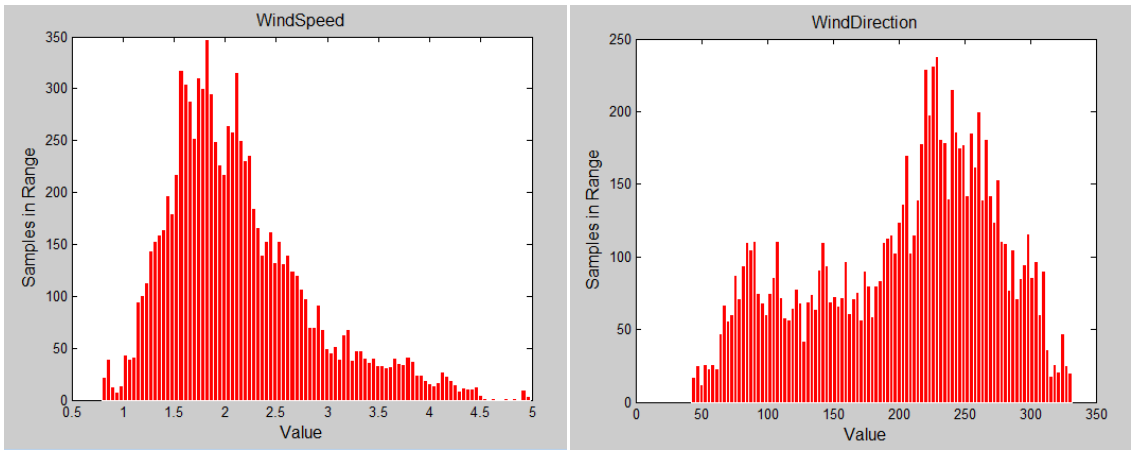

Figure 74: Jerónimos Monastery, Wind Data

5.2.7 General Notes on Jerónimos Monastery

The structural health monitoring of Jerónimos Monastery show that the structure is stable. Due to the cultural importance of the structure, the slender masonry columns, and the existing concerns on the structural stability, it is best to continue monitoring the structure to provide a greater depth of sensor history, and re-analyze to provide a more accurate prediction on the structure.

5.3 General Remarks

Two case studies were investigated with the numerical tool. MIROVY provided the user with both graphical and numerical data on the sensor results, and investigated possible relations between environmental inputs and structural responses. With this data some general conclusions can be drawn, and any major damage can be detected. Neither case study showed any data indicating existence of any urgent problems.

6 MODELING THE STRUCTURAL RESPONSE FOR ALARMS DEFINITION

Creation of alarms for structural health monitoring is an active area of research with many current approaches. Simple damage detection methods include routine visual review of signal histories in search of significant changes in the structure. This method can be automated, using mean and standard deviation to detect changes in the signal. Other more direct methods focus on the natural frequencies of the structure, where any significant change can trigger the alarm.

Slightly more complex damage detection methods are discussed by Chintalapudi et al. at the international conference on information processing in sensor networks. This method uses stiffness matrixes and eigenvalues in detecting and locating structural damage (Chintalapudi, et al., 2006).

Peeters presents an alternative damage detection method based on the structural responses, environmental effects, and the ARX model (Peeters, 2000). This method uses a collection of ARX models to determine the predicted structural response, and if the recent signal data begin to have greater than expected error when modeled, the alarm is triggered.

Due to the type of data input into the numerical tool, the damage detection method proposed by Chintalapudi et al. would be difficult to implement. Therefore the focus will be on basic detection and detection using ARX models.

6.1 Architecture

The architecture of the damage detection analysis is displayed in Table 25. The program provides three damage detection options, direct ARX and visual ARX, to assist the user in determining damage or instabilities. Before any of these three analyses can be run, the program separates the base and test data, the lengths of which are determined by the signal length, in years.

Table 25: Architectural Outline of Damage Detection Program

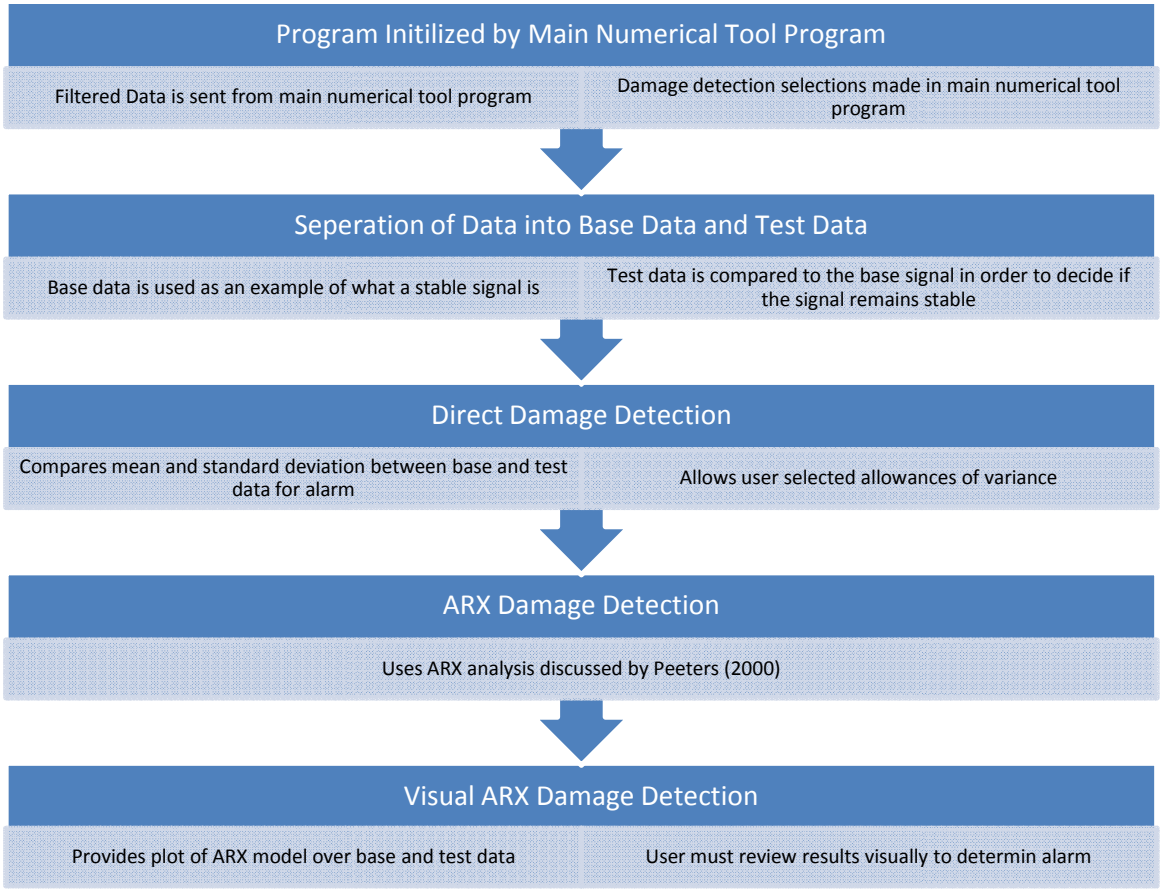
Program Initilized by Main Numerical Tool Program
Filtered Data is sent from main numerical tool program
Damage detection selections made in main numerical tool program
Seperation of Data into Base Data and Test Data
Base data is used as an example of what a stable signal is
Test data is compared to the base signal in order to decide if the signal remains stable
Direct Damage Detection
Compares mean and standard deviation between base and test data for alarm
Allows user selected allowances of variance
ARX Damage Detection
Uses ARX analysis discussed by Peeters (2000)
Visual ARX Damage Detection
Provides plot of ARX model over base and test data
User must review results visually to determin alarm

6.2 Procedures

The main numerical tool is used for the base of the damage detection procedures. It has been included as a sub-program in the numerical tool, and displays the message "→ START OF DAMAGE DETECTION←" in the command window at the start of the sub-program.

The damage detection sub-program of the signal analysis numerical tool is composed of four sections, one; the separating of base data and test data, two; direct damage detection, three; ARX damage detection, and four; visual ARX damage detection. For direct and ARX damage detection base data is defined as the data modeled as normal or undamaged, while the test data is defined as data that must be verified to be normal or undamaged, or conversely to be abnormal or damaged. Both the direct and ARX damage detection calculations require the previously separated base and test data for analysis.

The procedure for separating base and test data finds the number of years covered by the signal data. It assumes that there are not significant gaps in the data. If fewer than two years are available the

numerical tool provides a warning that this will case the damage detection analysis to be noticeable less accurate. In the opinion of the author the ideal data should have at least four years of data available for the analysis. Depending on the number of years of data, the numerical tool selects a certain amount of data from the start of the signal and a certain amount of data from the end to create the base and test data groups. The numerical tool attempts to have the base and test data groups made up of whole year values, so that seasonal variation is not a problem. Table 26 shows how the base and test data lengths were selected based on original signal length.

Table 26: Base and Test data lengths

Signal length (years)	Base data length	Test data length	Notes
< 1	First ¾ of signal	Final ¼ of signal	Warning displayed
1 – 2	1 year from start	1 year from end	Overlap exists
2 – 2.5	1 year from start	1 year from end	
2.5 – 3	2 years from start	1 year from end	Overlap exists
3 – 4	2 years from start	1 year from end	
4 – 5	3 years from start	1 year from end	
>5	3 years from start	2 years from end	

This data is then used for both damage detection calculations.

6.2.1 Direct Damage Detection

The direct damage detection alarm is based on the theory that the mean and standard deviation should not change significantly from one year to the next. A small, user selected, variable is used to give some leniency before comparing base and test data.

The mean of each signal is calculated, for both base and test data. The analysis first checks if the test data is larger than the base data, the base data having a small margin added that is based on standard deviation. Second the analysis checks if the test data has a smaller mean than the base data, the base data having the margin subtracted. No signal should have alarms in both the higher mean alarm and the lower mean alarm. Signals that do cause alarms are displayed in the command window, under the relevant category.

For the standard deviation alarm the data is only tested for an increase in the standard deviation. A decrease in the standard deviation is not important. If there is no change in the mean and a

reduction in the standard deviation, it suggests that the structure is becoming more stable. The standard deviation of the test data is compared to the standard deviation of the base data, plus a user selected percentage margin. Any test data that is larger triggers the alarm and is displayed in the command window.

The environmental signals are intentionally analyzed in the direct analysis. It is increasingly common for climate to change drastically from year to year due to climate change. If the temperature, humidity, or wind, are drastically different in the test year, when compared to the base year, this will have an effect of structural response, and the user should be aware of this.

6.2.2 ARX Damage Detection

The ARX damage detection analysis is run in three main steps. First step consists of normalizing all the data, second step separates the environmental input signals from the remaining data, and the third step carries out the analysis of the data.

When the data is normalized the base and test data is combined in one matrix before the normalization techniques begin. This is aimed at avoiding errors introduced such as changes in mean between data signals. Each column of the data is treated separately, the mean is calculated, the standard deviation is calculated, and each new value in the column is calculated based on standard deviation, mean, and past value of record. The columns are separated into base and test data once again, and provided for the next part of the ARX damage detection routine.

Separation of environmental inputs and structural responses is processed as the next step. The provided to be computationally difficult in the attempt to keep pre-numerical tool data manipulation to a minimal. Upon completion there exist four data matrixes, containing: base data environmental inputs, base data structural responses, test data environmental inputs, test data structural responses. The sorting is carried out using several data loops and comparative expressions.

The final part of the ARX damage detection sub-program is the most important. The analysis part of the program methodically approaches each of the structural response signals, and runs several ARX analyses on each base signal. The final prediction errors are compared, and the signal analysis with the lowest error is also run on the test data for that signal. If the final prediction error is higher on the test signal the alarm is triggered, and the signal name is displayed in the command window. The user is able to input an acceptable tolerance on the error.

6.2.3 Visual ARX Damage Detection

The visual damage detection has three main sections, the final of these sections containing two sub-sections. First step for the visual ARX damage detection is to normalize the data. Once the data is normalized the environmental parameters are separated from the structural responses, producing two matrixes. The final, most complex step uses a data loop, and two sub-routines.

The data loop runs once for every structural response signal in the data set, each loop dealing with one of the response signals. The data signal is combined with the environmental response matrix in order to run the ARX models. These models are created and calculated in the first sub-routine, in a similar manner used by the ARX damage detection. The best model is selected, and is returned to the visual ARX program. The final sub-routine uses the previously created ARX model for simulation, and graphic plots. Two plots are created in each loop, the first plot shows the actual signal, the ARX model, with upper and lower bounds based on the number of standard deviations selected by the user. The second plot looks at the residuals from the ARX model, plotting them in the upper and lower bounds. If damage is present the user should see a trend of the signal leaving the assigned bounds.

As well as visual output, shown in Figure 75 and Figure 76, the visual ARX damage detection also provides the loss function, final prediction error, and determination of coefficient to assist the user. The sample figures show a signal with some questionable data at the initial stages, however as Figure 76 shows more clearly, the error does not appear to have a consistent deviation in either negative or positive direction.

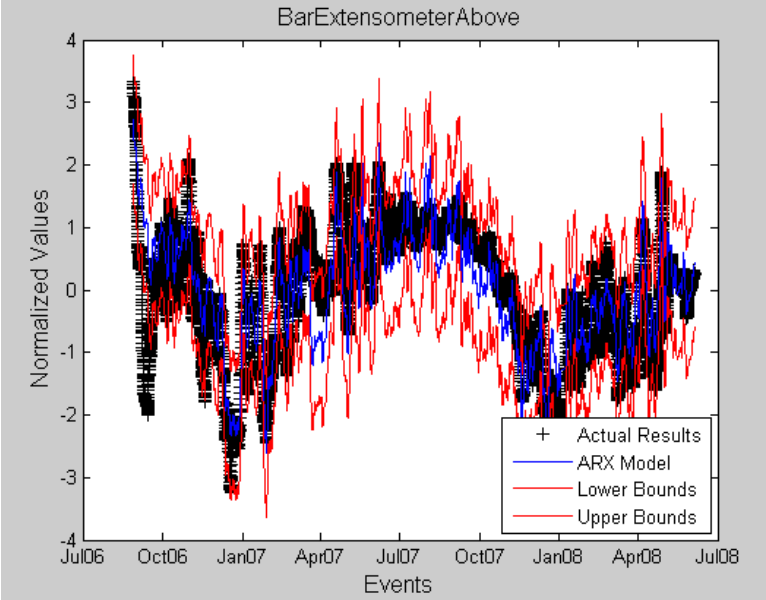

Figure 75: Visual ARX Damage Detection, First Plot

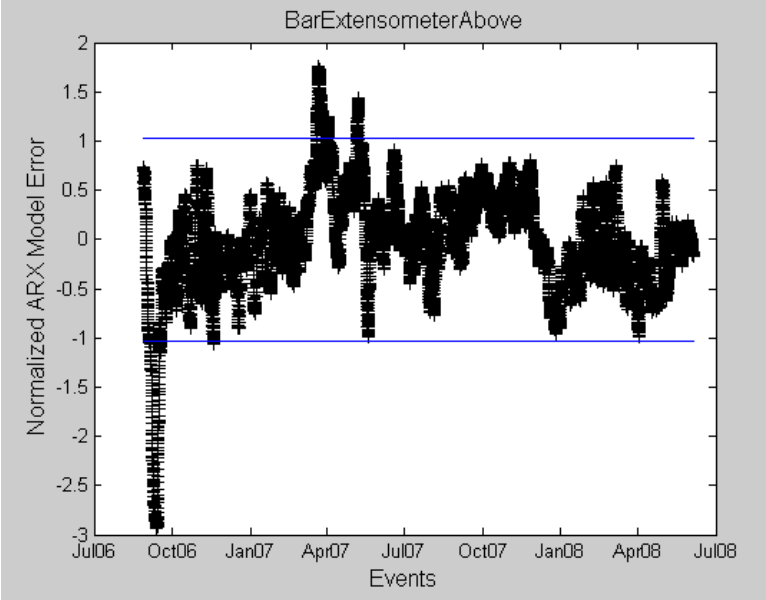

Figure 76: Visual ARX Damage Detection, Second Plot

6.3 Application to Oporto Cathedral

The damage detection routine is run on the Oporto Cathedral case study data. The analysis is done twice, first time using the data with a longer history, but no dependable extensometers, while the second analysis uses the data with shorter history, but containing the extensometers. The data input

into the analysis is given in Table 27. The various alarms triggered for each analysis is shown in Table 28.

Table 27: Input Variables for Damage Detection of Oporto Cathedral

Input Variable	Value
Margin for Mean Alarm (% STD)	5
Margin for Standard Deviation Alarm (% STD)	5
Environmental Inputs for ARX Alarm	Relative Humidity Relative Temperature Wind Direction
Margin for ARX Alarm (% of FPE)	5

Table 28: Resulting Alarms from Damage Detection Analysis of Oporto Cathedral

Original Data	High Mean Alarm	Low Mean Alarm	High STD Alarm	ARX Alarm
No Extensometers, longer signal history	Tilt Meter 2 Dir B Rel. Temperature Wind Velocity Surface Temp. 1 Surface Temp. 2	Crack Meter 2 Crack Meter 1 Crack Meter 3 Crack Meter 4 Tilt Meter 1 Dir A Tilt Meter 1 Dir B Tilt Meter 2 Dir A Rel. Humidity Wind Direction	Tilt Meter 1 Dir B Rel. Humidity	Crack Meter 1 Crack Meter 3 Crack Meter 4 Tilt Meter 1 Dir A

Table 28: Resulting Alarms from Damage Detection Analysis of Oporto Cathedral (continued)

Original Data	High Mean Alarm	Low Mean Alarm	High STD Alarm	ARX Alarm
With Extensometers, shorter signal history	Crack Meter 4 Tilt Meter 2 Dir B Wind Velocity Surface Temp. 1	Crack Meter 2 Crack Meter 1 Tilt Meter 1 Dir A Tilt Meter 1 Dir B Tilt Meter 2 Dir A Rel. Humidity Rel. Temperature Wind Direction Surface Temp. 2 Extensometer A Extensometer B	Tilt Meter 1 Dir A Tilt Meter 1 Dir B Tilt Meter 2 Dir B Rel. Humidity Wind Direction	Crack Meter 2 Crack Meter 1 Crack Meter 3 Crack Meter 4 Tilt Meter 1 Dir A Tilt Meter 1 Dir B

First impressions from when reviewing the alarms triggered by the damage detection analysis is that despite previous data review, more alarms appear that were expected. However, it also become clear the value of running the direct analysis on the environmental inputs.

Table 28 shows the results of the damage detection analysis. Analysis of the data with a longer signal history shows that the temperature and one tilt Meter have higher mean values than expected, while the remaining tilt Meters and all crack Meters have lower average means. Higher temperature would cause expansion and the further closing of cracks, and potentially affect the structural tilt. Therefore both mean alarms are inconclusive, requiring either a greater amount of base data, further study, or adjustment of the user inputs. The increased standard deviation of tilt Meter 1, direction B, causes some concern. If the tilt movements in this direction are increasing it suggests instability in the structure in resisting movement in this axis. The data containing the extensometers, but a shorter history, demonstrates similar results, and analysis of the data alone will not provide significant new findings. However, comparing both sets of data provides additional information. Relative air temperature has a higher mean in one category, while it has a lower mean in a second category. For an unknown reason the surface temperature 1 has a higher mean in both categories. This change in relative temperature mean has no affected the tilt Meter 2 direction B results, nor the other tilt meters and crack meters 1 and 2. Other results, such as crack Meters 3 and 4, can therefore be assumed to be safe. If the original data is reviewed, all tilt Meters have negative values, therefore, assuming that zero degrees is vertical, a higher value is better for the structure; tilt Meter 2, direction B, has improved. For the crack Meters all signals have positive means, so a lower mean is also a positive result. With

the extensometers, a lower mean indicates the two walls coming closer together, which should be positive, but could be a further indicator of problems with structural twisting. Tilt Meter 1, and tilt Meter 2 direction B, require further study.

The ARX alarm triggers for several signals in both data groups, shown in Table 28. Both groups contain crack Meter 1, crack Meter 3, crack Meter 4, and tilt Meter 1 direction A. As reviewed in the direct damage detection section, the crack Meters do trigger alarms, but do not appear to be causing structural instabilities, and therefore can be justified. Tilt Meter 1, direction A, cannot be justified, and appears to show actual structural damage. The margins can be adjusted and the analysis rerun in order to have a better appreciation of the severity.

Using the visual ARX damage detection several interesting trends appeared. Crack Meter 2 appears to be getting worse in the recent signal, as seen by the error of the ARX model in Figure 77. Crack Meter 1 shows a similar trend. The loss function, final prediction error, and coefficient of determination all return values indicating a good model, however, this final section of the signal requires future investigation. With more data it may appear as only a localized disturbance.

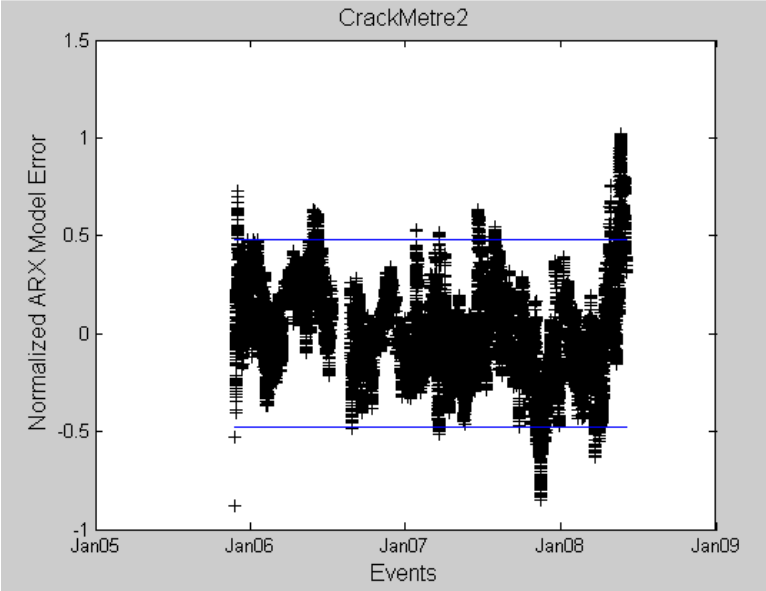

Figure 77: Oporto Cathedral, Crack Meter 2, visual ARX damage detection

Tilt Meter 1, direction A, was an alarm in the previous damage detection methods; the visual ARX method produces information which helps explain the alarm. Figure 78 shows the sudden unexplained drop in the signal, and return to a lower average signal. This appears to occur fall 2006, and the history of the structural intervention should be reviewed for possible explanations. The resulting error

of the model, shown in Figure 79, is most likely a result of this occurrence. If the start of the signal is dropped and connected to the remainder of the signal would produce the error values expected from a stable structure. This unexplained drop in the signal also occurs in tilt Meter 1 direction B, and tilt Meter 2 direction A. It does not appear in tilt Meter 2 direction B.

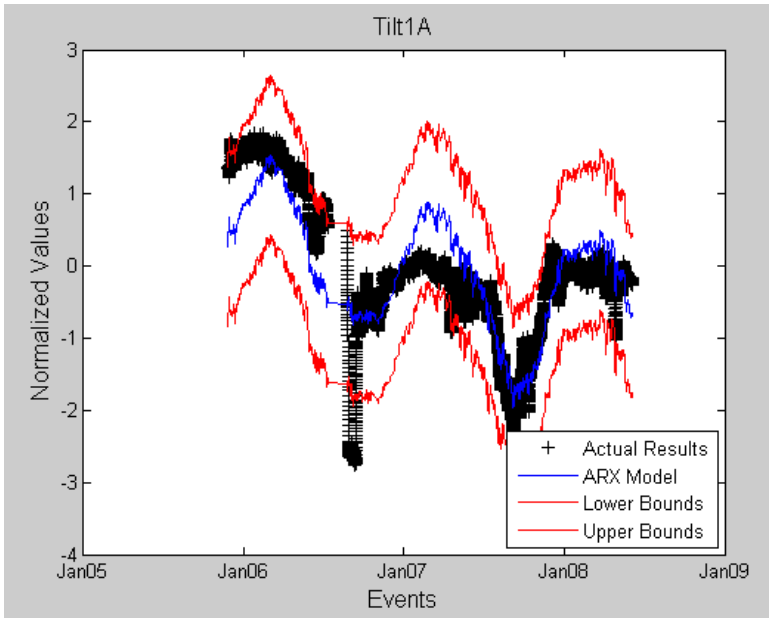

Figure 78: Oporto Cathedral, Tilt Meter 1 A, Visual ARX plot 1

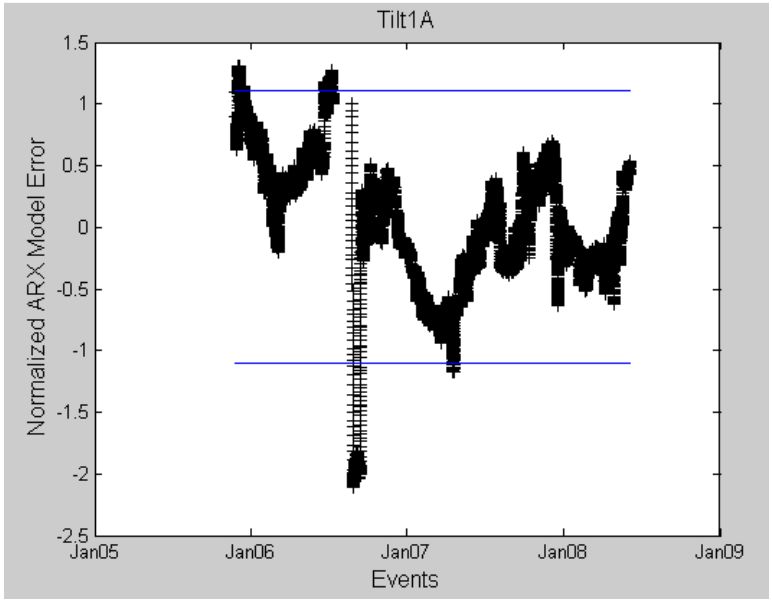

Figure 79: Oporto Cathedral, Tilt Meter 1 A, Visual ARX plot 2

General findings of the damage detection analysis of Oporto Cathedral, is that the structure is not in critical state, but some sensors require further monitoring, especially crack Meters 1 and 2, while other sensors, such as the tilt Meters, require some historical research and numerical analysis. No urgent structural issues appeared in the analysis.

6.4 Application to Monastery of Jerónimos

Jerónimos Monastery has two sensors detecting structural response, an original six sensors detecting environmental input, which an additional four sensors for monitoring environmental input added later. For this case study the longer data history is over two years long, while the shorter history is just over a year. The numerical tool input is provided in Table 29, while alarms announced in the command window, which excludes the visual ARX damage detection, are shown in Table 30. Both tilt Meters trigger the high mean alarm; this should not be a surprise, as in section 5.2.6 where general signals are discussed, Figure 64 and Figure 65 show one unexplained spiked value, this is again confirmed in Figure 80. The cause of this spike, which appears to take place over more than one day, is unknown. The south tilt Meter also triggers the high standard deviation and ARX alarm. Possible relations to lower exterior temperature or this data spike require further investigation.

Table 29: Jerónimos Monastery, Damage Detection Input Values

Input Variable	Value
Margin for Mean Alarm (% STD)	5
Margin for Standard Deviation Alarm (% STD)	5
Columns assigned as Environmental Input	4 to 9, 4 to 13
Margin for ARX Alarm (% of FPE)	5

Table 30: Jerónimos Monastery, Damage Detection Alarms

Original Data	High Mean Alarm	Low Mean Alarm	High STD Alarm	ARX Alarm
Longer history, no wind or humidity data	Tilt Meter North Tilt Meter South Temp. Int. South	Temp Ext North Temp Ext South	Tilt Meter South	Tilt Meter South
Short history	None	None	None	None

The short history, which does not contain the unexplained data, triggers no alarms. However, this data is of such short duration that further monitoring is required before these test results can be trusted.

The visual ARX damage detection results are similar for both the North and South tilt Meters. The results from the full history with fewer environmental monitors and from the shorter history are displayed in Figure 80 and Figure 81 respectively. Both results show a stable structure.

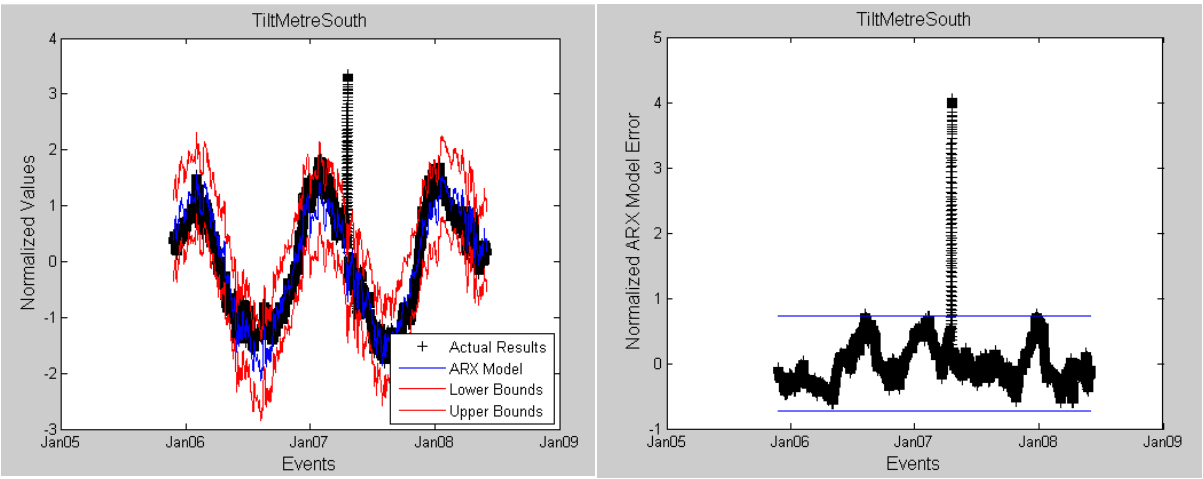

Figure 80: Jerónimos Monastery, South Tilt Meter Visual ARX damage detection

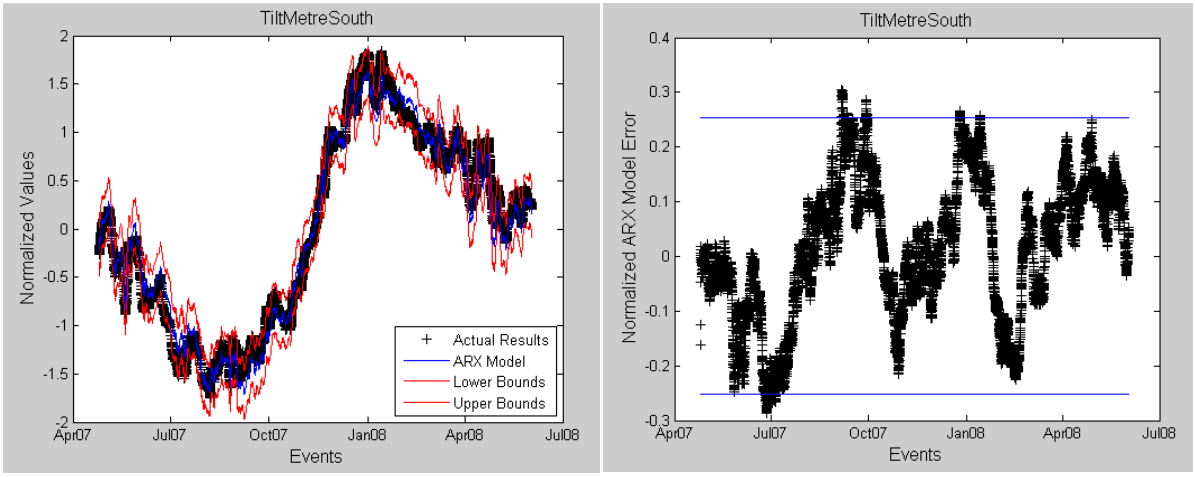

Figure 81: Jerónimos Monastery, South Tilt Meter, Visual ARX, Short History

The error from both ARX models, the bases of the visual ARX detection, provides interesting results. Table 31 provides the loss function, final prediction error, and coefficient of determination for both south tilt Meter models. Nothing here indicates possible damage, however, it is interesting to note that

the coefficient of determination indicates noticeably better model results with the short history model, but the loss function and the final prediction error, are very slightly worse.

Table 31: Jerónimos Monastery, Visual ARX, Error in ARX model

South Tilt Meter	Loss Function	Final Prediction Error	Coefficient of Determination
Long History	1.41499×10^{-5}	1.41859×10^{-5}	0.8714
Short History	1.58139×10^{-5}	1.59594×10^{-5}	0.9841

The damage detection analysis of Jerónimos Monastery highlights some concern for the south tilt Meter, but much of this concern can be dispelled referencing the other results. Data from the monitoring system indicates the structure is stable, and no urgent structural issues are apparent. Regardless, some questions have arisen from both the damage detection and early signal review that further monitoring would be beneficial in answering.

6.5 General Remarks

The damage detection analysis provides a beneficial addition to the numerical tool. Through modeling the data with direct and ARX models this addition to the numerical tool is able to provide users with further information to report on the structural stability. This program provides a solid basis for the structural alarms; however, future work is required on calibrating the modeling of structural response and creating proper alarm definition. Presently the damage detection can be analyzed by the user, and conclusions drawn on the severity of damage. Future potential includes MIROVY automatically providing feedback on the urgency of any structural problems discovered. This work would require a significant amount of further research and programming, and falls outside the scope of this thesis.

7 CONCLUSIONS

MIROVY was designed to assist users by automatically undertaking many processes that would otherwise be very labour intensive. Graphical displays and print outs provide users with large amounts of easy to analysis data with like input. This advanced numerical tool was designed within the context of historical structures, with case studies on historic cultural landmarks.

7.1 Critical Review of the Numerical Tool

A critical analysis of the value of MIROVY should progress in the same manner as the program, section by section.

Data input required some data pre-processing, however this could be undertaken for each case study in under an hour, requiring only combining of data, slight formatting, and the addition of the column headlines. No special order of columns or manipulation of data values was required.

The time selection part of the program was tested, and works. This sub-program is used once to investigate the integrity of daytime data, proving to be easy and fast to use with real life data.

Direct results analysis provided the graphical results assisting the user in determining upper and lower bound and selecting window size on the moving average filter. Adjusting these filters is easy and MIROVY is able to produce the new results quickly. One potential shortfall is that the only filters available are the outlier removal and the moving average filters. Some data contains abnormalities that if removed would improve sensor results. Other than the special cases the filters remove normal noise and random outliers without difficulty.

Simple statistical analysis provided all basic statistical information clearly and without difficulty. The most complex calculations undertaken in this section are standard deviation and histogram, and while even these are not difficult to undertake in a case by case basis the speed and ease that the numerical tool produces these results is a definite advantage.

The second time selection, and the specific data filter were both tested and work successfully if selected, however these were not used in either case study. One future adjustment that would potentially be beneficial to users is the ability to filter out a specific week or month from the data.

This is one potential method to deal with unexplained phenomena, removing it briefly to check other data, and return to the unexplained at a later point in time.

The static regression analysis section of the MIROVY is clear, quickly providing both graphics and printed information on relations between different signals. Single static regression gives clear plots showing relations, while the multiple static regressions provides easy to view information on modeled signal accuracy. These can be done easily and quickly, allowing the user to try several combinations in a short period of time.

The dynamic regression analysis section of the advanced numerical tool is capable of undertaking complex ARX computations. Here MIROVY requires some basic knowledge of ARX models and can take several attempts before the user finds the best combination of orders for the ARX model to give optimal results. This proves to be the most difficult part of the numerical tool; however, when compared to processing these calculations without using MIROVY, the program continues to provide the advantage to its user.

Modeling the structural response for alarm detection provides powerful assistance in detection of damage and structural instability. There is significant room for advancement and improvement in this section of MIROVY, but as a base this provides several pieces of information for the user to review and compare when making a decision on the structural stability.

On a whole MIROVY significantly reduces the work required in the analysis of structural monitoring data. Like any early version of a program there are many places for potential improvements, but this program provides a major step forward in creating fully automated structural monitoring systems.

7.2 Future Potential for Numerical Tool

The present user interface of the MIROVY requires a basic knowledge of Matlab, and requires the user to scroll down a long page of information to select the precise analysis desired. Creation of a user interface would assist future users, making it possible for those unfamiliar with computer programming to use the numerical tool. This would require someone familiar with the creation of user interfaces in Matlab, but little else as the main program window has been designed to make this step easier.

Providing the user with further data selection and filtering options would also be an improvement. Future data selection possibilities include processes like selection of only three dispersed data columns for analysis. While additional filters could be designed to target locations in the data were system adjustments have been done, and automatically manipulation the earlier data to match a similar trend as the later data. Of course care must be taken to not miss important data in these processes.

Presently the advanced numerical tool does not consider the layout of the sensors on a structure. Separate programs could be created to deal with different shaped structures, providing the user the ability to entre what wall sensors are located in, and eventually combine the sensor analysis with finite element models. This has the advantage of not only helping users visualize what is occurring in the structure, but could also help locate any problems developing in unmonitored areas.

Damage detection of the numerical tool presently gives feedback based on the bound set by the user. Advanced study and testing could be used to calibrate this section and determine what bounds should be used to determine different levels of severity in different structures.

Review of the results provided by the MIROVY with the Oporto Cathedral shows a gradual change in weather. This would agree with expected climate changes. MIROVY could potentially be used to assist in the study of climate change and its effect on historical structure as well as its effect on monitoring systems. One method of damage detection is to check for seasonal variations of signal means. With climate change changing our weather at a faster rate than any time on record, structural monitoring could be undertaking to investigate how significantly climate change will alter the seasonal movements of historic structures. This would be particularly important for structures whose movements or seasonal tilts reach the edge of structural stability in present climates.

References

Allen, M., & Maute, K. (2004). Reliability-Based Design Optimization of Aeroelastic Structures. *Structural and Multidisciplinary Optimization* , 228 - 242.

Altus, E., Totry, E., & Givli, S. (2005). Optimized Functional Perturbation Method and Morphology Based Effective Properties of Randomly Heterogeneous Beams. *International Journal of Solids and Structures* , 2345 - 2359.

Andersen, P. (1997). *Identification of Civil Engineering Structures using Vector ARMA Models.* Denmark: PhD Thesis, Aalborg University.

Azevedo, C. A. (2001). *Oporto Cathedral.* Oporto: Cabido Porucalense.

Binda, L., & Tiraboschi, C. (1999). Flat-Jack Test as a Slightly Destructive Technique for the Diagnosis of Brick and Stone Masonry tructures. *Int. Journal for Restoration of Buildings and Monuments* , 449 - 472.

Boone, S. (2001). Assessing Construction and Settlement Induced by Building Damage: A return to fundamental principles". *Underground Construction* (pp. 559 - 570). London: Institution of Mining and Metalurgy.

Canbay, E., Ersoy, U., & Tugrul, T. (2004). A Three Component Force Transducer For Reinforced Concrete Structural Testing. *Engineering Structures* , 257 - 265.

Chintalapudi, K., Paek, J., Gnawali, O., Fu, T. S., Dantu, K., Caffrey, J., et al. (2006). Structural Damage Detection and Localization Using NETSHM. *Information Processing In Sensor Networks: Proceedings of the fifth international conference on Information processing in sensor networks* (pp. 475 - 482). New York: Association for Computing Machinery.

Coleman, H. W., & Steele, W. G. (1999). *Experimentation and Uncertainty Analysis for Engineers.* Chichester: John Wiley & Sons, Inc.

Deutsch, C., Leuangthong, O., Nguyen, H., Norrena, K., Ortiz, J., Oz, B., et al. (2001). *Principles of Monte Carlo Simulation .* Retrieved April 24, 2008, from University of Alberta: www.ualberta.ca/~cdeutsch/MCS-course.htm

DGSI. (2008). *Durham Geo Slope Indicator - Total Pressure Cells*. Retrieved May 9, 2008, from http://www.slopeindicator.com/instruments/tpc.intro.html

Drdacky, M. (2008, February). Testing and Monitoring of Historic Structures and Materials. *SA 4: Presentation 10* . Prague, Czech Republic: Erasmus Mundus European Masters Program: Advanced Masters in Structural Analysis of Monuments and Historic Constructions.

Duncan, W. J., & Collar, A. R. (1934). A Method for the Solution of Oscillations Problems by Matrices. *Phil. Mag. Series 7* , 865.

Durham Geo. (2008). *EL Tiltmeter.* Retrieved July 15, 2008, from Durham Geo: Slope Indicator: http://www.slopeindicator.com

EMPA, CityU, COWI, LTU, NFBC, OU, et al. (2004). *Evaluatio of Monitoring Instrumentation and Techniques - Technical report.* Sustainable Bridges Project co-funded by the European COmmission within the Sixth Framework Programme.

Enckell, M. (2006). *Structural Health Monitoring using Modern Sensor Technology - Long-term Monitoring of the New Arsta Railway Bridge.* Stockholm: Department of Civil and Architectural Engineering, The Royal Institute of Technology, Sweden.

Felippa, C. A. (2001). A Historical Outline of Matrix Structural Analysis: A Play in Three Acts. *Computers & Structures* , 1313 - 1324.

Freire, P. (2008). *Lisbon.* Retrieved July 7, 2008, from NATIONAL ASTRONOMY AND IONOSPHERE CENTER: http://www.naic.edu/~pfreire/paulo/lisboa.html

FUTEK. (2008). *FUTEK - Advanced Sensor Technology Inc.* Retrieved May 8, 2008, from http://www.futek.com

Garcia, O., Vehi, J., Matos, J. C., Henriques, A. A., & Casas, J. R. (2007). Structural Assessment Under Uncertain Parameters Via Interval Analysis. *Journal of Computational and Applied Mathematics* , In Press, available online 29 June 2007.

Geomechanics. (2008). *Applied Geomechanics Inc.* Retrieved April 11, 2008, from http://www.geomechanics.com/

GEOSIG. (2008). *GSR-18 Strong Motion Recorder / GSD-18 Digitiser.* Retrieved April 14, 2008, from GEOSIG Ltd. - Measuring solutions: http://www.geosig.com

Green, P., & Silverman, B. (1995). *Nonparametric Regression and Generalized Linear Models: A roughness penalty approach.* London: Chapman & Hall / CRC.

Henriques, A. A., Veiga, J. M., Matos, J. A., & Delgado, J. M. (2008). Uncertainty Analysis of Structural Systems by Pertubation Techniques. *Structural and Multidisiplinary Optimization* , 201 - 212.

Honeywell. (2004). *Honeywell Sensotec Accelerometers*. Retrieved May 2, 2008, from Honeywell Sensotec: http://sensotec.com/accelerometers.asp

Hosmer, D. W., & Lemeshow, S. (2000). *Applied Logistic Regression: Second Edition.* Chichester: Wiley - Interscience .

Hubin, W. N. (2002). A Course in Computer Based Data-Acquisition. *American Journal of Physics* , 80 - 85.

Huiping, L., Guoqun, Z., Shanting, N., & Chuanzhen, H. (2007). FEM Simulation of Quenching Process and Experimental Verification of Simulatin Results. *Materials Science and Engineering* , 452 - 453.

IQS. (2008). *Industrial Quick Search,Inc. - Load-cells.org*. Retrieved May 8, 2008, from http://www.load-cells.org/info/load-cells/

ISIS Canada. (2004, August). *ISIS Educational Module 5: An Introduction to Structural Health Monitoring.* Retrieved April 9, 2008, from ISIS Canada: http://www.isiscanada.com

Jang, W.-S., Healy, W. M., & Skibniewski, M. J. (2008). Wireless sensor networks as part of a web-based building environmental monitoring system. *Automation in Construction* , 729 - 736.

Joo, J. W., Na, K. S., & Kang, D. (2002). Design and evaluation of a six-component load cell. *Measurement* , 125 - 133.

Kabelle, P. (2007). SA 2: Structural Analysis Techniques - Finite Element Method 1. - Principles. *Advanced Masters in Structural Analysis of Monuments and Historical*

Constructions (p. 57). Prague: Presented 5/12/2007 at Czech Technical University in Prague.

Laboratory Electronics. (2008). *LAB-EL*. Retrieved May 2, 2008, from LAB-EL: Thermometer-Hygrometer LB-710 (LB-710H): http://www.label.pl/en/rek710.html

Lancaster, H. O. (1974). *An Introductino to Medical Statistics.* John Wiley and Sons.

Lanco, P. (2006). *Structural Analysis of Multi - Ribbed vaults: Application to the high choir of Jeronimos Monastery (in Portuguese).* University of Minho (www.civil.uminho.pt/masonry).

Ljung, L. (1999). *System Identification: Theory for the User, Second edition.* Upper Saddle River, NJ: Prentice Hall.

Lourenco, P. B., Melo, A., & Carneiro, M. (2005). *Remedial Measures for the Cathedral of Porto: A post-modern conservation approach.* Retrieved July 2, 2008, from Universidade do Minho Archive: https://repositorium.sdum.uminho.pt/bitstream/1822/3060/1/2004_Lourenco_Melo.pdf

Lourenco, P., Krakowiak, K., Fernandes, F., & Ramos, L. (2007). Failure Analysis of Monastery of Jeronimos, Lisbon: How to learn from sophisticated numerical models? *Engineering Failure Analysis* , 280 - 300.

Lynch, J. P. (2007). A Overview of Wireless Structural Health Monitoring for Civil Structures. *Philosophical Transactions of the Royal Society A* , 345-372.

Lynch, J. P. (2005). Design of a Wireless Active Sensing Unit for Localized Structural Health Monitoring. *Structural Control and Health Monitoring* , 405 - 423.

Lynch, J., Y., W., Swartz, R. A., Lu, K. C., & Loh, C. H. (2008). Implementation of a Closed-Loop Structural Control System Using Wireless Sensor Networks. *Structural Control and Health Monitoring* , In press - Published online in Wiley InterScience.

Marques, L. (2007). *Monitorizacao Estatica e Dinamica: Aplicacoes.* MSc Thesis (in Portuguese): Universidade do Minho.

Mourao, S. (2002). *Study of the Seismic Behaviour of the Monumental Compound of Monastery of Jeronimos (in Poruguese).* University of Minho (www.civil.uminho.pt/masonry).

NovaLynx Corporation. (1988). *NovaLynx Corporation*. Retrieved April 10, 2008, from NovaLynx Corporation - Weather Monitoring Instruments and Systems: http://www.novalynx.com/products-wind-sensors.html

Oliveira, D. V. (2003). *Experimental and Numerical Analysis of Blocky Masonry Structures Under Cyclic Loading.* Universidade do Minho (www.civil.uminho.pt/masonry).

Oliveira, D., Ramos, L., Lourenco, P., & Roque, J. (2005). Structural Monitoring of the Monastery of Jeronimos. *Proceeding of the International Conference on the 250th Annicersary of the 1755 Lisbon Earthquake*, (pp. 466 - 473). Lisbon.

OMEGA. (2007). *Data Acquisition*. Retrieved April 11, 2008, from OMEGA.com: http://www.omega.com

OMEGA. (2003). *Omega: 3-Element Strain Gage Rosettes, 0º/45º/90º*. Retrieved May 2, 2008, from omega.com - Your One-Stop Source for Process Measurement and Control: http://www.omega.com/ppt/pptsc.asp?ref=SGD_TRIAXIAL&nav=PREE02

Peeters, B. (2000). *System Identification and Damage Detection in Civil Engineering.* Belgium: PhD Thesis, Catholic Univeristy of Leuven.

Pei, J.-S., Kapoor, C., Graves-Abe, T. L., Sugeng, Y. P., & Lynch, J. P. (2008). An Experimental Investigation of the Data Delivery Performance of a Wireless Sensing Unit Designed for Structural Health Monitoring. *Structural Control and Health Monitoring* , In press - published online in Wiley InterScience.

Peng, C., & Zhang, B. (2008). A note on goodness-of-fit test of continuation ratio logistic regression models under case–control data. *Journal of Statistical Planning and Inference* , 2355 - 2365.

Ramos, L. F. (2007). *Damage Identification on Masonry Structures Based on Vibration Signatures.* PhD Thesis: Universidade do Minho - Escola de Engenharia.

Ramos, L. F., & Lourenco, P. B. (2007). *Relatorio sobre a Monitorizacao Estatica da Torre Sul da Se do Porto.* Guimaraes: Universidade do Minho.

Ramos, L. F., & Lourenço, P. B. (2005). Static and Dynamic Structural Monitoring of the Santa Maria of Belem Church, in Lisbon. *II Eccomas Thematic Conference on Smart Structures and Materials.* Lisbon: C.A. Mota Soares et al. (Eds.).

Rankin, W. (1988). Ground Movements Resulting from Urban Tunnelling: Predictions and effects. *Geological Society - Engineering geology special publications* , 79 - 92.

Rao, C. R. (1973). *Linear Statistical Inference and Its Applications.* Chichester: John Wiley & Sons.

Salawu, O. S. (1997). Detection of Structural Damage Through Changes in Frequency: A Review. *Engineering Structures* , 718 - 723.

Sandrolini, F., & Franzoni, E. (2006). An operative protocol for reliable measurements of moisture in porous materials of ancient buildings. *Building and Environment* , 1372 - 1380.

SENSHE TECH. (2007). *SENSHE TECH: Geophone*. Retrieved May 2, 2008, from XI'AN SENSHE Electronic Technology Corp.: http://www.senshe.com/cp.asp?classid=439

Shames, I., & Dym, C. (1991). *Energy and Finite Element Methods in Structural Mechanics.* Taylor & Francis.

SISGEO. (1993). *SISGEO*. Retrieved April 11, 2008, from http://www.sisgeo.com

Smith, S. W. (2003). *Digital Signal Processing: A Practical Guide for Engineers and Scientists.* London: Newnes - An Imprint of Elsevier Science.

Society of Robots. (2008). *Society of Robots*. Retrieved May 8, 2008, from http://www.societyofrobots.com

Soong, T. T. (2004). *Fundamentals of Probability and Statistics for Engineers.* Chichester, West Sussex, England: Wiley-Interscience.

Virtual Porugal. (2008). *Vitrual Porugal, Porto the City*. Retrieved June 17, 2008, from http://www.portugalvirtual.pt

Window, A. (1992). *Strain Gauge Technology.* Kluwer Academic Publishers.

Wu, S., & Knott, J. (2004). On the statistical analysis of local fracture stresses in notched bars. *Journal of the Mechanics and Physics of Solids* , 907 - 924.

Appendix A: Post Report Enhancements to Numerical Tool

Relative Value Creator

The relative value creator was designed in response to requested relative values in the analysis. This program will shift the selected signal mean to zero without changing the standard deviation; and is located after the data import and before the single signal option. The main numerical tool program provides the data and headlines, as well as user selected signals to be translated into relative values.

Upon initializing the program displays "→ RELATIVE DATA CREATOR SELECTED TO RUN←". The program uses a loop to progress through all selected signals, displaying the headline for each signal it sets to a relative value. Each column processed has the mean calculated, and each value in the data column has the mean subtracted from the actual value. The old signal is replaced with the shifted signal in the data matrix, and the sub-program continues to the next signal. Once all selected signals have been shifted, the new data matrix is exported back to the main numerical tool program, and "→ RELATIVE DATA CREATOR SUCCESSFULLY COMPLETED←" is displayed in the command window.

Addition to Statistical Analysis

Signal to noise ratio and coefficient of variation may produce different results after the data has been filtered, leading the user to potentially false conclusions. Therefore a new option has been added to the simple statistical analysis allowing the user to run these calculations on the original imported data.

Addition to Static Regression Analysis

In order to provide easier comparison between single and multiple regression analysis an additional plot, in the same form as for the multiple regression relations, has been added to the single regression analysis outputs.

Save Function

A save function has been added to the program. While the program is designed to export all data of interest to the command window, and this continues to provide more information than the program saves, a save command has been added to assist with certain key data values. This final part of the program can be turned on or off like all other sections of the program, with all commands existing in the "MIROVY_MAIN.m" file.

Appendix B: Numerical Tool User Manual

This user manual will cover the following topics:

1. General
2. Input Data
3. Relative Value Creator
4. Single Signal Option
5. Time Selection
6. Direct Results Analysis
7. Simple Statistical Analysis
8. Specific Data Filter
9. Regression Analysis – Static Modeling
10. Regression Analysis – Dynamic Modeling
11. Damage Detection
12. Saved Data
13. Matlab Files
14. Program Interactions

User Manual 1: General

This user manual is organized in the same manner as the numerical tool, after the introduction the manual covers the following topics: importing data, the single signal option, time selection, direct results analysis, simple statistical analysis, time selection and specific data filter, regression analysis static and dynamic, and damage detection.

The tool is run by the MIROVY_Main.m file, in this file the user make various selections on what analysis the program should carry out, as well as what results are to be displayed in either plots, or in the command window. Switching on and off the various options is done by placing a 1 or 0 in the proper locations.

The suggested approach to data analysis is to initially switch all sub-programs, plots, and results displays to off. The user should then progress through the analysis one step at a time to ensure the data is being properly treated. This will make it easier to control the quality of results, ensuring the best quality data. Resetting data displays to off, or zero, once the user has ensured the data is being properly analyzed and recorded results will also simplify the amount of data to sort.

To run this numerical tool the user should have a computer with Matlab, version 7 or newer, and with additional toolboxes, signal analysis and system identification installed.

User Manual 2: Input Data

The data file input into the program must be a tab separated ASCII file, containing no blank spaces. For users less familiar with Matlab, it is easiest if this file and all the numerical tool program files are saved in the work folder of Matlab. First row of the data should be column headlines, providing the title of the signal. The titles must have no spaces. First three columns should provide the data in standard data acquisition form. First column contains year, second column contains day of year, out of three hundred and sixty five (three hundred and sixty six in leap years), and third column containing time on a twenty four hours clock, and with no punctuation between hour and minute. This is the date format typically used by data acquisition systems. Final note on input format is that the data matrix must be rectangular with no blank spaces.

Easiest way to input the file into this format is by using a combination of Microsoft Excel and notepad, although many other ways work as well. Input the data file created by your data acquisition into Microsoft Excel, Excel will provide guidelines on importing this data so that each signal is inside its own column.

In Microsoft Excel 2007 the data import wizard is activated under the "Data" tab, "Get External Data," and "From Text." The file being imported may actually be a ".dat" file, therefore "All Files" should be selected as what the user is searching for. The text import wizard will take you through several steps where the comma can be selected as the delimiter, as well as the initial row selected.

Most data files exported by data acquisition systems use the initial row as an identifier, and this row should be removed, and replaced with a row containing column headlines. These headlines must have no spaces. The first column is also an identifier, and must be removed.

Often several files from the data acquisition system are combined to form the file being analyzed; this can be done simply by locating the overlap in each file, and adding on the new data at this point. In this case the user should wait until all data in combined before removing the initial identifier column.

Once all the data is input into the excel file, select all the columns across the top. The method of select all will ensure that no additional blank spaces appear. Copy the data. Open notebook, and paste the data into the blank notepad. The data will now be set as tab delimited data, which is what the program is designed to receive. Save the text, or ASCII, file with the program files before running the numerical tool. The file is now prepared to run.

Open the numerical tool file "MIROVY_Main.m." This is the only file that will be opened to run the program. Got to "STEP ONE: IMPORT DATA." Here enter the file name that your data has been saved as. If all other sub-programs are turned off, save and run the program, and the command window will notify you if the data uploaded successfully.

User Manual 3: Relative Value Creator

Relative value creator will allow you to set signals to a relative value, shifting the mean to zero. This will provide feedback for some signals that is more intuitive. Such as the extensometer plots, if taken of the relative values, will be based on zero, and show the amount positive or negative from that mean.

Other signals, such as temperature, should not be turned into relative values. If you want certain signals to have relative value set “rRVC = 1;” then input which signals you want shifted to zero mean under sRVCS=[...];.

User Manual 4: Single Signal Option

Single signal option let you investigate the direct and statistical results for any one signal. To run this analysis set “rSSO=1;” and entre the number of the signal you wish to analyze for “sSSOS.”

User Manual 5: Time Selection

Time selection is a filter that allows you to remove any data that does not fit into the specified time period. To run this filter set “rTS=1;” and select the start and stop times for your period of interest in “signalStart” and “signalStop.” For example, if you are interested in all times between 8h00 and 16h00, set “signalStart=8” and “signalStop=16,” or alternatively, if you are interested in the night data, from 20h30 to 6h15, set “signalStart=20.5” and “signalStop=6.25.”

User Manual 6: Direct Results Analysis

Direct results analysis conducts the noise filtering of the signal. Therefore, it is important to use the plot and display information to help find the best filtered data, and then continue to run the program with displays turned off so that the following sub-programs use the filtered data. The description of each option is given in the program, and you can follow those guidelines.

Suggested moving average window sizes depend on frequency of data records and signal history. Often window sizes of one, two, or seven days are used. For example, if your signal takes a reading every hour, a one day window size would be composed of 24 records, and “mAFW” would be set to equal 24. Use the plot and compare filtered and unfiltered data to decide if the best moving average window has been chosen or not.

User Manual 7: Simple Statistical Analysis

Simple statistical analysis provides statistical information on the signal. Unlike the direct results sub-program the simple statistical analysis only provides information, and if this information is of no interest can be turned off without effecting following sub-programs. In the main program window the steps in the program are clearly outlined.

User Manual 8: Time Selection and Specific Data Filter

The time selection sub-program at this point is the same as discussed earlier in "User Manual 5: Time Selection."

The specific data filter works similar to the time selection filter, only allowing you to select data ranges from any signal, and exclude anything not in that range. Follow the simple guidelines provided in the main program window.

User Manual 9: Regression Analysis – Static Modelling

The steps involved with the static modeling regression analysis are outlined in the main program.

User Manual 10: Regression Analysis – Dynamic Modelling

The steps involved with the dynamic modeling regression analysis are outlined in the main program. It is suggested to use low orders (the na, nb, and nk values), as higher valued orders produce models that attempt to model signal noise. Low values are from zero to, and including, four.

User Manual 11: Damage Detection

Damage detection steps are outlined in the main numerical tool program.

User Manual 12: Saved Data

The final option in MIROVY is to save some of the files. If this option is selected the files will be saved into the same folder as the program (typically the work folder of Matlab). The files can be identified by the "Results_" at the start of each file name. Each file is saved in the ASCII format, as a ".out" file. These files can be opened as text files. If the values have not been calculated due to a section of the program being turned off, the file will only contain a zero.

User Manual 13: Matlab Files

Although only one file must be opened to run the numerical tool (MIROVY_Main.m), the program actually requires many Matlab files for full operations. These files are listed below in alphabetical order:

- MIROVY_Main.m
- MIROVY_Relative.m
- SignalAnalysis_DamageDetection.m
- SignalAnalysis_DamageDetection_ARX.m
- SignalAnalysis_DamageDetection_ARX_Analysis.m
- SignalAnalysis_DamageDetection_ARX_Norm.m
- SignalAnalysis_DamageDetection_ARXOne.m
- SignalAnalysis_DamageDetection_ARXThree.m
- SignalAnalysis_DamageDetection_ARXTwo.m
- SignalAnalysis_DamamgeDetection_Direct.m
- SignalAnalysis_DirectResults.m
- SignalAnalysis_DirectResults_MovingAverage.m
- SignalAnalysis_DirectResults_RemoveOutliers.m
- SignalAnalysis_DynamicRegression.m
- SignalAnalysis_DynamicRegression_ARX.m
- SignalAnalysis_DynamicRegression_Normalized.m
- SignalAnalysis_Import.m
- SignalAnalysis_Import_TimeVector.m

- SignalAnalysis_Normalized.m
- SignalAnalysis_PlotWBounds.m
- SignalAnalysis_SDF.m
- SignalAnalysis_SimplePlot.m
- SignalAnalysis_SingleSignal.m
- SignalAnalysis_StaticRegression.m
- SignalAnalysis_StaticRegression_Linear.m
- SignalAnalysis_StaticRegression_Multiple.m
- SignalAnalysis_StaticRegression_Normalized.m
- SignalAnalysis_Statistical.m
- SignalAnalysis_Statistical_PMF.m
- SignalAnalysis_TimeSelection.m
- SignalAnalysis_TwoPlot.m

User Manual 14: Program interactions

A chart showing interaction between programs, if everything is running, is shown below. In order to shorten file names the initial "SignalAnalysis_" or "MIROVY_" has been removed.

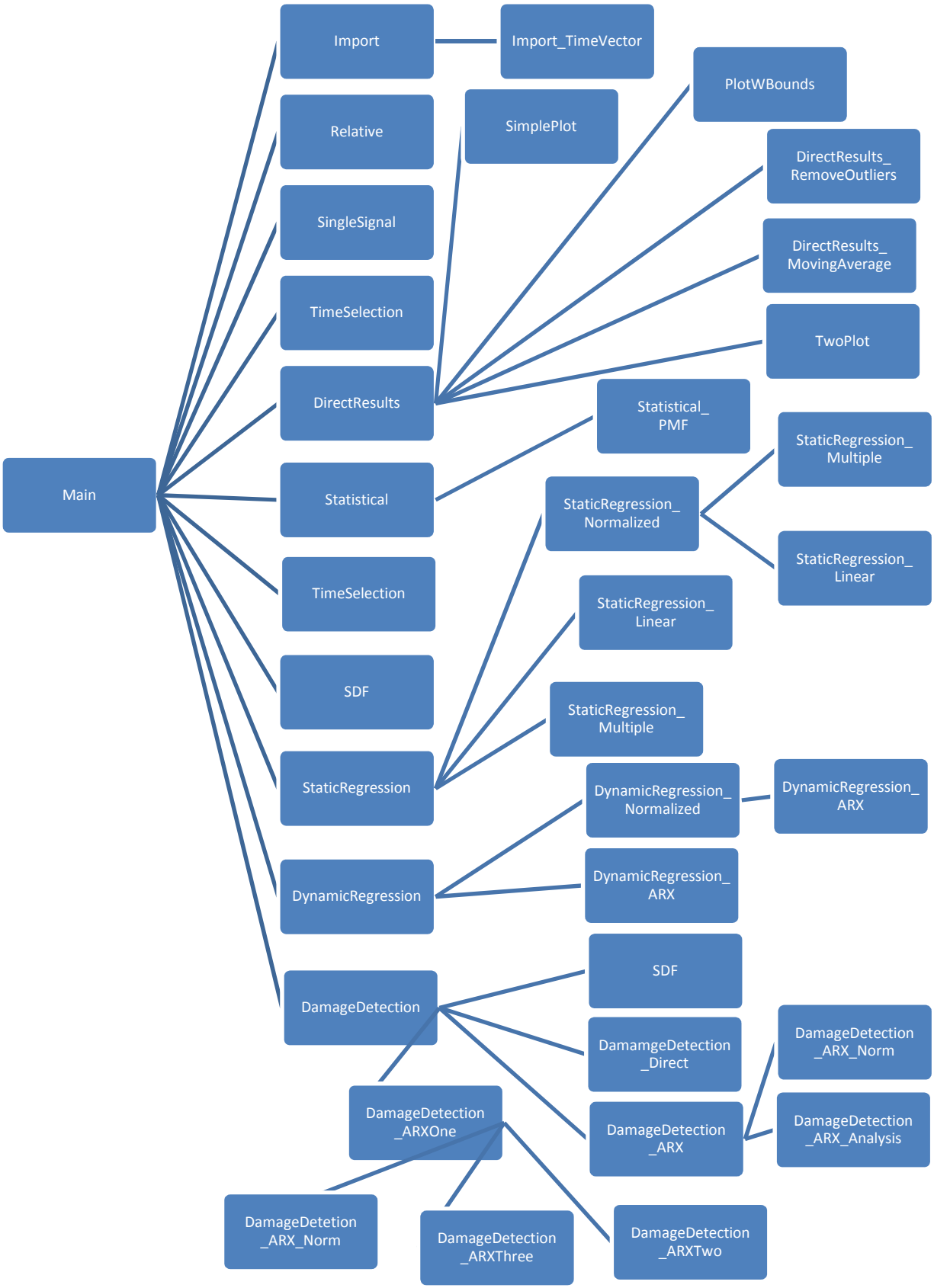
Main
Import
Import_TimeVector
Relative
SimplePlot
SingleSignal
TimeSelection
DirectResults
PlotWBounds
DirectResults_ RemoveOutliers
DirectResults_ MovingAverage
TwoPlot
Statistical_ PMF
Statistical
StaticRegression_ Multiple
StaticRegression_ Normalized
StaticRegression_ Linear
TimeSelection
StaticRegression_ Linear
SDF
StaticRegression_ Multiple
StaticRegression
DynamicRegression_ Normalized
DynamicRegression_ ARX
DynamicRegression
DynamicRegression_ ARX
SDF
DamageDetection
DamamgeDetection _Direct
DamageDetection _ARX_Norm
DamageDetection _ARXOne
DamageDetection _ARX
DamageDetection _ARX_Analysis
DamageDetetion _ARX_Norm
DamageDetection _ARXThree
DamageDetection _ARXTwo